THE JOURNAL
OF
CHEMICAL PHYSICS

VOLUME 2 SEPTEMBER, 1934 NUMBER 9

X-Ray Diffraction Study of Carbon Black*

B. E. WARREN, *Eastman Laboratory of Physics, Massachusetts Institute of Technology, Cambridge, Massachusetts*

(Received June 25, 1934)

X-ray diffraction patterns of carbon black have been made with strictly monochromatic radiation. Without making any assumptions as to the crystallinity of the material, the distribution of atoms about any one atom has been determined directly from the experimental scattering curve by the method of Fourier integral analysis. The results indicate definitely the existence of single graphite layers. Whether these layers have definite orientation and position with respect to one another (graphite crystal) or whether carbon black is a mesomorphic form of carbon, cannot be definitely decided from the experimental results. It is probable that carbon black is a heterogeneous mixture of particles which range from single graphite layers up to graphite crystals several layers thick. The intense small angle scattering is due to the difference between grain density and average density, caused by the loose packing of the extremely small grains.

INTRODUCTION

X-RAY diffraction studies of carbon black have been reported by a number of workers.[1] In most cases a pattern was obtained which comprised two or three broad diffuse rings, the rings having roughly the same position as the strongest lines in the powder pattern of graphite. A number of workers have concluded from this fact alone that carbon black is simply a fine grained form of crystalline graphite. However, since the appearance of the pattern is very similar to that of a typical liquid or amorphous solid, this immediate conclusion does not seem justified. In order to get as much information as possible from the diffraction pattern without making any *a priori* assumptions as to the crystallinity of the material, the scattering curve has been interpreted in the present work by the more powerful method of Fourier integral analysis. By this method, one obtains directly from the experimental scattering curve, the distribution of atoms about any one atom, regardless of whether the material is crystalline or amorphous.

EXPERIMENTAL

In order to eliminate the extraneous background blackening, it is necessary to use a strictly monochromatic beam and to evacuate the camera to avoid air scattering. The radiation from a copper target Müller tube was monochromatized by reflection from a rocksalt crystal and the cylindrical camera was evacuated during the exposure. The details of the experi-

* Paper presented at Washington meeting, American Physical Society, April, 1934.

[1] (*a*) Ewald and Hermann, Strukturbericht, 1913–1928: (*b*) G. L. Clark, Coll. Sym. Mon. **4**, 155 (1926): (*c*) P. Krishnamurti, Ind. J. Phys. **5**, 473 (1930): (*d*) U. Hofmann, Zeits. angew Chem. **44**, 841 (1931): U. Hofmann and D. Wilm, Zeits. f. physik. Chemie **B18**, 401 (1932): (*e*) C. Mongan, Hel. Phys. Acta **5**, 341 (1932): (*f*) F. Trendelenburg, Hel. Phys. Acta **6**, 477 (1933); Naturwiss. **20**, 655 (1932); Zeits. f. tech. Physik **14**, 489 (1933): (*g*) Berl, Andress, Reinhardt and Herbert, Zeits. f. physik. Chemie **A158**, 273 (1932): (*h*) S. B. Hendricks, Zeits. Krist. **83**, 503 (1932): (*i*) P. C. Mukherjee, Zeits. f. Physik **88**, 247 (1934).

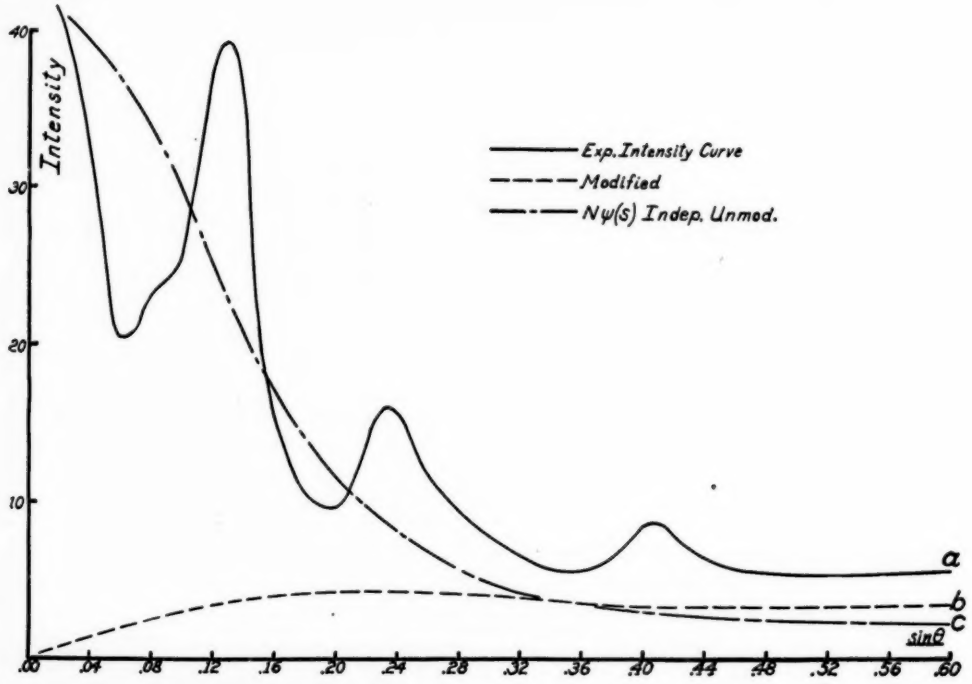

FIG. 1 (a) Experimental intensity curve for carbon black corrected for absorption in sample. (b) Intensity of modified scattering. (c) Independent unmodified scattering.

mental arrangement have been described in a previous paper.[2]

The material used was the commercial carbon black of the Cabot Carbon Co. The material was packed into a small cylinder of cigarette paper of diameter 1.6 mm. With the tube running at 15 m.a. and 30 kv peak, an exposure of 20 hours was sufficient. The microphotometer record of the film was changed into an intensity curve in the usual way. Fig. 1a shows the experimental intensity curve corrected for absorption in the cylindrical sample.[3]

Method of Fourier integral analysis[4]

We assume that in carbon black each atom is surrounded in the same way as every other atom.* Introducing a density function $\rho(r)$ such that $4\pi r^2\rho(r)dr$ gives the number of atoms between r and $r+dr$ from any given atom, the intensity of scattering is given by the relation

$$I(s)=N\psi(s)\left\{1+\int_0^\infty 4\pi r^2\rho(r)\ (\sin sr)/sr\ dr\right\}, \quad (1)$$

where

$$\psi(s)=I_0e^4f^2((1+\cos^2 2\theta)/2)/m^2c^4R^2,$$

$s=4\pi\sin\theta/\lambda$ and N is the effective number of atoms in the sample.

Let

$$i(s)=I(s)/N\psi(s)-1,$$

$$si(s)=4\pi\int_0^\infty r\rho(r)\sin sr\ dr. \quad (2)$$

By the Fourier integral theorem this can be written

$$r\rho(r)=(1/2\pi^2)\int_0^\infty si(s)\sin sr\ ds. \quad (3)$$

The integration over the scattered intensity $I(s)$ is from zero to large angles, and hence includes the diffraction maximum at zero angle (000 order) which is not experimentally observable. Replace $I(s)$ by $I'(s)+I(s)$ where $I'(s)$ is the intensity distribution in the 000 order beam, and $I(s)$ is the observable intensity curve.

[2] B. E. Warren, Phys. Rev. **45**, 657 (1934).
[3] F. C. Blake, Rev. Mod. Phys. **5**, 180 (1933).
[4] B. E. Warren and N. Gingrich, Phys. Rev. **46**, 368 (1934).
* If there are two kinds of carbon atom then $\rho(r)$ is the average of the two density functions.

That part of the integral in Eq. (3) which involves $I'(s)$ is readily evaluated and takes the same value for either an amorphous or crystalline material. Eq. (3) then takes the final form

$$4\pi r^2\rho(r) = 4\pi r^2\rho_0 + (2r/\pi)\int_0^\infty si(s)\sin sr\,ds, \quad (4)$$

where ρ_0 is the average density of the sample in atoms per cc. The curve $si(s)$ can be obtained directly from the experimental intensity curve and the integration involved in Eq. (4) then readily carried out with a harmonic analyzer. By a purely mechanical, straightforward method, one obtains the distribution curve $4\pi r^2\rho(r)$ directly from the experimental intensity curve.

Application of carbon black

The experimental intensity curve is given by Fig. 1a, the intensity being expressed in arbitrary units. As seen from Eq. (1) at large angles of scattering $I(s)$ approaches $N\psi(s)$ and hence at sufficiently large values of $\sin\theta/\lambda$ the experimental curve is given by the modified and *independent* unmodified scattering of N atoms.

Independent unmodified $I = N\psi(s)$

Modified[5] $I = NI_0\dfrac{e^4}{m^2c^4R^2}\left(\dfrac{1+\cos^2 2\theta}{2}\right)\{Z-\Sigma f_n^2\}$.

Assuming that the scattering can be taken as independent at $\sin\theta/\lambda = 0.6$, the fractional parts of unmodified and modified scattering are calculated. Since $I = I_{\text{unmod.}} + I_{\text{mod.}}$ this determines the ordinates at $\sin\theta/\lambda = 0.6$ for both the modified and independent unmodified curves. Both of these curves are readily calculated as a function of the angle, from the tables of scattering factors[6] and, the scale of ordinates having been fixed at one point, the two curves are then plotted on the same scale as $I(s)$. The unmodified part of the experimental scattering curve is then obtained by subtracting 1*b* from 1*a*. The difference divided by 1*c* gives the quotient $I(s)_{\text{coh}}/N\psi(s)$ from which the curve $si(s)$ is constructed. Although the assumption of independent scattering at large angle is only an approximation, it is nevertheless a sufficiently good one, and affords a very simple method of putting the $si(s)$ curve upon a quantitative basis.

The curve $si(s)$ obtained in this way is plotted against s (Fig. 2) and the integration involved in Eq. (4) carried out on a Coradi harmonic analyzer. The coefficients which the analyzer delivers for the different harmonics give directly the values of the integral for various values of r.

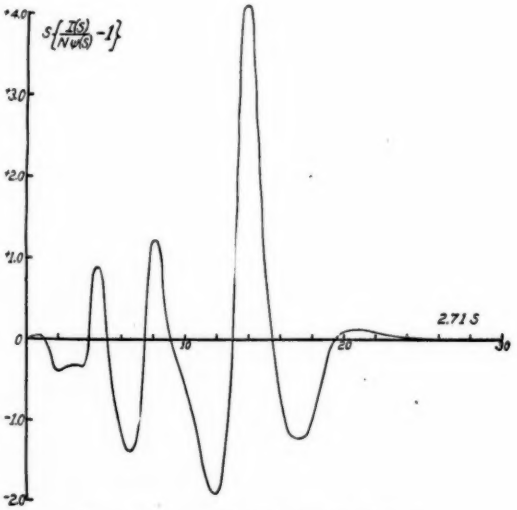

FIG. 2. Curve $si(s)$ plotted against s.

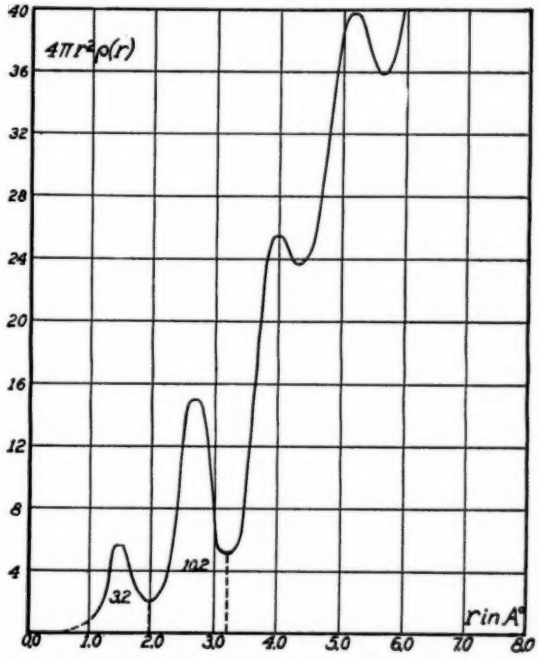

FIG. 3. Distribution of surrounding atoms in carbon black.

[5] E. O. Wollan, Rev. Mod. Phys. **4**, 233 (1932).

[6] James and Brindley, Phil. Mag. **12**, 81 (1931).

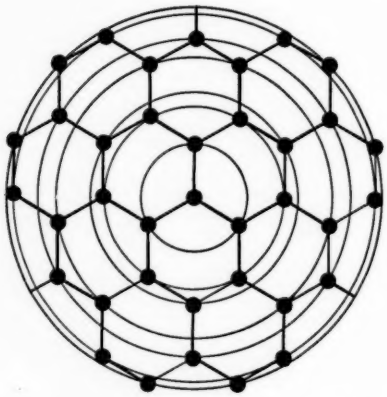

FIG. 4. Atomic arrangement in a single layer of the graphite structure.

TABLE I. *Number of neighbors and distances in a single graphite layer.*

No.	Distance	Aver. Distance
3	1.42A	
6	2.46	2.6A
3	2.84	
6	3.75	4.0
6	4.25	
6	4.92	5.0
6	5.11	

The scale of abscissae used in Fig. 2 corresponds to 0.425A per harmonic and the integration was carried out for the first 15 harmonics, thus giving points on the r scale from 0 to 6.4A. By then altering the scale of abscissae in Fig. 2, intermediate points were obtained.

The density curve so obtained is shown in Fig. 3. From the curve one gets directly the concentration of atoms at any distance from a given atom and, furthermore, since the work has been carried through on a quantitative basis, the areas under the peaks give directly the number of atoms in that range of distances.

At a distance of about 1.5A there is a peak containing 3.2 atoms, at 2.7A a peak containing 10.2 atoms and further concentrations at 4.05A and 5.15A. The curve indicates that the atomic arrangement in carbon black is definitely not diamond-like, since in the diamond structure there are 4 neighbors at 1.54A, 12 at 2.52A and 12 at 2.95A. Allowing for slight errors in the number of atoms and positions of the peaks due to overlapping, the distribution of Fig. 3 is in very close agreement with that of a *single* graphite layer.

The atomic arrangement in a single layer of the graphite structure is represented in Fig. 4 and the number of neighbors and their distances are tabulated in Table I.

The correspondence with the distribution of Fig. 3 is sufficiently close to justify the conclusion that *single* graphite layers exist in carbon black. Beginning at about 3.6A, there is a marked continuous distribution which is due to the atoms in neighboring layers. If these neighboring layers have a definite position and orientation with respect to the first layer, the configuration is that of graphite; if they do not, then carbon black is a mesomorphic form of carbon (regular arrangement in two dimensions only). It is very difficult to decide between these two possibilities.

Fig. 5 (a) shows the atom distribution for graphite crystals. Fig. 5 (b) gives the distribution for a material consisting of single graphite layers,

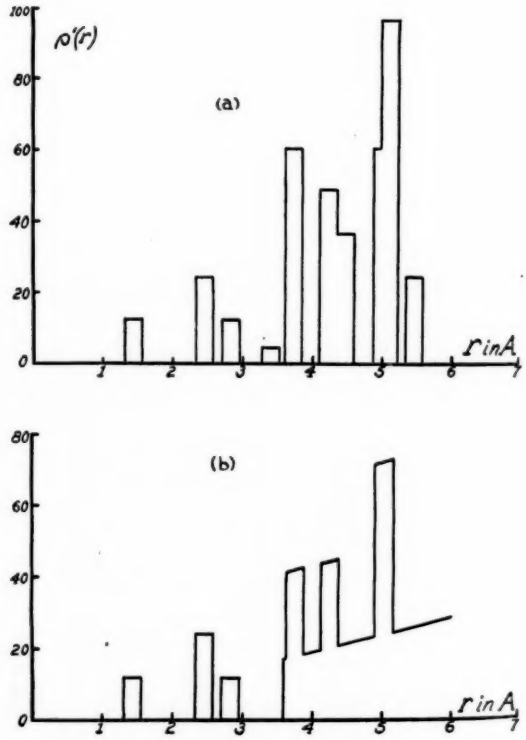

FIG. 5. (a) Atom distribution in a graphite crystal. (b) Atom distribution in a mesomorphic form of carbon, consisting of single graphite layers stacked roughly parallel to one another.

roughly parallel to one another and having an average separation of 3.6A. For a non-crystalline stacking of the single graphite layers, it would, of course, be expected that the layer separation would be slightly larger than the distance 3.4A, characteristic of graphite.

The two distributions are not sufficiently different to allow either one to be definitely excluded. In fact, from the experimental distribution curve one can only conclude that carbon black consists of either extremely small graphite crystals or single graphite layers roughly parallel to one another or a heterogeneous mixture of these two. The fact that the experimental scattering curve *could* be satisfactorily interpreted on a basis of single graphite layers roughly parallel to one another is extremely interesting and should be a warning against drawing too hasty conclusions from a diffraction pattern which shows only two or three diffuse peaks. Although the exact numerical values involved in the distribution curve of Fig. 3 should not be relied upon too closely, it is, however, worth noting that the area under the curve is in better agreement with a structure of single graphite layers roughly 3.8A apart than with a structure of small graphite crystals. On the other hand, the small angle scattering, discussed in the next section, indicates that at least a fraction of the material is in the form of small graphite crystals. It is probable that the average sample of carbon black is a heterogeneous mixture of particles ranging from single graphite layers up to graphite crystals several layers thick.

Small angle scattering

Referring to Fig. 1a it will be noticed that the diffraction pattern of carbon black shows one feature which is very unusual for homogeneous solids and liquids. Instead of the intensity falling to a small value with decreasing angle, it rises to a value which is actually greater than that of the strongest peak. This fact has been noticed by other investigators[1c, h] and several rather complex explanations have been put forward.

The effect appears to be due solely to the fact that the material consists of extremely fine grains which, because of their very flat non-uniform shape, pack together very loosely in the sample. About any atom there is accordingly a region of high density extending out to a distance which is of the order of magnitude of the grain size and beyond this an average density which is necessarily lower due to the loose packing of the grains. If this type of distribution be inserted in Eq. (1), we find that the intensity at small angle may have very appreciable values depending upon the amount of excess density. If we assume that a fraction of the material is in the form of small graphite crystals several layers thick, the difference between the density of graphite and carbon black is enough easily to account for the observed intensity at small angle. The decrease of the small angle scattering with increasing angle depends upon the dimensions of the high density region and is thus a rough measure of grain size.

Conclusions

Carbon black is not a truly amorphous form of carbon. The existence of single graphite layers is very definite and therefore the material is at least mesomorphic. The diffraction data indicate a heterogeneous mixture containing particles which range from single graphite layers up to graphite crystals several layers thick. The size of the grains will vary widely from one sample to another, depending upon the method of formation, and it is probably true that carbon black comprises a continuous series extending from the mesomorphic to the crystalline state.

The Reduction of Oxygen to Hydrogen Peroxide by the Irradiation of Its Aqueous Solution with X-Rays*

HUGO FRICKE,† *The Walter B. James Laboratory for Biophysics, The Biological Laboratory, Cold Spring Harbor, Long Island*

(Received June 11, 1934)

Irradiation with x-rays produces no chemical change in air-free water. With oxygen present, hydrogen peroxide is formed due to a primary activation of the water. The initial production of hydrogen peroxide is independent of the oxygen pressure, from 4 to 70 cm Hg and is dependent on the hydrogen ion concentration according to:

$$\frac{H_2O_2}{1000r \times 1000 \text{ cc}} = [2.2 + 2.2\left[\frac{10^{9.6-pH}}{1+10^{9.6-pH}}\right]10^{-6}\text{N}.$$

IRRADIATION with x-rays produces no chemical change in air-free water.[1] With oxygen present, hydrogen peroxide is formed due to a primary production of activated water molecules.[2] This reaction has been studied at a temperature of 30°C. The effect of variation of x-ray dosage, oxygen pressure and hydrogen ion concentration has been determined.

The analysis for hydrogen peroxide was carried out by adding a surplus of acid potassium bichromate to the irradiated solution and titrating back with ferrous sulfate. A high degree of purity of the water, particularly with respect to organic matter is essential. The water was purified by distillations from basic permanganate and acid bichromate solutions, in an all-Pyrex system, and thereafter the vapor mixed with air was passed through a quartz tube heated to 900°C. The water was next transferred to a de-aerator, saturated with oxygen at the desired pressure, and passed into the irradiation cells. The cells and de-aerator could be heated to 500°C for the purpose of removing possible traces of organic material.

Irradiation of the gas-free water gives a convenient test for the presence of organic impurities which are thereby decomposed with the formation of carbon dioxide and hydrogen. Even with the precautions used, the order of one micro-mol/liter of these gases was produced in the water. This value may be increased several times by less exacting means of purification and handling.

All solutions irradiated have been tested for organic impurities by this method. Its general usefulness will be obvious.

The oxygen pressure has been varied over the range of 4 to 70 cm of mercury, for water and for sodium hydroxide at pH=13. The initial production of hydrogen peroxide is independent of the oxygen pressure. The results for water are shown in Fig. 1. The x-ray dosage was determined by irradiation of ferrous sulfate solutions in

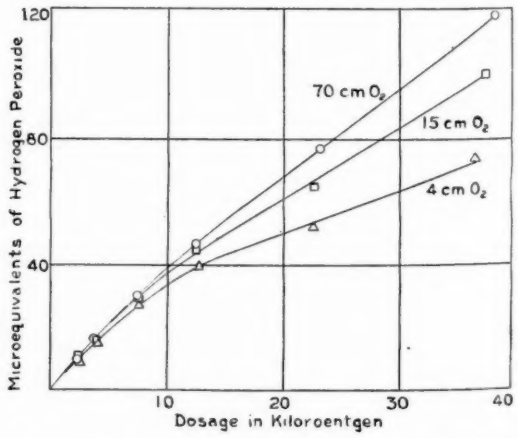

FIG. 1. The production of hydrogen peroxide as a function of the x-ray dosage for different values of the oxygen pressure.

* The general investigation, of which this work forms a part, is carried out with the support of the Carnegie Corporation, the Rockefeller Foundation and the L. K. and D. W. Elmhirst American Committee. The Committee on Biological Effects of Radiations, of the National Research Council, provided part of the equipment through the courtesy of a group of manufacturers, including The Corning Glass Works, The General Electric Company, The National Carbon Company and The Westinghouse X-Ray Company.

† I am indebted to Dr. E. R. Brownscombe for assisting me with these measurements.

[1] H. Fricke and E. R. Brownscombe, Phys. Rev. **44**, 240 (1933).

[2] H. Fricke and E. R. Brownscombe, J. Am. Chem. Soc. **55**, 2358 (1933).

0.8N sulfuric acid.[2] The deviation of the dosage curves from a straight line is accounted for by the decomposition of the hydrogen peroxide by the rays, as was established by the irradiation of solutions to which hydrogen peroxide had been added.

The dependence on the hydrogen ion concentration has been studied in the range pH = 3 to 13. The results are shown in Fig. 2 where the

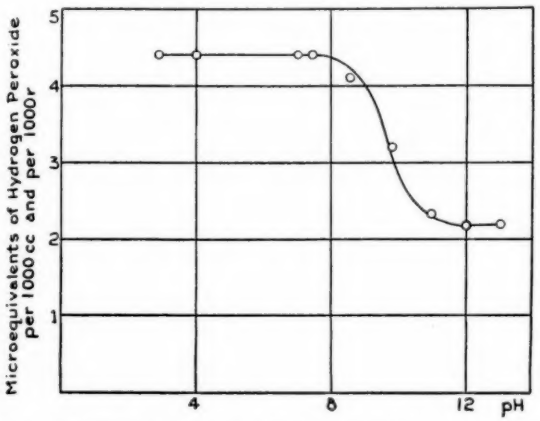

FIG. 2. The production of hydrogen peroxide as a function of the hydrogen ion concentration.

numbers of microequivalents of hydrogen peroxide produced per 1000 cc of solution and per 1000 r of dosage are plotted as a function of the hydrogen ion concentration of the irradiated solution. The values given represent the initial formation of hydrogen peroxide and are determined by taking the tangent of the dosage curve at the origin. The experimental accuracy may be placed at ±5 percent. Representative dosage curves are shown in Fig. 3.

The value given at pH = 7 refers to water. In the acid range sulfuric and phosphoric acids were used and no difference in the results was found. Hydrochloric and nitric acids exert a specific influence. For alkaline solutions, sodium hydroxide was used from pH = 11 to 13 and the results checked at pH = 11 and 12, with calcium hydroxide and with potassium hydroxide. From pH = 7.5 to 9.6 sodium phosphate and borate buffers were used. For each particular value of the pH the concentration of the buffer was changed from 0.5 to 5.0 millimolar with no variation in the results, indicating that the anions exerted no influence in the reaction. The concentration of chemicals used in all solutions was so low that the x-ray absorption was not appreciably different from that of pure water.

The curve shown in Fig. 2 is calculated from the function

$$\frac{H_2O_2}{1000\text{ cc}\times 1000r}=\left[2.2+2.2\frac{10^{9.6-pH}}{1+10^{9.6-pH}}\right]10^{-6}\text{N}. \quad (1)$$

The deviations of the experimental points from the theoretical curve may be within the limits of experimental error.

The change in hydrogen peroxide production which takes place between pH = 7.5 and 11.5 is linked with a change in the form of the dosage curve which becomes more nearly a straight line as the pH increases. For the higher dosages the curves appear to have the same slope.

The results indicate that the two terms in (1) are associated with two different reactions which in acid solution contribute equally to the production of hydrogen peroxide. One of these reactions is independent of the hydrogen ion concentration and only slightly interfered with

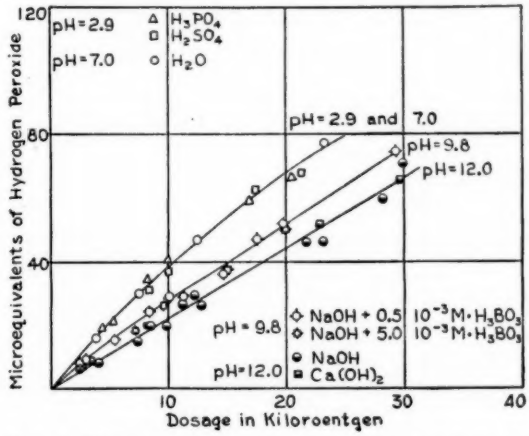

FIG. 3. The production of hydrogen peroxide as a function of the x-ray dosage for different values of the hydrogen ion concentration.

by the presence of hydrogen peroxide. The other reaction is inhibited by hydrogen peroxide in low concentration and its dependence on the hydrogen ion concentration indicates that its course involves the reversible combination of an intermediate (activated) product with the hydrogen ion.

Comparison of X-Ray Diffraction Curves of Water and Deuterium Oxide at 25°C

G. W. STEWART, *University of Iowa*

(Received June 29, 1934)

The difference in freezing point temperatures, maximum densities and molecular volumes and other physical constants of water and deuterium oxide indicate that the molecular forces do not remain entirely invariant with the isotopic change in mass. A comparison of the diffraction of x-ray curves for the two substances at 25°C indicates that the liquid structure of deuterium oxide is much like that of water. The peaks in the deuterium oxide curve are slightly sharper, apparently explicable in the fact that, at 25°C, this substance, compared with water, is nearer to its freezing point.

ONE would expect the forces in the water molecule to remain nearly invariant with the isotopic change of mass to deuterium oxide. Nevertheless, these two compounds differ in freezing points, boiling points, temperatures of maximum density[1] and molecular volumes.[2] It is of interest to ascertain if the liquid structure of these two compounds, as determined by the diffraction of x-rays, is noticeably different.

The deuterium oxide was supplied by Professor G. N. Lewis of the University of California and was 99 percent pure. The conductivity water was prepared by Professor J. N. Pearce of this University. The apparatus used is the same as that referred to in previous work.[3] The effect of Mo $K\alpha$ radiation was obtained by differential readings with $SrCO_3$ and ZrO_2 screens. The liquids were placed in very thin-walled cylindrical glass containers, these being nearly of the same diameter, 6.8 and 6.6 mm, and same thickness of wall. The transmission for the Mo $K\alpha$ radiation of the containers was found to be 0.81 and 0.79 percent. Corrections were made for the penetration and scattering of the Soller slits, the scattering from the glass container and the absorption of the liquid and container. No correction was made for the slight variation in effective thickness with angle of diffraction, for the beam was confined to a width of 2 mm by an additional single slit, thus making such a correction small. Nothing was to be gained by correcting for the incoherent scattering. The results of the observations are plotted in Fig. 1. The lower full line is that of water and the upper that of deuterium oxide, the zero for the ordinate being shifted for convenience. Approximately nine independent observations were made at each degree of angle of diffraction from 1° to 40° and 20° to 40°, and at each half degree from 10° to 20°. These curves essentially agree with previous observations[4] on water.

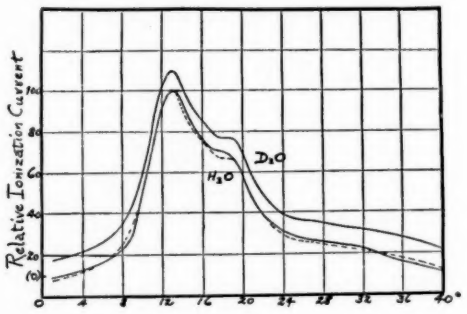

FIG. 1.

Bernal and Fowler[5] have discussed the liquid structure of water as indicated by the position of the two peaks and the course of the diffraction curve. The consideration of the moment may therefore be limited to whether or not there is any significant differences in these curves of water and deuterium oxide. The variations between the two noticed, other than in the middle portion, are within the uncertainties of the experiments.

The experimental errors in the middle portion

[1] Lewis and McDonald, J. Am. Chem. Soc. **55**, 3057 (1933). D_2O freezing point is 3.8°C, boiling point, 101.42°C and maximum density at 11.6°C.

[2] Luten, Phys. Rev. **43**, 161 (1933), gives the specific gravity as 1.1056 at 25°C. The value 1.111 would be required for no change in molecular volume.

[3] Stewart, J. Chem. Phys. **2**, 147 (1934).

[4] Meyer, Ann. d. Physik **5**, 701 (1930); Stewart, Phys. Rev. **37**, 9 (1931); Amaldi, Phys. Zeits. **32**, 914 (1931). The curve of Meyer matches the present one very closely throughout the middle portion, differing only in the end regions. The former curves of Stewart were taken with a zirconium filter only and general radiation was reduced to a small amount by a low voltage.

[5] Bernal and Fowler, J. Chem. Phys. **1**, 515 (1933).

of the curves are not as large and, while the differences of the curves in that region are not certain, yet they merit some confidence. It is probably not without significance that in deuterium oxide there are noticed slightly sharper peaks, particularly in the case of the smaller one. This one has been found[3] to disappear with rising temperature in the case of water, being unobservable at 40°C, and to be more marked as the freezing point is approached. In fact, with water the two peaks are distinctly sharpened in going from 21°C to 2°C, with the one at the diffraction angle of 13°C being displaced to the left and the one at 19° displaced to the right. The sharper peaks with D_2O are precisely what would be anticipated from these earlier experiments for the D_2O is nearer to its freezing point, as well as its temperature of maximum density. To use the new term of Bernal and Fowler,[5] the "structural temperature" of the deuterium oxide is less than that of water. It would be valuable to extend the careful comparisons of x-ray diffraction curves of deuterium oxide and water over a wide range of temperature, in order that the correctness of the tentative interpretation just made may be ascertained.

I wish to make appropriate acknowledgments to Professor G. N. Lewis for the deuterium oxide, to Professor J. N. Pearce for the conductivity water and to Dr. W. D. Phelps, research assistant, who is responsible for the observational data upon which this report is based.

The Infrared Absorption Spectrum of Water Containing Deuterium

JOSEPH W. ELLIS AND BARTHOLD W. SORGE, *University of California at Los Angeles*

(Received June 6, 1934)

Absorption percentages for the region 1–10μ are presented for one sample of water, 60 percent of whose hydrogen is deuterium, and for a second sample containing 99.5 percent deuterium oxide. Maxima are picked out as the three fundamental frequencies for the molecules DOD and HOD. These are compared with values predicted by an isotopic shift calculation based on data chosen from the spectrum of ordinary water. All other higher frequency maxima are interpreted as overtones or combination bands, but only after a fourth fundamental frequency is chosen in the examples of HOH and DOD.

THIS paper reports the experimental determination of the infrared absorption spectrum in the region 1–10μ of two samples of water containing different percentages of deuterium. On the basis of data selected from infrared and Raman spectra of ordinary water a calculation has been made to locate approximately the three fundamental frequencies of each of the molecules DOD and HOD. Certain absorption bands found in the newly determined spectra are identified with those calculated frequencies and the higher frequency bands are interpreted in terms of overtones and combinations of these fundamentals. Complete identification of all of the bands is possible, however, only after a fourth fundamental, associated with polymers, is selected.

SAMPLES OF WATER USED

The first sample studied was one kindly given us by Dr. Kaplan who had previously obtained it for another purpose through the courtesy of Professor G. N. Lewis of the University of California at Berkeley. It was rated as containing 60 percent of its hydrogen as deuterium. The second specimen was purchased from the California Isotope Company, Berkeley, California, and was guaranteed by this firm to contain originally 99.5 percent of deuterium oxide. This company's density determination yielded 1.117 g/cm^3, this somewhat larger value than usual arising from an excess of O^{18}.

THE EXPERIMENTAL EQUIPMENT

For the region 2.5–10μ a Hilger wave-length spectrometer, type D35, with a single 60° rock-salt prism was used. Temperature variation in the index of refraction of the prism was held to a minimum by making the observations in a sub-basement. Because of the large losses of light in the absorption cells, rather large slit widths had

to be used. The greatest slit width was 0.25 mm, corresponding to an average $\Delta\lambda$ range of 0.17μ. A Hilger linear thermopile, non-evacuated, and a Leeds and Northrup high sensitivity galvanometer were used in conjunction with this instrument.

For the region $1-2.5\mu$ a recording quartz spectrograph,[1] yielding a far greater resolving power than the Hilger instrument, was employed. The slit subtended an average $\Delta\lambda$ range of 0.002μ. A vacuum thermocouple and a Leeds and Northrup high sensitivity galvanometer are parts of this recording device.

For part of the longer wave measurements a cell was made up using 0.1 mm mica windows, separated by platinum strips 0.01 mm thick. This cell was set before the slit of the spectrograph so that the light rays coming from the spherical condenser mirror made a 30° angle of incidence with the windows. The usual procedure was followed of placing alternately before the slit the filled cell and two similar pieces of mica also held at a 30° angle. The purpose of using the mica sections at an angle was to prevent the formation of interference maxima and minima in the spectrum.[2] Although precaution was taken to guard against interference effects, no attempt was made to align the windows with respect to the plane of the optic axes. This lack of precaution is held responsible for the appearance in two of the spectra of a spurious apparent absorption band at 5.6μ, the location of a well-known absorption band of mica. Tests made after the spectra were recorded revealed that the magnitude of the absorption by mica at 5.6μ was dependent upon the orientation of the plane of the optic axes. The assumption is made that here, as in most crystals, the absorption coefficient is greatly dependent upon the plane of polarization of the light beam. A large amount of plane polarization gets introduced into the beam in the spectroscope used because of reflection at the prism, cell and mirror surfaces, thus affording the necessary lack of symmetry in the light beam required by the above explanation of the 5.6μ maximum.

The practical limit of observation through a mica cell is about 7μ. Therefore, to increase the range of observation to 10μ a cell with rocksalt windows was used for the more concentrated deuterium sample. It was practically impossible to determine the cell thickness here but from an examination of the intensity of absorption it is estimated to have been about twice as great as the mica cells containing the less concentrated sample and the ordinary water used for comparison purposes, i.e., about 0.02 mm.

In the shorter wave region glass cells ranging in thickness from 0.25 to 6 mm were used.

As sources of radiation a Nernst filament and a tungsten lamp were used for the longer and shorter wave-lengths, respectively.

The Absorption Spectra

Fig. 1*C* records the percentage curves for ordinary distilled water. The percentage absorption values have been computed directly from galvanometer readings in the longer wave region and from the photographically recorded deflections in the shorter wave region. The maxima of well-known bands occur at 6.20, 4.70, 3.03, 1.93 and 1.445μ. Considerable asymmetry exists in the 6.20μ band, suggesting that it is probably not a simple band. The somewhat low value for the 1.93μ peak is yielded through the use of very narrow slits, the width being indicated by a ruled line above 1.8μ. Had much wider slits been used, doubtless the band would have appeared more symmetrical and the maximum would probably have occurred near 1.96μ, as usually found. That the difference between 1.93 and 1.96μ represents an experimental error is impossible, for the errors in calibration do not exceed 0.005μ. The 5.6μ maximum is the spurious one referred to above. Absorption at 1.78μ, once erroneously interpreted as a doublet,[3] appears as a single band with this instrument of high resolving power.

Fig. 1*B* represents the observed spectrum for the water containing 60 percent of deuterium. The following maxima occur: 6.75, 6.2, 3.95, 3.03, 2.44, 2.015, 1.915, 1.650, 1.570, 1.425 and 1.360μ. Again the 5.6μ mica band appears. For the short wave spectrum the light beam was sent directly through the small capillary stem of the glass capsule container, yielding an effective thickness of about 0.5 mm. The existence of the weaker bands was verified also by using a thicker

[1] Ellis, R. S. I. **4**, 123 (1933).
[2] Meyer and Bronk, Astrophys. J. **59**, 252 (1924); Ellis, J. O. S. A. **23**, 88 (1933).
[3] Ellis, Phys. Rev. **38**, 693 (1931).

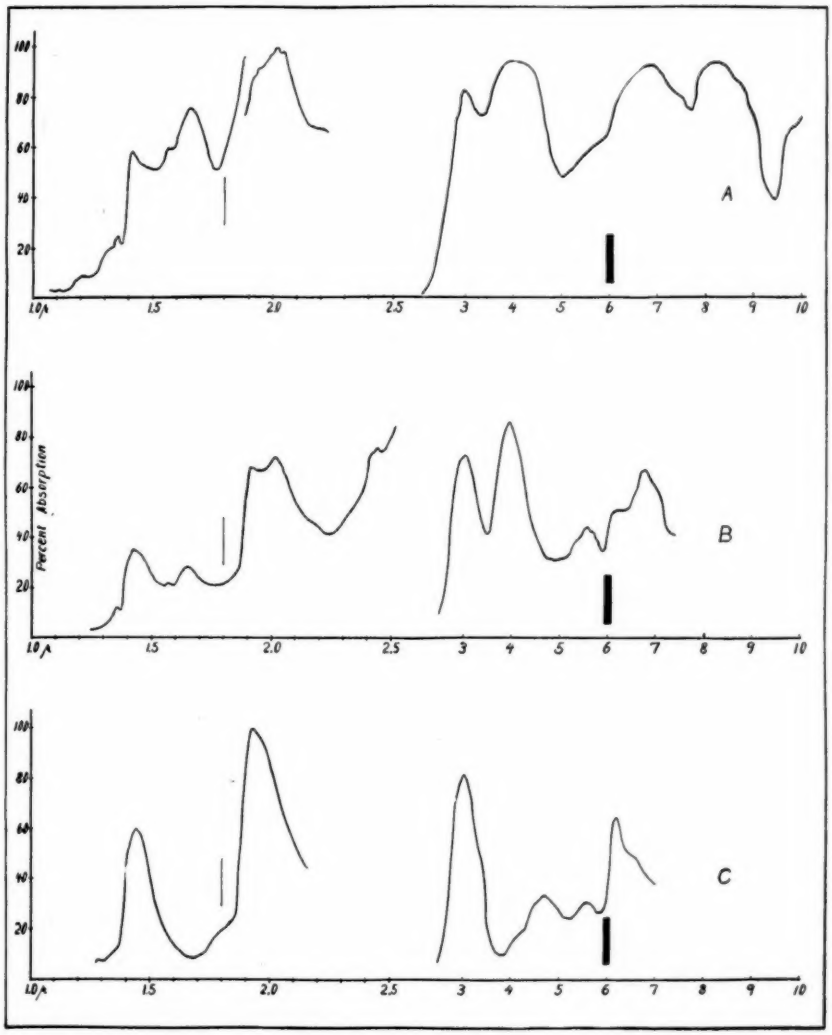

FIG. 1. *A*, percentage absorption through 99.5 percent deuterium oxide; *B*, water containing 60 percent deuterium; *C*, ordinary distilled water.

portion of the capsule. The single drop of water was later transferred to the mica cell and some days after the longer wave measurements were made it escaped by evaporation through a crack in the seal of this cell.

The record for the 99.5 percent sample of deuterium oxide is given in Fig. 1*A*. The maxima occur at 8.20, 6.85, 4.00, 2.95, 2.040, 2.015, 1.940, 1.655, 1.565, 1.415, 1.355, 1.310 and 1.20μ. Absorption is increasing at 10μ but the small deflections did not permit a complete study of this region. There is apparently absorption in the region of 5.6μ but, since rocksalt cell windows were used, this can bear no relation to similar absorption in Fig. 1*C*. The short wave record represents absorption by about 6 mm and 0.5 mm layers for the regions 1.0–1.9μ and 1.9–2.2μ, respectively. The former was obtained directly through the original cylindrical tube and the latter through a small drop enclosed in a capillary.

CALCULATION OF THE FUNDAMENTAL FREQUENCIES OF THE MOLECULES DOD AND HOD IN THE LIQUID STATE

Mecke's[4] analysis of the vibration-rotation spectrum of ordinary water vapor leads him to

[4] Mecke, Zeits. f. Physik **81**, 313 (1933).

the choice of 6.269, 2.8 and 2.663μ as the wave-length values associated with the three fundamental frequencies of the vapor HOH molecule. In liquid water we associate absorption bands at 6.20 and 3μ with the 6.269 and the 2.8, 2.663μ bands, respectively. More detailed information about the 3μ region is obtained from the Raman spectrum,[5] which usually yields three components, the average of the maxima being approximately 3.11, 2.92 and 2.80μ. Since the 3.11 band disappears or diminishes greatly in intensity with the addition of nitric acid and with a rise in temperature, we choose the remaining two as corresponding to Mecke's 2.8 and 2.663μ bands, respectively. The shift in wave-length for the liquid state is not surprising, especially since many of the molecules contributing to these bands are doubtless parts of polymer molecules.

Assuming that the HOH molecule in the liquid state retains a symmetrical triangular shape, even though it couples with other molecules to form a polymer, and that the potential energy of the molecule can be written in terms of valence and bending force coefficients, f and d, respectively, a calculation of these two constants as well as the valence angle θ has been made. Values for the three possible normal frequencies have been taken as follows, using Mecke's[4] notation: $\delta(\pi)$, 1610 cm^{-1}, 6.20μ; $\nu(\pi)$, 3420 cm^{-1}, 2.92μ; $\nu(\sigma)$, 3560 cm^{-1}, 2.80μ. In this calculation the general theory outlined by Lechner[6] for triangular molecules has been followed.

For the special geometrically symmetrical triangular molecule made up of particles of masses m_1, m_2 and m_3 with valence distances $s^\circ_{12}=s^\circ_{23}=s$, and $f_{12}=f_{23}=f$ the three normal frequencies can be readily expressed by

$$\delta^2(\pi)+\nu^2(\pi)+\nu^2(\sigma)=\left[\frac{f}{\mu_{12}}+\frac{f}{\mu_{23}}+\frac{d}{\mu_4}\right]\left[\frac{1}{2\pi c}\right]^2$$

$$\delta^2(\pi)\nu^2(\pi)+\delta^2(\pi)\nu^2(\sigma)+\nu^2(\pi)\nu^2(\sigma)=\left[\frac{f^2}{\mu_{12}\mu_{23}}\left(1-\frac{\mu_{12}\mu_{23}}{m_2^2}\cos^2\phi\right)+\frac{fd}{\mu_{12}\mu_4}\left(1-\frac{\mu_{12}\mu_4}{m_2^2}\sin^2\phi\right)+\frac{fd}{\mu_{23}\mu_4}\left(1-\frac{\mu_{23}\mu_4}{m_2^2}\sin^2\phi\right)\right]\left[\frac{1}{2\pi c}\right]^4$$

$$\delta^2(\pi)\nu^2(\pi)\nu^2(\sigma)=\left[\frac{f^2d}{\mu_{12}\mu_{23}\mu_4}\left(1-\frac{\mu_{12}\mu_{23}}{m_2^2}\right)\right]\left[\frac{1}{2\pi c}\right]^6$$

in which $\phi=(\pi-\theta)$, $c=3\times10^{10}$ and

$$1/\mu_{12}=1/m_1+1/m_2;\quad 1/\mu_{23}=1/m_2+1/m_3;$$
$$1/\mu_4=1/\mu_{12}+1/\mu_{23}+(2/m_2)\cos\phi.$$

When $m_1=m_3$, as is the case for HOH and DOD, these expressions simplify considerably.

The values for f, d and θ obtained are

$$f=6.80\times10^5 \text{ dynes/cm}$$
$$d=6.92\times10^4 \text{ dynes/cm}$$
$$\theta=136°.$$

No great accuracy should be attached to this value of the valence angle as it is very sensitive to slight changes in the choice of fundamental frequencies. If the vapor molecule value of θ, 107°, worked out from rotational structure by Mecke,[4] is used in place of 136°, the values of f and d become, respectively,

$$f=7.76\times10^5 \text{ dynes/cm}$$
$$d=7.56\times10^4 \text{ dynes/cm}.$$

This shows, therefore, in the calculations which follow, that the choice of θ introduces no large errors in the predicted approximate locations of the fundamental absorption bands. It seemed advisable, however, in working with the HOH molecule to fit the observed data to three constants rather than to two, i.e., rather than to use the vapor value for θ.

The calculation of the three fundamental frequencies for the molecules DOD and HOD is

[5] See K. W. F. Kohlrausch, *Der Smekal-Raman-Effekt*, p. 129, for a summary of the measurements on water in this region.

[6] Lechner, Monatshefte für Chemie **61**, 385 (1932).

essentially one of vibrational isotopic shifts. The values for f, d and θ computed for the HOH molecule were assumed to hold for the two molecules containing deuterium. The values obtained for DOD were: $\delta(\pi)$, 1190 cm^{-1}, 8.40μ; $\nu(\pi)$, 2450 cm^{-1}, 4.08μ; $\nu(\sigma)$, 2650 cm^{-1}, 3.78μ. For HOD they were: $\delta(\pi)$, 1410 cm^{-1}, 7.10μ; $\nu(\pi)$, 2510 cm^{-1}, 3.98μ; $\nu(\sigma)$, 3520 cm^{-1}, 2.84μ. Because of the inequality in the H and D masses in HOD, the π vibrations will be accompanied by σ components in the electric moment changes and *vice versa*. The $\delta(\pi)$ etc., notation is retained, however, for HOD for comparison purposes.

The Interpretation of the Spectra

Not all of the absorption and Raman frequencies observed for ordinary water can be interpreted in the usual manner as overtone and combination frequencies of the three fundamental frequencies chosen above. All of those represented in Fig. 2 may be so interpreted if a fourth fundamental 2130 cm^{-1} (4.70μ) is also chosen. Assigning a vibration quantum number V^* to this and V_1, V_2, V_3 to $\nu(\sigma)$, $\nu(\pi)$ and $\delta(\pi)$, respectively, the first column of Fig. 2 has been made up. The appearance of a fourth fundamental is not surprising considering the almost certain existence of polymers. Even if no polymer heavier than dihydrol exists, twelve fundamental frequencies are possible. Some others of these twelve fundamentals are probably found in the low frequency Raman bands found by Bolla[7] but which are not included in Fig. 2. Although the 2130 cm^{-1} band itself may be a combination frequency in as much as it is equal to the sum of $\delta(\pi)=1610$ cm^{-1} and a 510 cm^{-1} Raman frequency,[7] in the present paper we shall assign a quantum number V^* to it. The weak 5620 cm^{-1} band then is represented by one or both of V^*+V_1 and V^*+V_2. The 3215 cm^{-1} (3.11μ) band may represent another of the polymer fundamentals, although in as much as it is equal to twice the 1610 cm^{-1} fundamental, some double excitation explanation might be looked for. Its great Raman intensity in cold water and its diminution with temperature preclude the possibility of its being an overtone of 1610 cm^{-1}.

It will be observed that bands at 1.47 and 1.42μ

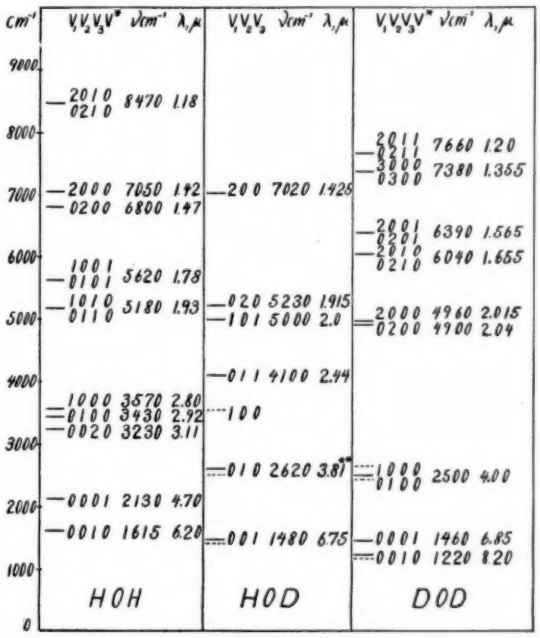

FIG. 2. Observed frequencies assignable to HOH, HOD and DOD. Raman band observed by Wood is indicated by double asterisks.

are indicated in Fig. 2*A*. These two components of the 1.445μ band, the latter of which is the more intense, have been clearly distinguished in the spectrum of two different samples of water at 99°. No systematic effort has been made to resolve other bands at higher temperatures.

In the spectrum of Fig. 1*A*, because of the high purity rating of the deuterium oxide furnished, it might be anticipated that only bands characteristic of DOD or its polymers should appear. However, the bands at 2.95, 1.940 and 1.415 must, we believe, be partly construed to indicate the presence of ordinary water. This contamination, especially when the water was transferred to the rocksalt cell for the longer wave study, probably came about through the hygroscopic nature of deuterium oxide. Part of the band at 2.95μ may, however, be due to a combination frequency associated with the 8.2 and 4.0μ fundamentals.

The 1.415μ position is one which is approached because of the unsymmetrical sharpening of the 1.44μ band when concentrated nitric acid is studied.[8] Its sharpness and its low wave-length value are indicative of a low concentration of

[7] Bolla, Nuovo Cimento **10**, 101 (1933).

[8] Kinsey and Ellis, Phys. Rev. **36**, 603 (1930).

HOH. The fact that this band does not appear as a doublet in Fig. 1*B* is probably because of a further superposition of a band arising from HOD.

The 8.20μ band is interpreted as $\delta(\pi)$ and 4.00μ as $\nu(\pi)$ and $\nu(\sigma)$ unresolved. Bands near these positions should be found for heavy water vapor. The strong band at 6.85μ is assumed to be a polymer band corresponding to 4.70 in ordinary water. It occupies a position intermediate between 4.0 and 8.2μ, just as 4.70 occupies such an intermediate position between 6.2 and 3.0μ. The relatively great intensity of the 6.85μ band suggests a greater degree of polymerization in deuterium oxide than in ordinary water. That this may be expected to be the case has been suggested by Bernal[9] on the basis of diminished molecular rotation.

All of the other bands of Fig. 1*A* can be regarded as overtones and combinations of four fundamentals. The assignments of quantum numbers V_1, V_2, V_3 and V^* are shown in Fig. 2*C*. In this figure, also, the frequency positions for the three calculated fundamentals are shown by dotted lines.

R. W. Wood[10] found a 2517 cm^{-1} Raman band which he assigned to the molecule DOD. This agrees well with our 2500 cm^{-1} band.

Wood also found a 2623 cm^{-1} Raman band which he assigned to HOD. We have included this frequency in Fig. 2*B* rather than our absorption value under the assumption that it may represent a value less influenced by other bands than the infrared maximum.

The band at 2.44μ, and perhaps the one at 1.915μ, represent the only features of the spectrum in Fig. 1*B* which may be credited to the unsymmetrical HOD molecule, representing V_2+V_3 and $2V_2$, respectively. Other predicted combinations and overtone bands would be superposed upon bands also belonging to DOD.

It is believed that the agreement between observed wave-number values in Fig. 2 and values anticipated on the basis of the quantum assignments are as good as could be expected in consideration of the widths and the overlapping of bands which exist.

During the course of this experiment there appeared a brief paper by Casselman[11] giving his results on a sample of heavy water comparable to our 60 percent water. There is a great similarity between his record and our Fig. 1*B* although we believe there are considerable errors in wavelength determination in Casselman's record. There is apparently a broad false minimum in his curves around 5.6μ which might be explained on the basis of failure properly to orient mica windows, an effect opposite to that which we have outlined above but which could be explained by the same mechanism. It is not stated whether mica windows were used but the termination of his spectrum near 7μ would indicate that they were.

Conclusion

The fair agreement between the observed frequency values for heavy and intermediate water with those resulting from an isotopic shift calculation with light water data, should not be construed to indicate with certainty the existence in the liquid state of molecules HOH, HOD and DOD similar to those in the vapor state. Realizing that H atoms in a vast variety of molecules always give rise to absorption and Raman bands near 3μ and 6–7μ, it is possible that the degree of agreement obtained in this experiment might still be obtained even though there is in the liquid state as radical a departure from the vapor molecule configuration as the model of Kinsey and Sponsler[12] requires. The one thing which the experiment does definitely show, we believe, is a large degree of polymerization in pure deuterium oxide, apparently a larger degree than in ordinary water.

[9] Bernal, Proc. Roy. Soc. **A144**, 24 (1934).
[10] Wood, Phys. Rev. **45**, 732 (1934).
[11] Casselman, Phys. Rev. **45**, 221 (1934).
[12] Kinsey and Sponsler, Proc. Phys. Soc. **45**, 768 (1933).

The Infrared Absorption of Alcoholic Solutions of Hydroxides

E. K. PLYLER AND F. D. WILLIAMS, *Department of Physics, University of North Carolina*

(Received July 12, 1934)

Bands have been observed at 0.76μ, 0.95μ, 1.05μ, 1.27μ, 1.30μ, 1.73μ, 1.89μ, 2.30μ, 2.60μ, 3.80μ and 5.20μ in alcoholic solutions of hydroxides. Solutions of NaOH and KOH gave the same positions for the bands. It was found that if the bands at 3.80μ and 5.20μ were considered as fundamentals, the remaining bands could be classified as harmonics. The similarity of the observed bands of the alcoholic solutions to the bands of aqueous solutions is mentioned.

A RECENT study[1] of the infrared absorption bands of aqueous solutions of certain hydroxides has shown that intense bands exist at 3.65μ and 5.2μ. These bands were found to be due to changes in energy levels of the hydroxide molecule when attached to water molecules. Collins[2] had previously found that different hydroxides in alcoholic solutions had similar bands in the regions of 0.96μ, 1.10μ and 1.26μ. He concluded that the absorption was due to the OH ion. The present work was undertaken to see if any bands existed at the longer wave-lengths in alcoholic solutions of the hydroxides which were related to the bands observed by Collins. The region studied was from 0.8μ to 7μ. The infrared absorption spectra of the alcohols have been studied by several workers[3] but the work has been repeated in order that the absorption for the same cell thickness of alcohols and the solutions would be available.

The experimental method was the same as has been previously described.[4] The absorption spectra of solutions of NaOH and KOH in both methyl and ethyl alcohol were measured. All the solutions were saturated at 22°C. Since these hydroxides are very soluble in water, it was necessary to have alcohols free from water. Absolute alcohols were obtained and tested for the presence of water with anhydrous copper sulphate and also by density measurements. These tests indicated that the alcohols were free from water in any appreciable amount. An additional proof that water was not present in any appreciable amount became apparent when the strong absorption bands due to water failed to appear at all.

In Fig. 1 are shown the results obtained in the region from 3μ to 5.4μ. No absorption which

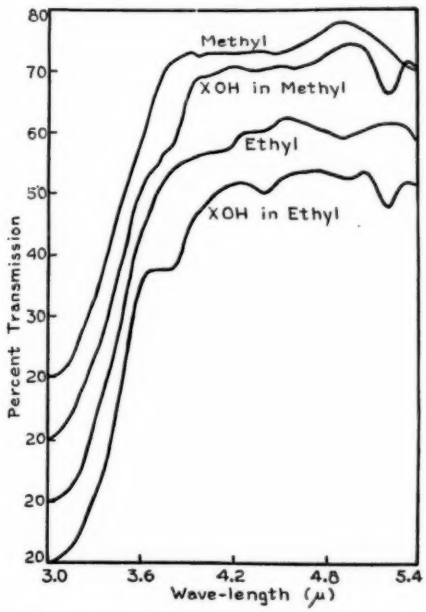

FIG. 1. Bands at 3.8μ and 5.2μ produced by hydroxides in alcoholic solutions. The cells were about 0.1 mm thick.

might be attributed to hydroxides was found in the region from 5.4μ to 7μ and this part of the spectrum was omitted from the figure. Two bands which were not observed in the pure alcohols were found in the solutions at 3.8μ and 5.2μ. These bands occurred in the same region for NaOH and KOH solutions and at approximately the same wave-length when the solvent was methyl or ethyl alcohol. The region from 4μ to 5.4μ transmits about 80 percent of the radiation

[1] E. K. Plyler and W. Gordy, J. Chem. Phys. **2**, 470 (1934).
[2] J. R. Collins, Phys. Rev. **20**, 486 (1922).
[3] W. Weniger, Phys. Rev. **31**, 388 (1910); J. W. Sappenfield, Phys. Rev. **33**, 37 (1929); E. K. Plyler and T. Burdine, Phys. Rev. **35**, 605 (1930).
[4] E. K. Plyler and E. S. Barr, J. Chem. Phys. **2**, 307 (1934).

and the percent transmission would have been greater if corrections had been made for the reflection of the fluorite windows in this region.

The band at 5.2μ is the most intense of all the bands observed. It is found at approximately the same position in aqueous solutions of the hydroxides. The band at 3.8μ occurs at a longer wave-length than the corresponding band in aqueous solutions. Since these bands are characteristic of different hydroxides in solution, they are designated as XOH in the figure.

The results obtained in the region from 0.8μ to 2.0μ are shown in Fig. 2. There are many small

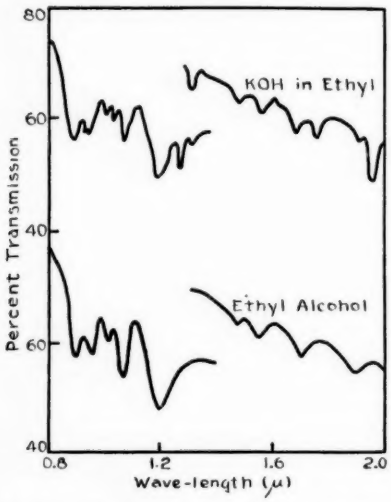

FIG. 2. Small bands produced in the region from 0.8μ to 2μ by hydroxide solutions. The cells were 1 cm thick.

bands in this region due to the alcohols and the additional bands are not so easily detected. Small bands were located at 0.96μ, 1.05μ, 1.27μ, 1.30μ, 1.73μ and 1.89μ.

Also a small band was located at 0.76μ but it is not shown in the figure. The region from 2.0μ to 2.8μ was studied with thinner cells and the results are shown in Fig. 3. Two bands with greater intensity were found at 2.30μ and 2.60μ. The observed bands have been classified as given in Table I. The bands at 3.8μ and 5.2μ are considered as fundamentals and called ν_2 and ν_1, respectively. All the other observed bands except the band at 2.30μ are found to be harmonics of these bands. The calculated band for the combination $\nu_1+\nu_2$ does not check closely with the observed band at 2.30μ and this band may be

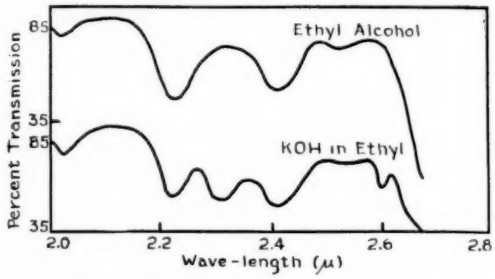

FIG. 3. The bands at 2.3μ and 2.6μ produced by hydroxides in alcoholic solutions. The cells were about 1 mm thick.

a fundamental. No correction term was introduced in the calculation of harmonic frequencies but the check is very good. The intensity of the harmonic bands does not decrease rapidly. The fourth harmonic of each fundamental was observed.

Except for the shift of the band at 3.65μ in aqueous solutions of the hydroxides to 3.8μ for the alcoholic solutions, there appears to be little change in the absorption of the hydroxides in solutions of water or alcohol. It has already been shown that the two fundamental bands of the hydroxide solutions are due to the energy levels between the undissociated hydroxide molecule and water molecules. The present work shows that the energy levels between hydroxide molecules and the alcohol molecules are very similar

TABLE I. *Classification of observed bands.*

Term	Frequency in cm^{-1}		Wave-length in microns	
	Calc.	Obs.	Calc.	Obs.
ν_1	1923*	1923	5.20*	5.20
ν_2	2632*	2632	3.80*	3.80
$2\nu_1$	3846	3846	2.60	2.60
$\nu_1+\nu_2$	4554	4348	2.20	2.30
$2\nu_2$	5264	5291	1.90	1.89
$3\nu_1$	5769	5780	1.73	1.73
$4\nu_1$	7692	7692	1.30	1.30
$3\nu_2$	7896	7874	1.26	1.27
$5\nu_1$	9615	9524	1.04	1.05
$4\nu_2$	10528	10526	0.95	0.95
$5\nu_2$	13160	13158	0.76	0.76

* Observed values taken as calculated values.

to the energy levels where water is the solvent. This result is in agreement with the general observation that aqueous and alcoholic solutions of the same substance usually give rise to the same color.

Raman Spectrum of Fluorobenzene*

F. W. Crawford and J. Rud Nielsen, *Department of Physics, University of Oklahoma*

(Received July 5, 1934)

The Raman spectrum of fluorobenzene has been investigated with a Hilger E1 quartz spectrograph, the following frequency shifts being obtained: 241, 517, 613, 804, 829, 997, 1009, 1157, 1220, (1265), (1414), 1496, (1561), 1599, 3076 and 3677 cm^{-1}. Relative intensities were measured with a Zeiss three-prism glass spectrograph and a Moll microphotometer.

THE Raman spectrum of benzene has received much attention[1] and the spectra of chlorobenzene, bromobenzene and iodobenzene have been studied by several investigators.[2] At the time that the present work was undertaken, no data were available on the Raman spectrum of fluorobenzene. Recently, however, measurements on this compound have been reported by Pai[3] and by Murray and Andrews.[4]

Experimental Arrangement

The experimental arrangement used was essentially that proposed by Wood.[5] The primary light source was a 220-volt vertical quartz mercury arc backed by a reflector. A Pyrex tube, 25 mm in diameter and filled with a solution of 20 cm^3 of carbon tetrachloride to 1 cm^3 of a saturated solution of iodine in carbon tetrachloride, served as filter and condensing lens. It suppressed the continuous background from the mercury arc without reducing too greatly the intensities of the mercury lines between 3341A and 4358A. Because of the photochemical decomposition of the filter solution, it was renewed twice a day. An air blast was directed against the filter tube, the mercury tube being partially shielded. Screens of black paper kept unfiltered light from reaching the fluorobenzene; for, though none of the mercury lines transmitted by the filter caused appreciable photochemical action, light filtered only through Pyrex glass produced a dark brown precipitate. The fluorobenzene, obtained from the Eastman Kodak Company, was distilled under normal pressure directly into the Wood's tube. This was surrounded by a water jacket, two-thirds of the exterior wall of which was covered by a closely fitting reflector. The scattered light passed through a plane Pyrex window and a totally reflecting prism and was focussed by a condensing lens on the 0.04 mm wide slit of a Hilger E 1 quartz spectrograph.

Four plates were taken with exposures varying from three to ten days. To enhance the weak Raman lines, enlargements were made on process plates. Contact prints were made of these enlargements and the wave numbers of the Raman lines were measured, linear interpolation from the closest known iron lines being used.

Since the configuration of the 3650A group is readily recognized in the scattered spectrum, much aid in the assignment of the Raman lines was gained by including this group in the exciting light. Moreover, it is advantageous from the point of view of dispersion, scattering efficiency and photographic sensitivity to use as short wave-lengths as the absorptivity and photochemical stability of the irradiated substance permit.

In order to measure the relative intensities of the Raman lines, two plates were taken with a Zeiss three-prism glass spectrograph.[6] The time of exposure of each plate was three days, the slit

* From a thesis submitted by F. W. Crawford to the Graduate Faculty of the University of Oklahoma in partial fulfillment of the requirements for the degree of Doctor of Philosophy. A report of this work was made before the Oklahoma Academy of Science on November 31, 1933.

[1] K. W. F. Kohlrausch, *Der Smekal-Raman-Effekt*, Springer, Berlin, 1931; P. Grassmann and J. Weiler, Zeits. f. Physik **86**, 321 (1933).

[2] K. W. F. Kohlrausch, ref. 1; W. D. Harkins and R. R. Haun, J. Am. Chem. Soc. **54**, 3920 (1932); J. W. Murray and D. H. Andrews, J. Chem. Phys. **1**, 406 (1932).

[3] N. Gopala Pai, Nature **132**, 968 (1933).

[4] J. W. Murray and D. H. Andrews, J. Chem. Phys. **2**, 119 (1934).

[5] R. W. Wood, Phil. Mag. **6**, 729 (1928).

[6] The intensity measurements were made at the Massachusetts Institute of Technology. We are indebted to Professor George R. Harrison who generously placed the facilities of the George Eastman Research Laboratory at the disposal of one of us (F. W. C.).

width being in one case 0.10 mm and in the other case 0.20 mm. A step-weakener having ten steps, each 3 mm wide, was placed in contact with the exposed portion of the plate, which it covered completely. The central strip of the step-weakener was removed with a sharp pointed knife, and the absorbing steps were staggered on either side. The step-weakener was made from a photographic film by exposing adjacent strips for different times. The absorption of each step for the spectral region between 3600 and 5000A was measured with a Moll recording microphotometer, a Wratten No. 49 filter being placed in front of the thermocouple. The microphotometric record of a plate was made by recording step by step the complete Raman spectrum, as photographed through the step-weakener, on a single light sensitive sheet. Ten curves, one below the other, were thus obtained. Only the upper six of these were found to be useful, however, since the four steps of greatest density absorbed so strongly that only the most intense lines produced appreciable blackening on the plates. The calibration curves for the plates were made from selected portions of these records. With a slit width of 0.20 mm, most of the Raman lines gave density curves with flat tops.

It was found unnecessary to correct for the small variation of plate sensitivity with wave-length. The loss of light due to reflection in the spectrograph was estimated for the cases of completely polarized and completely depolarized Raman lines, respectively, due regard being taken for the mode of illumination. The difference between the losses in the two cases was about 12 percent of the incident intensity. Since the degree of depolarization was not measured for the Raman lines, it was not possible to apply the proper correction to the individual Raman lines. The relative intensities, given in Table II, are, therefore, not very accurate, the greatest possible error being as much as 20 percent.

Results

The Raman lines observed are listed in Table I in the order of decreasing wave numbers. The first column gives the ordinal numbers used to designate the lines. Three of the lines, indicated by a *z*, were observed only with the glass spectrograph with which more strongly exposed plates were obtained than with the quartz instrument; because of the wide slit used with the glass spectrograph, the wave numbers of these three lines are accurate only to about ± 10 cm^{-1}. In the third column are listed the approximate intensities, estimated visually, of the Raman lines. Exceptionally broad lines are indicated by the letter *b*. The assignment of the lines is given in the fourth column, the incident mercury lines being designated by the letters used by Kohlrausch[1] and other authors; namely, *d* 20336, *e* 22938, *f* 22995, *g* 23039, *h* 24335, *i* 24516, *k* 24705, *l* 25098, *m* 25592, *o* 27293, *p* 27353 and *q* 27388 cm^{-1}. The mercury line 29919 cm^{-1}, not listed by Kohlrausch, is denoted by *r*.

Some of the Raman lines can be assigned in more than one way. In such cases the two or more possible assignments are enclosed together in brackets. The intensities of several of these lines are definitely greater than would be expected if they were due to a single Raman transition. Moreover, in two cases the merging of two or more Raman lines is clearly indicated by a broadening.

In computing the frequency shifts, the values listed above for the wave numbers of the incident mercury lines were used. It will be noticed that for the exciting line *o* the stokesian shifts have values somewhat larger than the average, whereas the one observed antistokesian line ascribed to this incident line gives a shift lower than the average. This irregularity is doubtless due to the fact that the exciting line *o* is really double, 3662.29A and 3663.28A, the long wave-length component being the more intense and sharper of the two.

In the case of the weak Raman lines 59, 61 and 63, no assignment can be made that is supported by the assignment of other lines. It is tentatively assumed, therefore, that these lines are excited by the strong mercury line *e*. These doubtful assignments are enclosed in parentheses.

Of the assignments not designated as doubtful, those of the lines 43 and 46, involving the large frequency shift 3677 cm^{-1}, are the least certain. These two Raman lines have the same separation as the mercury lines *q* and *p*. The line $o-3677$ does not appear, but, since $p-3677$ is very weak, the absence of $o-3677$ may well be due to underexposure. The Raman lines having the

TABLE I. *Raman lines of fluorobenzene.*

Designation	Wave number cm^{-1}	Intensity	Assignment	Designation	Wave number cm^{-1}	Intensity	Assignment
1	29112	(1)	$r-807$	37	24276	(6*b*)	$i-240$, $p-3077$
2	28908	(1)	$r-1011$				
3	28881	(0)	$q+1493$				
4	28397	(0)	$q+1009$	38	24216	(6*b*)	$o-3077$
5	27629	(1)	$q+241$	39	24186	(1)	$k-519$
6	27594	(0)	$p+241$	40	24094	(0)	$k-611$
7	27530	(0)	$o+237$				
8	27149	(4)	$q-239$	41	23902	(10)	$i-614$, $k-803$
9	27113	(3)	$p-240$				
10	27047	(2)	$o-246$				
11	26873	(3)	$q-515$	42	23877	(0)	$k-828$
12	26835	(2)	$p-518$				
13	26776	(3)	$o-517$, $q-612$	43	23711	(2)	$i-805$, $k-994$, $q-3677$
14	26739	(0)	$p-614$	44	23695	(8)	$k-1010$
15	26668	(0)	$o-625$	45	23685	(1)	$i-831$
16	26585	(10)	$q-803$	46	23676	(1)	$p-3677$
17	26559	(0)	$q-829$	47	23549	(4)	$k-1156$
18	26548	(6)	$p-805$	48	23509	(0)	$i-1007$
19	26483	(4)	$o-810$	49	23486	(4)	$k-1219$
20	26391	(1)	$q-997$	50	22699	(4)	$e-239$
21	26381	(10)	$q-1007$	51	22420	(3)	$e-518$
22	26352	(0)	$p-1001$	52	22335s	(2)	$e-603$
23	26345	(8)	$p-1008$	53	22180s	(0)	$f-815$
24	26280	(6)	$o-1013$	54	22132	(4)	$e-806$
25	26231	(4)	$q-1157$	55	21941	(1)	$e-997$
26	26197	(3)	$p-1156$	56	21929	(4)	$e-1009$
27	26166	(3)	$q-1222$	57	21781	(2)	$e-1159$
				58	21721	(2)	$e-1217$
28	26135	(3)	$o-1158$, $p-1218$	59	21675s	(0)	$(e-1265)$
				60	21632	(10*b*)	$k-3073$
29	26072	(1)	$o-1221$	61	21524	(0)	$(e-1414)$
30	26014	(0)	$e+3076$				
31	25790	(3*b*)	$q-1598$	62	21439	(2*b*)	$e-1499$, $g-1598$, $i-3077$
32	25753	(1*b*)	$p-1600$				
33	25696	(0)	$o-1597$				
34	24946	(2)	$k+241$	63	21377	(0)	$(e-1561)$
35	24462	(4)	$k-243$	64	21340	(1)	$e-1598$
36	24313	(10)	$q-3075$	65	19863	(4)	$e-3075$

shift 3677 cm^{-1} and produced by other strong mercury lines would lie in the region of low photographic sensitivity. The frequency 3677 cm^{-1} is undoubtedly a combination frequency, $\leqq 613+3076$ cm^{-1}, similar in origin to the frequency 3680 cm^{-1} found by Grassmann and Weiler[1] for benzene. The line 43 is made up of several Raman bands superposed on each other, as indicated in Table I. One might be tempted to interpret line 46 as $l-1422$ and identify the shift with that of 1414 cm^{-1}, tentatively assumed for line 61. However, the low intensity of the incident line l and the large difference between the frequency shifts speak strongly against this assignment.

The weighted averages of the Raman shifts obtained are listed in the first column of Table II. As in Table I, uncertain shifts are placed in parentheses. The accuracy is indicated in the case of each shift by giving an estimated upper limit for the error. In the second column are listed the photometrically determined intensities. For comparison, the Raman shifts reported by Pai[3] and by Murray and Andrews[4] are given in the third and fourth columns of the table. The intensity values, estimated visually by these authors, are listed in parentheses after the wave numbers.

It will be seen from Table II that with regard to the strongest frequency shifts there is good

TABLE II. *Raman frequencies of fluorobenzene.*

Crawford and Rud Nielsen Raman shift	Intensity	*Pai* Raman shift	*Murray and Andrews* Raman shift
241±2 cm^{-1}	6	243 cm^{-1} (5)	244 cm^{-1} (8)
		424 (1)	
			502 (0)
517±2	3	521 (3)	520 (3)
613±2	2	617 (3)	615 (2)
			(705) (1)
		757 (2)	755 (1)
804±2	11	808 (5)	807 (9)
829±2	0.5		830 (1)
			883 (0)
997±2	4		997 (2)
1009±2	8	1012 (7)	1013 (10)
			(1025) (1)
		1065 (1)	1070 (1*b*)
1157±2	3	1157 (4)	1159 (3)
1220±2	2	1220 (4)	1222 (3)
(1265±10)	0.5	1275 (1)	
			1302 (0)
(1414±10)	—	1413 (1)	
1496±3	1		1498 (1)
(1561±3)	—		
1599±2	1	1600 (5)	1601 (4*b*)
			(1625) (0)
			2615 (1)
			(2917) (1*b*)
			(2986) (1*b*)
			3027 (1)
3076±1	14	3074 (7)	3075 (10)
			3090 (1)
3677±2	—		

agreement between the different observers. Although the agreement is within the experimental error, it may be noted that we find consistently somewhat lower values for the Raman shifts than do Pai and Murray and Andrews. As far as we know, Pai has not yet published a detailed account of his work. Murray and Andrews used a glass spectrograph whereas the present work was done with a quartz instrument. We have observed Raman lines over a wider spectral region and have worked with greater dispersion. On the other hand, it appears that Murray and Andrews obtained more strongly exposed plates, since they observed several weak Raman lines not found by us; yet they report no antistokesian lines.

Lines 59 and 61 are undoubtedly identical with two lines observed by Murray and Andrews. However, our assignment, in both cases indicated as doubtful, differs from theirs. There is little basis for preferring one assignment to the other. It would seem, however, that the large frequency shifts assumed by Murray and Andrews are less probable than the lower values assumed by us. The shift 1414 cm^{-1} agrees with Pai's value 1413 cm^{-1}, and the shift 1265 cm^{-1}, computed from the inaccurately measured line 59, may be identical with Pai's shift 1275 cm^{-1}.

Among the lines observed by Murray and Andrews but not by us, the lines 23,822 cm^{-1} and 22,436 cm^{-1}, both of which are assumed to give shifts not otherwise found, may perhaps be more reasonably assigned as $h-513$ and $g-1603$, respectively.

Line 37 might have been assigned as $k-429$, in which case we should have obtained a frequency shift nearly equal to Pai's value 424 cm^{-1}. The double assignment given in Table I cannot well be in error, however, since 3077 cm^{-1} is excited also by the other members of the 3650A group, and since 241 cm^{-1} is a very intense Raman frequency.

Line 53 might be assigned as $e-758$, thus giving a shift practically equal to the value 757 cm^{-1} reported by Pai. However, the assignment $f-815$ seems more reasonable in view of the great intensity of the 804 cm^{-1} shift. The discrepancy between the values 815 and 804 cm^{-1} is explained by the inaccuracy in the measurement of line 53 which was observed only with the glass instrument. The weak Raman line 23,950 cm^{-1}, reported by Murray and Andrews and interpreted by them as due to a shift of 755 cm^{-1}, was not observed by us.

DISCUSSION

It has been suggested by Mecke[7] that the Raman frequencies 266 cm^{-1}, 317 cm^{-1} and 420 cm^{-1}, represent the "valence vibrations" of iodobenzene, bromobenzene and chlorobenzene, respectively. On the assumption that this is correct, one may compute the frequency of the valence vibration of fluorobenzene approximately by plotting these frequencies against the reduced masses of the molecules, considered as quasi-diatomic, and extrapolating to the reduced mass of fluorobenzene. In this way a value of about 500 cm^{-1} is obtained. Hence, it may be assumed that the Raman frequency 517 cm^{-1} represents the valence vibration of the fluorobenzene molecule. On the other hand, Pai, on the basis of thermochemical data not given in his brief note, suggests

[7] R. Mecke, *Leipziger Vorträge 1931*, p. 45.

that the frequency 1220 cm^{-1} is associated with the carbon-fluorine bond. This is not very likely to be correct, since all of the monohalides of benzene have frequencies in the neighborhood of 1200 cm^{-1}.

From the existing data, it is not yet possible to draw definite conclusions with regard to the structure of benzene and its monohalides. When an assumption is made as to the symmetry of the fluorobenzene molecule, it is possible, by the methods developed by Brester[8] and Placzek,[9] to make certain statements about the normal vibrations of the molecule. If it be assumed, for example, that the fluorobenzene molecule is plane and has the symmetry C_{2v} (i.e., one two-fold symmetry axis and a symmetry plane passing through the axis) there will be 11 normal vibrations that are symmetrical with respect to both symmetry elements. The strongest and most highly polarized Raman lines will belong to this group. In addition, there will be 3 normal vibrations which are symmetrical with respect to a rotation of π about the axis and antisymmetrical with respect to a reflection in the symmetry plane. This group of frequencies is forbidden in the infrared absorption but will occur in the Raman effect as lines with a depolarization of 6/7. Further, there are 6 normal vibrations that are antisymmetrical with respect to a rotation and symmetrical with respect to a reflection and, finally, 10 normal vibrations which are antisymmetrical with respect to both symmetry elements. Both of the last groups give Raman lines with a depolarization of 6/7.

If, on the other hand, the benzene molecule has a three-fold rather than a six-fold symmetry axis, as indicated by the Kekulé formula and by recent work of Weiler,[10] the fluorobenzene molecule would probably have at most just a single symmetry plane. The normal vibrations would then fall into two groups, 21 vibrations which are symmetrical with respect to a reflection in the symmetry plane and 9 that are antisymmetrical with respect to such a reflection. The symmetrical vibrations should, on the whole, be more intense in the Raman spectrum than the antisymmetrical vibrations.

The data on the Raman and infrared spectra of fluorobenzene and the other monohalides of benzene are not yet sufficiently complete to determine which, if either, of these models is the correct one.

[8] C. J. Brester, *Kristallsymmetrie und Reststrahlen*, Utrecht, 1923.

[9] Cf. G. Placzek, *Rayleigh-Streuung und Raman-Effekt*, Marx: Handbuch der Radiologie, 2nd ed., Vol. 6, Part II, Braunschweig, 1934.

[10] J. Weiler, Zeits. f. Physik **89**, 58 (1934).

The Constancy of the Polarization of Non-Polar Molecules

C. P. Smyth and K. B. McAlpine, *Princeton University*

(Received June 28, 1934)

The dielectric constants of the vapors of *n*-hexane and *n*-heptane are measured over a range of temperature and used to show that the molecules of these substances have no detectable dipole moments. The constancy of the polarizations of non-polar vapors in contrast to the slight rise with temperature of the polarizations of the same substances in the liquid state is attributed to the elimination of the intermolecular action which lowers slightly the polarizability of the molecules in the liquid state.

BECAUSE of the general use of hexane and heptane as solvents in dipole moment measurements, it was deemed desirable to check the zero values assigned to their moments from measurements upon the liquids by examination of the vapors. At the same time, it has been possible to obtain further information upon the more general question of the constancy of the polarization of non-polar molecules.

The dielectric constants of the vapors were measured as before.[1] The polarization P at each absolute temperature T was calculated from the

[1] K. B. McAlpine and C. P. Smyth, J. Am. Chem. Soc. **55**, 453 (1933); J. Chem. Phys. **2**, 499 (1934).

dielectric constant ϵ and the molar volume V as $P=[(\epsilon-1)/(\epsilon+2)]V$. The extrapolation to zero pressure to eliminate the error in V caused by deviation of the vapor from ideal behavior was less satisfactory than usual because of the magnitude of the deviation due to the large size of the molecules. Consequently, in the case of heptane, the extrapolated values, P_0, are given only to one decimal place. For hexane, the values are more accurate and are taken from the polarization-pressure curve at 760 mm also, these being recorded as P_{760}. P_{760} contains, of course, the error caused by use of the ideal gas law to calculate V.

Purification of Materials

n-Hexane

A sample of a high degree of purity was lent by Dr. A. L. Henne and Dr. A. F. Shepard of the Midgley Foundation of the Ohio State University, to whom the writers wish to express their gratitude.

n-Heptane

Material from the Ethyl Gasoline Corporation was shaken with successive portions of concentrated sulfuric acid until the acid ceased to develop color. After removal of the acid layer, the heptane was washed with water, with potassium hydroxide solution and again with water. It was then shaken with mercury, filtered, dried over calcium chloride and distilled from sodium; b.p. 98.3°; n_D^{20}, 1.38763.

Experimental Results

The experimental results are given in Table I.

Table I. *Polarization values.*

n-Hexane			*n*-Heptane	
T, °K	P_{760}	P_0	T, °K	P_0
337.7	31.55	30.10	348.2	34.7
388.3	30.80	30.08	357.4	34.7
428.2	30.39	30.02	396.8	35.1
484.3	30.13	29.94	460.9	35.0
558.4	(29.40)	(29.40)	501.3	34.9

Discussion of Results

The polarization values for hexane show how the effect of deviation from ideal behavior diminishes with rising temperature, the difference between P_{760} and P_0 becoming small. The apparent small decrease in P_0 with rising temperature becomes greater as the temperature is higher, while, as the function of the reciprocal of the absolute temperature given by the Debye equation, it should become smaller if the molecule possesses a dipole moment. Although the thermal decomposition of hexane at these temperatures should be negligibly small,[2] it seems probable that the large surface of the gold-palladium alloy of the cell in which the vapor is measured causes a slight decomposition into smaller molecules of lower polarization, the increased decomposition with rising temperature being so pronounced at 558.4° that the polarization value is enclosed in parentheses. It is probable, therefore, that the true polarization is approximately constant at 30.1. This is in contrast to the small linear rise with temperature shown by hexane and other hydrocarbons in the liquid state.[3,4] Liquid *n*-hexane at 323°K has a polarization 29.92 and its polarization-temperature curve extrapolated to about 370°K would give a polarization equal to that of the vapor. It may be remarked here that the tendency previously observed in several cases for the points to fall below the slowly ascending straight line of the polarization-temperature curve when temperatures not far below the boiling point are reached may be attributed to the separation of gas which is in solution at low temperatures and to the consequent formation of bubbles between the condenser plates.

The variation with temperature of the polarization of heptane is no greater than the possible error in the values and shows no definite trend. The mean 34.9 would seem to be approximately correct. At room temperature the polarization of the liquid is 34.5 and extrapolation of its polarization-temperature curve gives 34.9 at about 410°K. For both hexane and heptane, the absence of any decrease in polarization with rising temperature, other than that presumably arising from slight decomposition, points to zero moment for both molecules in conformity with

[2] F. E. Frey and H. J. Hepp, Ind. and Eng. Chem. **25**, 441 (1933).
[3] C. P. Smyth and W. N. Stoops, J. Am. Chem. Soc. **50**, 1883 (1928).
[4] R. W. Dornte and C. P. Smyth, J. Am. Chem. Soc. **52**, 3546 (1930).

previous results on the substances in the liquid state and with the zero values found for gaseous methane,[5] ethane[6] and propane.[1]

In the liquid paraffins[3, 4] and in liquid carbon tetrachloride and carbon bisulfide, investigated recently in this laboratory by Professor A. E. Stearn, the polarization is an approximately linear function of temperature, increasing about 1 percent for each 100° rise in temperature. The measurements on the vapors cannot be as accurate as those on the liquids but the experimental errors in the vapor values are not so large as to obscure a tendency toward a 1 percent per 100° rise in the polarizations of the seven non-polar hydrocarbon vapors which have been accurately measured. Over temperature ranges of 150° to 260° the maximum difference between the lowest and the highest polarization value of each substance investigated was not more than 1.2 percent with the exception of the early values for ethane, which showed a difference of 1.7 percent. A variation like that in the liquid would give an increase of about 1.5 to 2.6 percent in the vapor over these temperature ranges, a change which would make itself readily apparent in the measurements. In liquid carbon bisulfide, the polarization increases from 20.96 at 203°K to 21.20 at 303°K, while Zahn[7] reported a mean value 22.36 for the vapor, the maximum difference between three values from 325.1° to 489.2°K being 0.4 percent.

It was suggested in earlier work[3] that the force fields of adjacent molecules in the liquid might slightly reduce the ease of displacement of the electrons in the molecules and hence the polarization, while, as the molecular separation and motion increased with rising temperature, the effect of the force fields would decrease and the polarization increase. As an argument against this hypothesis, it was pointed out later[4] that, in binary mixtures of heptane with substances having strongly polar molecules, the refractions of the components were practically independent of the composition of the mixtures,[8] although the internal field must have varied considerably with the concentration of the dipoles in the liquid. In recent work upon the effect of solvent upon the moment of ethylene chloride in solution,[9] it was found that the solvent raised the moment of the ethylene chloride molecule above that found for the vapor but that chloroform, which has a moment 1.05×10^{-18}, did not raise the moment more than did non-polar solvents. It was suggested, therefore, that the effect of the solvent was due to the electric field associated with the outer part of the molecule and falling off inversely as a high power of the distance. If the lowering of the polarizability of a molecule in the liquid is due to this field, it might well vary with concentration by an undetectable amount. It is possible, therefore, that the polarization of a liquid may be slightly lowered by these molecular force fields, the effect of which diminishes with rising temperature and disappears when the molecules are separated by vaporization of the liquid, leaving the very slightly higher and constant polarization observed for the vapor. Actually, it is only the condition of the molecule in the vapor state to which the Lorentz-Lorenz and the Debye equations should apply.

[5] R. Sänger, Phys. Zeits. **27**, 556 (1926).
[6] C. P. Smyth and C. T. Zahn, J. Am. Chem. Soc. **47**, 2501 (1925).
[7] C. T. Zahn, Phys. Rev. **35**, 848 (1930).
[8] C. P. Smyth, E. W. Engel and E. B. Wilson, Jr., J. Am. Chem. Soc. **51**, 1736 (1929).
[9] A. E. Stearn and C. P. Smyth, J. Am. Chem. Soc. **56** (1934).

On the Structure of Monolayers of Myristic Acid

N. W. H. ADDINK,* *Laboratory of Colloid Science, Cambridge, England*

(Received June 5, 1934)

IT IS well known that on compression of a monolayer of myristic acid on water or on dilute acid solutions there are breaks in the force-area (F, A) curve. More recently similar changes of gradient have been observed in the phase boundary potential-area ($\Delta V, A$) curve. N. K. Adam has termed that portion of the curve lying between the vaporous and liquid condensed state the liquid expanded, the nature and structure of which has been a matter of some discussion.

On compression of a vaporous film at *ca.* 860A² per molecule the commencement of the new phase, the liquid expanded, is observed and on continued compression at a constant F the two phases are present together until an area of *ca.* 50A² at 18°C is reached. We would naturally expect a compression of the liquid expanded phase to commence here and at some point a transition into the liquid condensed to occur. It is found, however, that such a phenomenon is not noted but the F, A curve exhibits marked hysteresis as observed by Langmuir[1] and Adam and Jessop[2] and no portion of constant F is obtained.

The transition point at 20°C into the liquid condensed was obtained at 31A² and 15 dynes/cm by Adam and Jessop.[2] Harkins and Fischer[3] obtained nearly the same value.

On the other hand, Schulman and Rideal[4] by measurement of the phase boundary potential noted a change at 40A² and 220 mv. Fosbinder and Lessig[5] obtained 39A² and 205 mv. On compression to areas less than 40A² Schulman and Rideal[4] observed that a metastable liquid expanded film could be obtained which, on standing, became converted into the more stable condensed film. Adam and Harding[6] on repeating this work found a break in the F, A curve at 31A² but their phase boundary potential measurements showed no break between 30 and 35A². Thus they obtained only what Schulman and Rideal termed the metastable expanded film; these authors attributed the transition observed by Rideal and Schulman to some collapse phenomenon and accordingly cast doubt upon the existence of a uniform condensed film.

A re-examination of both the force-area and surface potential area curve for areas less than 40A² has been undertaken to discover whether a true hysteresis or a collapse phenomenon is involved so as to obtain some information as to the nature of the liquid films.

The apparatus employed consisted essentially of a Langmuir trough of the type described by Adam and Jessop (1° on the torsion head = 0.13 dyne/cm) and a phase boundary potentiometer described by Schulman and Rideal. Several purified specimens of myristic acid were employed and no differences outside the range of experimental error were observed.

In Table I are given the values of the phase boundary potential differences caused by a film of myristic acid placed on a solution of 0.01 N HCl by means of petrol ether. In general five different portions of the film were examined for uniformity.

TABLE I. *Variations of surface potential due to myristic acid at 44A².*

Time in minutes	Observed potentials over surface					Mean
0	189	186	187	187	186	187
8	184	183	181	181	182	182
15	178	177	178	178	180	178
35	174	173	175	175	177	175
60	175	173	175	175	177	175

This fall of potential with time is not due to a leak since the value obtained after some 30 minutes could be maintained for several hours. It is clear that myristic acid is appreciably soluble in 0.01 N HCl and that some confusion in the time hysteresis is due to lack of appreciation of this point, first emphasised by Fahir[7] who,

* Ramsay Research Fellow.

[1] Langmuir, J. Am. Chem. Soc. **39**, 848 (1917).
[2] Adam and Jessop, Proc. Roy. Soc. **A112**, 362 (1926).
[3] Harkins and Fischer, J. Chem. Phys. **1**, 852 (1933).
[4] Schulman and Rideal, Proc. Roy. Soc. **A130**, 259 (1930).
[5] Fosbinder and Lessig, J. Frank. Inst. **25**, 425 (1933).
[6] Adam and Harding, Proc. Roy. Soc. **A138**, 411 (1932).
[7] Cf. Marcelin, Ann. de physique **104**, 459 (1925).

however, attributed all changes in force-area to solubility and neglected the change in phase. After carefully sweeping the film off the surface the potential of the cleaned surface is found to fall 14 mv gradually in the course of two hours, indicating a return of dissolved acid to the clean surface; blank experiments revealed no such change. This effect due to bulk solubility can be partly eliminated by spreading a succession of films on the surface or by saturating the bulk phase with crystals of myristic acid. Small changes, however, do occur under these conditions since the solubility of myristic acid in the form of crystals is different from that as a film and this indeed varies with the state and compression of the film. The solubility of myristic acid in the form of crystals exceeds that of a film in the expanded state and will cause the surface potential to rise in three hours from 174 mv to 206 mv.

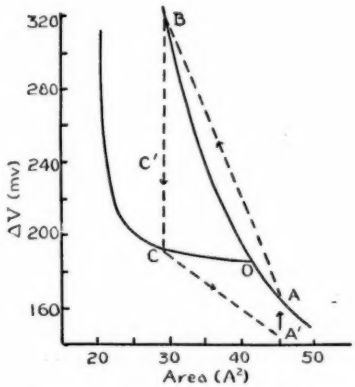

FIG. 1. Surface potential curve of myristic acid. Temp. 20°C. Transition point, 41A², 205 mv.

In Fig. 1 is shown the plot of a ΔV- area curve for myristic acid on 0.01 N HCl saturated with myristic acid in equilibrium with a film in the liquid expanded state at 45A².

The film is put on at $A = 45A^2$, $\Delta V = 187 \pm 1$ mv in the liquid expanded state and it is found that the film can be compressed to 42A² ($\Delta V = 200 \pm 1$ mv) or expanded to 48A² ($\Delta V = 175 \pm 1$ mv) and can be reversibly restored to 45A² without any change in phase boundary potential. If we now compress to areas less than 41A² (*O*), e.g., to *B* at 28A² we obtain a high value for the phase boundary potential of 340 mv which falls in the course of four hours to a value *C* of 210±1 mv for a homogeneous film. Similar results are obtained over the whole region of area 23A² to 33A². There is thus a stable homogeneous film over this region. On expansion to 45A² from *C*, however, the potential does not return to *A* but to a point *A'* some 20 mv below *A*; the potential shows a tendency to rise till it remains constant at 15 mv below *A*. Clearly for the metastable expanded film at *B* the solubility of myristic acid is greater than for the liquid condensed or stable expanded film, and during compression to *B* and the four hours waiting until *C* is attained some myristic acid goes into solution. This effect can be diminished by employing 0.1 N HCl in lieu of 0.01 N HCl. After compression to 28A² the same value, *viz.*, 340 mv, was obtained; the potential, however, did not fall to 210 mv but only to *C'* at 260 mv even after prolonged waiting (six hours) and after expansion to 45A² the value of the potential was only 3 to 4 mv less than the original value of *A* (175 mv) instead of the 15 mv on 0.01 N HCl.

If the solution were previously saturated with crystals of myristic acid a film on compression to *B* only falls to 270 mv and on expansion to 45A² instead of the potential being 3–4 mv less than *A* it is some 11 mv higher because molecules of myristic acid have entered the film from the solution, which is supersaturated in respect to a film although saturated in respect to the crystals.

It is clear that over the region 23A² to 33A² two states of film can exist; a metastable liquid expanded film *OB* and a stable homogeneous film. It is almost impossible to obtain an accurate value for the ΔV-area curve for the stable homogeneous film because on account of the difference in bulk solubilities of the films in various states and stages of compression the exact number of molecules in the film is unknown. It is clear, however, that the stable film must possess a surface potential area curve lying between *OC'* and *OC*.

If the film is compressed within the region 41A² to 38A² a similar metastable film is obtained which falls back to stable potentials along the curve *OC* but the film is not uniform in this region; thus, at 38A² the fluctuations amount to ±6 mv even after prolonged periods of time. In this case also *A'* is found to be slightly lower than *A* except on myristic acid saturated solutions.

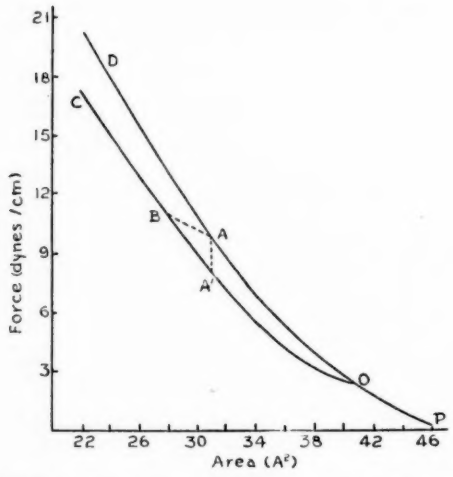

FIG. 2. Force-area curve of myristic acid. Temp. 20°C. Dotted line corresponds with Adam's curves.

In Fig. 2 are shown the force-area curves for myristic acid on 0.01 N HCl.

It will be seen that both the metastable expanded curve *OAD* and the stable curve *POBC* are obtained with the commencement of the curve *OBC* at *O* at 41A². The curve *POABC* is one of the type actually obtained by Adam and Jessop[8] since at higher compressions the change from the metastable to the stable film occurs fortuitously (in this case at 31A²) and the portion *OB* is not noted so readily. The forces obtained, however, are not as high as obtained by these investigators.[3]

If we compare the times necessary to obtain stable films as determined by the changes in force or change in phase boundary potential we observe the very interesting fact that no further change takes place in the force after *ca.* 25–30 minutes whilst a slow change takes place in the phase boundary potential for several hours.

This difference can be observed in Table II where the results of compressing a film to 22A² are given.

The greater solubility of the film both in the metastable expanded and in the condensed states than in the stable expanded state can be demonstrated by measuring the force as well as the phase boundary potential. On carrying out the cycle *POAA'OP* a lowering of *F* by 0.3 to 0.4 dynes per cm is obtained which, after waiting for half an hour at *P*, rises to almost the original value.

These observations lead us to confirm the reality of the metastable liquid expanded film commencing at 41A² and to conclude that this metastable film, on standing, is converted into a stable film which is homogeneous over the area 23A² to 33A² but inhomogeneous from 41A² to 38A². The conversion from the metastable to the stable form takes time; the process of conversion is partly reflected in a change in *F* (½ hour) but a slower process (4 hours) is only revealed by changes in the phase boundary potential. The view that in the liquid expanded state the tops of the chains cling together and the polar heads are freely moving in the water has been advanced on the basis of several considerations.[9] Cary and Rideal considered that the change from the liquid expanded to the liquid condensed state was due to a decreased hydration of the heads. Langmuir views the change from the liquid expanded to the liquid condensed state as due to the formation of orientated micellar aggregates presumably swimming in a liquid expanded film which grows smaller as compression continues.

These views suggest that one of the important factors in the transition is the squeezing out of water from the lower portions of the chains. It seemed possible to obtain some confirmation of this hypothesis by the adsorption of some dehydrating agent underneath the film. Bungenberg de Jong[10] employed 0.2 percent tannic acid as dehydrating agent for effecting a transition from emulsoids to suspensoids. After a few experiments it was found possible to spread a film of myristic acid on a solution containing 5 g tannic acid (Kahlbaum zur Analyse) in 1000 cc 0.01 N HCl.

TABLE II.

Time in minutes	Phase boundary potential difference in mv	Force in dynes/cm
0	335±10	20.2
5	332±13	19.6
10	332± 9	17.5
25	291± 3	17.2
180	251± 2	17.2

[8] Adam and Jessop, Proc. Roy. Soc. **A112**, 362 (1926).

[9] Langmuir, ref. 1 and J. Chem. Phys. **1**, 756 (1933); Schofield and Rideal, Proc. Roy. Soc. **A110**, 167 (1926); Cary and Rideal, Proc. Roy. Soc. **A109**, 301 (1925); Schulman and Rideal, ref. 4.

[10] Bungenberg de Jong, Rev. trav. chim. **42**, 437 (1923).

It was found that provided the film were not unduly expanded, thus permitting tannic acid to come up to the surface, the surface potentials did not differ from those on aqueous solutions containing no tannic acid. In Table III the changes in surface potential with time are given.

TABLE III. *Behavior of a film of myristic acid on a solution containing 0.5 percent tannic acid in 1 L 0.01 N HCl in water.* Temperature = 20°C. Zero potential = 193 mv.

Area A^2	Time (min.)	Observed ΔV values (mv)					Mean	Conditions of film
$43\frac{1}{2}$		190	190	193	192	192	192	homogeneous
28	0	301	283	304	309	305	300	heterogeneous
28	10	296	276	291	294	290	289	heterogeneous
28	20	293	274	285	289	281	284	heterogeneous
28	34	286	261	285	285	282	280	heterogeneous
28	65	259	252	222	243	259	247	heterogeneous
28	80	251	243	218	237	245	239	heterogeneous
28	90	230	227	222	227	228	227	heterogeneous
28	120	226	223	222	224	225	224	homogeneous
28	130	217	214	213	215	216	215	homogeneous
28	160	216	215	215	216	214	215	homogeneous
$43\frac{1}{2}$	0	148	147	146	154	155	150	
$43\frac{1}{2}$	5	160	160	157	157	164	160	
$43\frac{1}{2}$	10	161	154	161	159	166	160	
$43\frac{1}{2}$	20	168	165	169	168	168	168	

It will be noted that the equilibrium is attained in some two hours when tannic acid is present, instead of four to six hours in its absence.

As Langmuir has pointed out the change from the liquid expanded to the liquid condensed state may be regarded as, in effect, a change from molecules attached to one another by their chains with water separating their carboxyl heads to micellar aggregates in which the molecules are parallel to one another, these micelles floating about in a film of the liquid expanded state. If this be the case the stable film over an area of $41A^2$ to $22A^2$ should be inhomogeneous containing both micelles and residual expanded film. In point of fact the stable film has been found to be inhomogeneous from $41A^2$ to $37A^2$ but between $33A^2$ and $25A^2$ it appears to be homogeneous presumably because the micellar distribution is now so great that the travelling electrode cannot pick out the inhomogeneities. The changes observed in both ΔV and F with time are clearly associated with the formation of the micelle and, as we note, this operation takes place in two stages; one a fairly rapid one which affects both F and ΔV and a second one which scarcely affects F but is indicated by a slow change in ΔV.

If we regard the molecules in the liquid expanded state as being hydrated both in respect to their heads and at least the lower portion of the chains, the first operation on compression consists in squeezing out the excess water from between the chains. If we regard the two-dimensional pressure as due to the factors, the kinetic agitation of the solvated heads of the portions of the chains which are hydrated and the cohesion of the ends of the chains, then

$$F = \sigma_{COOH} - \sigma_{chain}$$

$$F = \sigma_{COOH} + \sigma_{(chain)\ interface} - \sigma_{chain\ (oil)}.$$

During the process of squeezing out the water, the contribution due to σ interface becomes smaller and that due to σ chain rises and consequently F falls. The much slower process which is revealed by the gradual change in the phase boundary potential is in all probability due to two operations which proceed relatively slowly. The compressed film from which the interchain water has been squeezed out consists initially of a two-dimensional liquid, i.e., the chains are more or less in random distribution although the polar groups of all the chains are in the substrate; during the process of conversion into the micelle and eventually the liquid condensed film, the originally irregularly orientated molecules orientate themselves parallel to one another, a process akin to the formation of a liquid crystal from a true liquid. The evidence that the molecules are orientated parallel in the liquid condensed state rests chiefly on the observations that in those films which form two-dimensional solids the conversion from the liquid condensed state to the solid is sharp; both the optical as well as the physical properties of the solid films suggest that they are two-dimensionally crystalline.

This process of molecular orientation in the film proceeds slowly; possibly in addition more water is exuded from between the head groups which affects the dielectric constant and the phase boundary potential of the film.

I wish to thank Professor E. K. Rideal for suggesting this investigation and to express my indebtedness to the Ramsay Memorial Fellowship Trust for financial assistance.

The Velocities of Adsorption of Hydrogen and Deuterium on Hydrogenation Catalysts

JAMES PACE[1] AND HUGH S. TAYLOR, *Frick Chemical Laboratory, Princeton University*

(Received July 6, 1934)

The velocities of adsorption of hydrogen and deuterium have been measured on the hydrogenating oxide catalysts, chromium oxide and zinc-oxide-chromium oxide and on a supported nickel catalyst. The velocities of adsorption of the two gases are identical, within the experimental error, over a range of temperature on each surface. The fundamental importance of these observations in the theory of activated adsorption and in chemical kinetics generally is emphasized.

WE have performed a series of experiments on the velocities of adsorption of hydrogen and deuterium on catalytically active surfaces which are of fundamental importance in the general field of reaction kinetics and in the more specialized field of activated adsorption. The availability of pure deuterium gas permits an extended examination of the collisional concepts of reaction velocity both in homogeneous and heterogeneous gas reactions, since the substitution of deuterium for hydrogen permits one to vary the collision velocity by the square root of 2 and, at the same time, to examine into the nature of the activation energy required owing to the known differences in zero-point energy of the two isotopes.

In the field of heterogeneous kinetics the simplest system to be studied is that of a surface taking up, by activated adsorption, one or other of the isotopes. In such kinetic systems, the complications induced by other reactant gases are absent. Concerning such measurable processes of adsorption there still remains some diversity of opinion and, also, obscurities of interpretation. It has already been pointed out[2] that the kinetic theory expression

$$\tfrac{1}{4}(N/v)\bar{w}e^{-E/RT}$$

for the number of molecules striking unit area of surface per second with an activation energy, E, gives a rate of adsorption which is several orders greater than that which is observed, for example, with a zinc oxide surface and hydrogen. This result indicates that the collision frequency is playing a subordinate rôle in the process. By using hydrogen and deuterium on a given surface, an additional check on this conclusion can be obtained, owing to the variation in the value of $\bar{w}$, the root-mean-square velocity, and in the value of E should zero-point energy differences of the two gases be involved. If the slow process be regarded as a diffusion process obeying, for example, the equation of Ward,[3]

$$s = 2ac_0(Dt/\pi)^{\frac{1}{2}},$$

where s is the amount of gas taken up in time t, a is the surface area, c_0 the surface concentration of gas and D the diffusion coefficient, there should be a difference in the velocities of diffusion of hydrogen and deuterium in the ratio $(2)^{\frac{1}{2}} : 1$.

If the rate-determining process is a slow velocity of migration of adsorbed hydrogen or deuterium from a center at which rapid activated adsorption occurs, there should also be differences in the observed velocities with which hydrogen and deuterium are taken up by the surface, because of the zero-point energy differences of the metal-isotope complexes which must be broken down in the process of activated diffusion or "hopping." Our experiments with hydrogen and deuterium reveal no velocity differences at all over a range of temperatures with the surfaces (*a*) chromium oxide, (*b*) zinc oxide-chromium oxide, (*c*) supported nickel.

Experimental Procedure

We have employed the constant volume technique described by Taylor and Williamson[4] for measuring the rate of adsorption of the two gases on the surfaces, at temperatures of 110°, 132° and 184°C, using suitable vapor baths for temperature control.

[1] Commonwealth Fund Fellow, Princeton University, 1932–34.

[2] Taylor, Trans. Faraday Soc. **28**, 137 (1932).

[3] Ward, Proc. Roy. Soc. **A133**, 522 (1931).

[4] Taylor and Williamson, J. Am. Chem. Soc. **53**, 2168 (1931).

Gases

The hydrogen employed was electrolytic gas from cylinders, purified by passage over heated platinized asbestos and dried over calcium chloride and phosphorus pentoxide. The deuterium was prepared by electrolysis of our purest D_2O, of density $D_{25}^{25}=1.1079$, made alkaline by interaction with sodium metal. It was purified by passage over heated platinized asbestos, through a solid carbon dioxide-ether trap and in certain experiments through a heated palladium tube. Helium for dead-space measurements was purified by passage over hot copper and through a charcoal-liquid air trap.

Adsorbents

The chromium oxide was prepared by the method of Lazier and Vaughen[5] from chromium nitrate and ammonium hydroxide. The zinc oxide-chromium oxide was prepared from zinc nitrate and ammonium chromate by the method described by Taylor and Strother.[6] These substances were ignited in hydrogen, evacuated and treated in adsorption runs with hydrogen until reasonably good reproducibility was obtained. The evacuation between each run was conducted for 10–12 hours at 375°C for chromium oxide and 430°C for zinc oxide-chromium oxide. The nickel catalyst was prepared from nickel oxide supported on kieselguhr, reduced in hydrogen at temperatures rising in 5 hours to 500°C. After a further reduction during one hour the system was closed and evacuated. Between each run the catalyst was evacuated at 420°C.

Experimental Results

With chromium oxide adsorption measurements were carried out in the following order (*a*) H_2 at 110°, (*b*) H_2 at 132°, (*c*) D_2 at 110°, (*d*) D_2 at 132°, (*e*) D_2 at 184°, (*f*) H_2 at 110°, (*g*) H_2 at 184°. In this way, the constancy of the surface characteristics during the experimental study was ensured. With the zinc oxide-chromium oxide the order was (*a*) H_2 at 110°, (*b*) D_2 at 110°, (*c*) D_2 at 184°, (*d*) H_2 at 184°, (*e*) H_2 at 110°. With the nickel experiments, all at 110°C, the order was (*a*) H_2, (*b*) H_2, (*c*) D_2, (*d*) D_2, (*e*) H_2. The

[5] Lazier and Vaughen, J. Am. Chem. Soc. **54**, 3080 (1932).
[6] Taylor and Strother, J. Am. Chem. Soc. **56**, 586 (1934).

TABLE I. *Velocity of adsorption of hydrogen and deuterium on chromium oxide.*

Temp. °C	Gas		*t–v* measurements				
110	$H_2(a)$	$t=$	1.5	15	26.5	44	69
		$v=$	1.07	1.52	1.72	1.97	2.17
110	$D_2(c)$	$t=$	1.5	15	26	46	65
		$v=$	1.06	1.56	1.71	2.01	2.16
110	$H_2(f)$	$t=$	1.5	15	22	50	68
		$v=$	1.05	1.55	1.65	2.05	2.15
132	$H_2(b)$	$t=$	1.5	7	15	26	35
		$v=$	1.03	1.43	1.78	2.13	2.43
	$D_2(d)$	$t=$	1.5	7	15	20	40
		$v=$	0.95	1.45	1.75	1.95	2.50
184	$H_2(g)$	$t=$	3	4	5	8	10
		$v=$	2.38	2.58	3.03	3.98	4.58
	$D_2(e)$	$t=$	2.5	4	5	8	10
		$v=$	1.97	2.58	2.92	3.97	4.52

TABLE II. *Velocity of adsorption of hydrogen and deuterium on zinc oxide-chromium oxide.*

Temp. °C	Gas		*t–v* measurements				
110	$H_2(a)$	$t=$	1.5		14	38	60
		$v=$	2.00		2.55	2.75	2.85
	$D_2(b)$	$t=$	1.5	7	18	36	60
		$v=$	1.95	2.35	2.55	2.70	2.80
	$H_2(f)$	$t=$	1.5		12	36	62
		$v=$	2.00		2.55	2.75	2.90
184	$H_2(e)$	$t=$	1.5	7	16	37	50
		$v=$	2.10	2.65	2.95	3.15	3.25
	$D_2(d)$	$t=$	1.5	7	16	34	48
		$v=$	2.16	2.71	3.04	3.21	3.36

TABLE III. *Velocity of adsorption of hydrogen and deuterium on supported nickel at 110°C.*

Temp. °C	Gas		*t–v* measurements				
110	$H_2(a)$	$t=$	1.5	7	17	47	
		$v=$	7.47	7.65	7.77	7.87	
	$H_2(b)$	$t=$	1.5	11	30	48	60
		$v=$	7.48	7.73	7.83	7.91	7.93
	$D_2(c)$	$t=$	1.5	11	20	48	60
		$v=$	7.54	7.79	7.89	7.99	8.02
	$D_2(d)$	$t=$	1.5	11	24	53	76
		$v=$	7.54	7.83	7.94	8.00	8.05
	$H_2(e)$	$t=$	1.5	8	20	63	
		$v=$	7.55	7.77	7.90	8.02	

velocity data in cc at N.T.P. for the stated time intervals are given in Tables I, II and III. The times are in minutes.

Discussion

Even the present, somewhat restricted series of measurements reveals that, within the limit of experimental error, there is no difference at all in the rates of adsorption of hydrogen and deuterium by the three surfaces and that this is true at several different temperatures. This startling result leads immediately to several important conclusions. Since the difference in zero-point energy between hydrogen and deuterium gas is 1800 calories, the exponential term $e^{-E/RT}$ should, at a mean temperature of 420°K, produce an 8.5-fold difference in velocity between the two processes, were such zero-point energies of the gas molecules involved in the rate-determining process. The zero-point energy of the gas molecules is, therefore, definitely excluded. Apart from this factor, however, the identity of velocities also excludes from the rate-determining process the rate at which the gas molecules strike the surface, since, in such case, a ratio of velocities $r_{H_2} : r_{D_2} = 1.414 : 1$ would be expected. The identity of the measured rates equally well excludes a diffusion process of the type already discussed since in this event a 20 percent difference in rates would be expected. Nor can an activated migration be concerned since zero-point energy differences are also here involved.

We are aware that, in the course of our experiments, there is occurring, to a certain extent, an interchange of the adsorbed deuterium with a source of hydrogen, whether adsorbed hydrogen gas or water vapor, on the catalytic materials we have used. The existence of this reaction in no way alters the conclusion to which the present experiments lead as to comparative velocities of adsorption. In itself, however, this exchange is of fundamental interest especially as regards the technique of preparation of pure deuterium. We hope to report on such exchange reactions shortly.

Since the adsorbent surface is the constituent common to both the hydrogen and the deuterium experiments, the assumption at once suggests itself that the activation energy of the adsorption process is required by the solid adsorbent. An increasing body of evidence is accumulating that the spacing of the surface atoms[7, 8] is an important determining factor in the problem of activation energies accompanying such slow processes of adsorption. One is tempted, therefore, to assign the activation energy to a slow temperature-sensitive process of production of surface atoms thus favorably spaced for adsorption. A theoretical examination of such a possibility, which involves, simultaneously, an analysis of the data on rates of slow adsorption hitherto obtained is being conducted in this laboratory by Dr. M. G. Evans.

The absence of the gas velocity factor in the experimental results at once raised the fundamental problem of the approach to chemical kinetics, in both homogeneous and heterogeneous systems involving gases, from the standpoint of collisions. Recent advances in this field have employed the quantum mechanics in an effort to determine what types of collision are kinetically favorable. This has developed into a formulation of the reaction process in terms of a potential energy surface map of the atoms involved, the activation energy being determined by a potential barrier, representing the energy of an activated *complex* of all the atoms participating, separating the two regions of energy representing the reactants and products of the process. Eyring and Topley are at present engaged in an inquiry as to how far the velocity characteristics of the individual molecular species enter into the determination of reaction speeds of the activated complexes. Their conclusions will be of intense interest in the general field of reaction kinetics. The present experimental research and others in progress in this laboratory, involving both homogeneous and heterogeneous systems, exhibit the advantages accruing to the investigator from the isolation of the hydrogen isotopes and their application in experimental kinetic studies, with a more refined kinetic theory of reactions as the immediate objective.

[7] Sherman and Eyring, J. Am. Chem. Soc. **54**, 2661 (1932).
[8] Eckell, Zeits. f. Elektrochemie **39**, 423, 433, 807, 855 (1933).

The Rate of Adsorption of Ethylene by Silica and Nickel

E. W. R. Steacie and H. V. Stovel, *Physical Chemistry Laboratory, McGill University, Montreal*

(Received May 26, 1934)

The adsorption of ethylene by silica has been investigated from 20 to 300°C. Over this range equilibrium is reached practically instantaneously in all cases. The adsorption of ethylene by reduced nickel has been investigated from −80° to 150°C. Definite slow effects and temperature hysteresis were observed. Since diffusion into the crystal lattice ("solubility") is extremely unlikely in this case, more definite conclusions can be drawn than have been possible in previous investigations.

Introduction

In recent years numerous cases have been observed in which "adsorption" equilibrium is attained only slowly. Such slow effects are usually accompanied by temperature hysteresis, and frequently the adsorption is found to increase with increasing temperature.[1]

To explain these phenomena Taylor suggested "activated" adsorption and assumed that all such slow effects were purely attributable to the surface. Without entering into any discussion of the validity of Taylor's fundamental postulates, objections have been raised to his interpretation of observed cases on the grounds that the behavior could be equally well explained by solubility and grain boundary diffusion.[2, 3]

Any attempt to show unequivocally the existence of activated adsorption is complicated by the fact that when a gas is admitted to a vessel containing a solid several slow processes are possible, *viz.*, activated adsorption, grain-boundary diffusion, solubility and chemical reaction. In many systems the amount of chemical reaction is negligible. In almost all previous investigations in which slow effects occurred, solubility was definitely known to exist.

Solubility of gases in solids is known to be confined to very simple molecules (almost invariably to diatomic molecules). The only cases in which such slow "adsorption" effects had been found involved such molecules. It therefore seemed of interest to investigate the rate of adsorption on a solid of a gas which is sufficiently complicated to make solubility extremely unlikely. We have therefore investigated the rate of adsorption of ethylene by silica and nickel.

Experimental

The usual method for the measurement of adsorption at constant volume was employed. A measured quantity of gas was introduced into a vessel containing the adsorbent. By previous calibration the pressure which would be exerted by this quantity of gas if no adsorption took place was known. The difference between this pressure and the pressure actually observed was a measure of the amount of gas taken up. The apparatus was similar to that previously described by Pease.[4]

The adsorbents were contained in Pyrex bulbs having a capacity of about 10 cc in the case of silica and about 40 cc with nickel. All parts of the apparatus containing gas, except the adsorption vessel and connecting tubing, were immersed in a thermostat. For runs between −80°C and −30°C the adsorption bulb was placed in a Dewar flask containing solid carbon dioxide and acetone. For runs at 0°C a Dewar flask containing ice and water was used. For 20°C and 50°C a water thermostat was employed. For higher temperatures an electric furnace was used, the bulb being packed in with iron filings to ensure uniformity of temperature. In all cases the temperature could be maintained constant to within ±0.5°C or better. Temperatures were measured with standard alcohol or mercury thermometers or by means of a chromel-alumel thermocouple, the choice depending on the temperature.

Nitrogen was employed for calibrating the apparatus, as is customary. There were indications of a small adsorption of nitrogen under

[1] See Taylor, J. Am. Chem. Soc. **53**, 578 (1931), and various papers in Faraday Society Symposium on Adsorption, 1932, etc.

[2] Steacie, J. Phys. Chem. **35**, 2112 (1931); Trans. Faraday Soc. **28**, 617 (1932).

[3] Ward, Proc. Roy. Soc. (London) **A133**, 506 (1931); Trans. Faraday Soc. **28**, 399 (1932).

[4] Pease, J. Am. Chem. Soc. **45**, 1197 (1923).

certain conditions. By making calibrations at various temperatures and pressures, however, it was possible to eliminate most of the effect. In any case an error due to the adsorption of nitrogen would affect only the absolute magnitude of the adsorption, and would have no effect on that portion of the adsorption which occurs slowly.

The description of the method of preparation of the adsorbents is given in the following section.

Ethylene was obtained in cylinders from the Ohio Chemical and Manufacturing Co. It was stated to be 99.5 percent ethylene. By fuming sulphuric acid it was found to be 99.7 percent C_2H_4 and by ignition 99.2 percent.

Nitrogen was obtained from cylinders. It was bubbled through alkaline pyrogallate to remove oxygen and dried with phosphorus pentoxide.

Hydrogen was also obtained from cylinders. Oxygen was removed by passage over hot copper. It was then dried by passage over phosphorus pentoxide.

Between runs the system was thoroughly evacuated by using a mercury vapor condensation pump backed up by a Hyvac oil pump. Pressures during evacuation were followed by means of a McLeod gauge. The evacuation was always carried on for at least 8 hours. After the first two or three hours the pressure was always less then 10^{-3} mm.

As a check on the method blank runs were made with a bulb containing no adsorbent. These indicated a very small slow drop in pressure amounting all told to not more than 0.07 cc at a pressure of 400 mm. This amount is practically negligible compared with the amounts of gas adsorbed. Most of the gas disappearing under these conditions was probably taken up by stopcock grease.

Experimental Results

I. Silica

Runs were first made with a 10 gram sample of ground quartz tubing, passing an 80-mesh sieve. There was no measurable adsorption of ethylene.

A sample of precipitated silica was therefore prepared. To 10 cc of sodium silicate solution (sp. gr. 1.170) were added 100 cc of 10 percent hydrochloric acid at a temperature of 50°C. The precipitate was broken up and washed by decantation with hot distilled water until the wash water gave no milkiness with N/10 Ag NO_3. The precipitate was pressed between filter paper and dried at 100°C. It was then pulverized and ignited for 2 hours at a red heat. A 2-gram sample was used.

In all cases equilibrium was reached practically instantaneously. The data obtained are summarized in Table I.

Table I. *The adsorption of ethylene by silica.*

Temp. °C	Pressure, cm	Adsorption, cc at N.T.P.
23.8	9.81	1.23
23.7	26.70	2.24
23.7	46.27	3.10
23.7	70.84	4.00
51.0	4.96	0.39
51.0	24.52	1.23
51.0	51.27	2.05
51.0	71.15	2.59
100.6	10.55	0.23
100.7	33.25	0.50
100.7	47.30	0.67
100.7	66.84	0.92
185.6	12.35	0.06
185.5	38.47	0.07
185.5	54.30	0.14
185.7	76.85	0.14
296.0	13.63	0.03
296.0	42.41	—
296.1	84.58	—

If the data are plotted we obtain typical adsorption isotherms. As is usually the case a log-log plot gives good straight lines.

The main conclusion to be drawn is that the adsorption of ethylene by silica is entirely of the van der Waals type, with no indication of any slow processes.

II. Nickel

An investigation was made of the adsorption of ethylene by nickel hydrogenation catalysts. The method of preparation was essentially that of Taylor and Burns.[5] Nickel nitrate (Merck) was heated to 400°C for 17 hours in a muffle furnace. The material was transferred to a Pyrex tube 2.5 cm diameter and 10 cm long. The tube was heated to 300°C in an electric furnace and hydrogen was passed through slowly for 15 hours. At the end of this period a calcium

[5] Taylor and Burns, J. Am. Chem. Soc. **43**, 1276 (1921).

chloride tube on the exit side showed no gain in weight in 3 hours. The furnace was then removed, the hydrogen flow stopped and the exit tube immediately sealed off and removed. The bulb was then evacuated to 0.001 mm at 300°C for 24 hours. On standing for 9 hours the pressure increased to only 0.005 mm. Three 30-gram samples of nickel were used.

Nickel I

This was prepared as above. Preliminary runs showed that the catalyst decomposed ethylene rapidly at temperatures above 100°C. At 20°C, in addition to a rapid adsorption there was also a definite slow drop in pressure. The data from a typical run are given in Table II.

It is apparent that about one-half the adsorption occurs immediately, the remainder being taken up very slowly. The same behavior was noted in other runs.

Nickel II

This series of runs was made on the previous sample of nickel after it had been heated to 520°C for about 1 hour. This treatment resulted in a general diminution in the activity.

Runs were made at −80, −30, 0, 20, and 50°C. At the lower temperatures equilibrium was reached practically instantaneously. At temperatures above 0°C, the initial rapid drop in pressure was followed by a slow decrease.

Runs at low temperatures. The data for −80, −30, and 0°C are given in Table III. Values marked *D* were obtained by withdrawing a definite part of the gas.

Runs at higher temperatures. Runs at 0°C showed traces of a slow effect, while at 20°C and 50°C the effect was marked. The complete data for a typical run at each temperature are given in Table IV.

It is apparent from Table IV that the rapid adsorption falls off with increasing temperature in the usual way. The slow effect, however, increases decidedly as the temperature rises. Thus at 50°C, the slow effect at the end of 9 hours amounts to 50 percent of the total adsorption. This is in accord with the usual behavior of systems which show slow adsorption effects.

Hysteresis effects were also noticeable. Thus a run was made at 50°C. The initial rapid adsorption was 0.64 cc. The adsorption in the next 10 hours was 0.59 cc, giving a total of 1.23 cc. The adsorption bulb was then cooled to 0°C and a total adsorption of 2.17 cc was found. The normal value from a run at 0°C would have been 1.78 cc, at the corresponding pressure. There is thus a hysteresis effect leading to an excess

TABLE II.

Time min.	Pressure, cm	Adsorption, cc at N.T.P.
1	19.66	1.73
3	19.38	1.95
10	19.08	2.18
32	18.64	2.52
59	18.35	2.75
155	17.84	3.14
186	17.73	3.24
240	17.58	3.35
365	17.32	3.55
569	17.04	3.76
651	16.95	3.84
736	16.87	3.90

TABLE III. *Nickel II. Runs at low temperatures.*

Pressure, cm	Adsorption cc at N.T.P.	Pressure, cm	Adsorption cc at N.T.P.	Pressure, cm	Adsorption, cc at N.T.P.
Temperature, −85.1°C		*Temperature, −30°C*		*Temperature, 0°C*	
6.19	4.72	2.00	0.81	0.49	0.41
15.60	5.09	9.02	1.67	9.76	0.93
18.51	5.12	20.25	2.73	21.73	1.33
25.80	5.22 *D*	26.10	2.62	22.24	1.52 *D*
35.67	5.09	51.29	3.02	35.33	1.60
40.78	5.23 *D*	54.46	3.11 *D*	41.46	1.92 *D*
53.11	5.40 *D*	71.83	3.18	59.11	2.05
54.07	5.32				
71.22	5.71				

TABLE IV. *Nickel II. Rate of adsorption.*

Time min.	Adsorp. cc at N.T.P.	Time min.	Adsorp. cc at N.T.P.	Time min.	Adsorp. at cc N.T.P.
Initial pressure cm (calc.) 23.33 Temperature, 0°C		*Initial pressure cm (calc.) 19.25 Temperature, 20°C*		*Initial pressure cm (calc.) 11.52 Temperature, 50°C*	
3	1.33	2	0.81	2	0.44
7	1.37	5	0.85	6	0.50
33	1.41	18	0.89	15	0.54
62	1.44	36	0.95	50	0.64
124	1.46	108	1.01	75	0.67
218	1.51	190	1.04	190	0.76
380	1.54	255	1.08	343	0.82
514	1.55	475	1.12	532	0.88
580	1.56	660	1.16	677	0.90

adsorption of 0.39 cc. There was no sign of desorption of this excess amount over a period of 2 hours.

Nickel III

Nickel III was a new sample prepared in the same way as nickel I. The time required for complete reduction was considerably greater and amounted to $4\frac{1}{2}$ days. It was then evacuated for 24 hours.

Runs were made at −80°, 0°, 20.8°, 50°, 142°, and 250°C. At 250°C there was a rapid increase in pressure due to decomposition of ethylene. At all temperatures slow adsorption effects were noticeable, although the effect was small at −80°C. The results were in general very similar to those obtained with nickel II although the sample was more active. Some typical adsorption-time curves are given in Fig. 1.

Hysteresis effects were very pronounced. Thus in one run at 142°C the total amount adsorbed after 10 hours was 7.83 cc. Virtually all of this was the slow type, the ordinary van der Waals adsorption having fallen to a low value at this high temperature. The bulb was then cooled to −80°C. The total adsorption at this temperature was 12.39 cc. The normal adsorption at −80°C would have been 5.5 cc. There is thus an excess adsorption of 6.89 cc, which is of the same order of magnitude as the slow adsorption at 142°C.

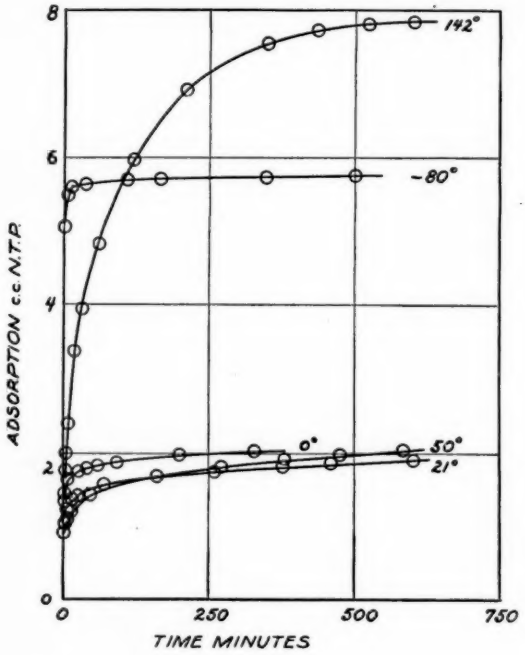

FIG. 1

DISCUSSION

It is apparent that the ethylene-nickel system resembles a number of other systems involving gases and catalytically active solids which have been previously investigated. It shows slow adsorption effects, adsorption hysteresis with changing temperature and, in certain temperature ranges, the adsorption increases with increasing temperature.

The ethylene-nickel system therefore shows all the criteria of activated adsorption. In virtually all previously investigated cases of this type solubility has been a likely complication.

In a few cases it is possible that the effects of solubility and adsorption have been successfully disentangled.[6, 7] In our opinion, however, this investigation represents the first case in which the criteria of activated adsorption have been obtained in a system in which solubility is exceedingly unlikely to be a complicating factor.

It is, of course, possible to calculate isosteric heats of activation for the ethylene-nickel system from the data given above, by using the method given by Taylor and Williamson.[8] The method, however, is open to criticism and it is very doubtful if calculations made in this way have any real meaning.

In any discussion of the bearing of activated adsorption on hydrogenation catalysis, it is apparent that it is necessary to take into account the slow adsorption of the substance being hydrogenated as well as that of the hydrogen.

---

[6] Benton and Drake, J. Am. Chem. Soc. **56**, 255 (1934).
[7] Drake and Benton, J. Am. Chem. Soc. **56**, 506 (1934).
[8] Taylor and Williamson, J. Am. Chem. Soc. **53**, 2168 (1931).

The Decomposition of Nitrous Oxide on the Surface of Platinum. I. The Retarding Effect of Oxygen

E. W. R. Steacie and J. W. McCubbin, *Physical Chemistry Laboratory, McGill University, Montreal*

(Received May 26, 1934)

An investigation has been made of the decomposition of nitrous oxide on the surface of spongy platinum in the temperature range 485 to 570°C. The results are in agreement with the previous work of Hinshelwood, Schwab and others using filament catalysts. Experiments have also been made on the effect of added oxygen. It is found that oxygen formed in the reaction has a much larger retarding effect than has added oxygen. Under certain circumstances oxygen and nitrogen also retard the reaction by hindering diffusion to the more remote parts of the catalyst. It is concluded that oxygen formed in the reaction is adsorbed in the atomic condition, while added oxygen is mainly adsorbed in the form of molecules.

Introduction

ONE important phase of heterogeneous catalysis is the retardation of a reaction by its products. In general, preferential adsorption of the reaction products seems to offer a satisfactory explanation. In almost all cases, however, the retarding effect of the products has been inferred from the form of the differential equation expressing the rate of reaction and very few experiments have been performed in which the product to which the retarding effect is ascribed has been added in varying amounts and under various conditions.

One of the most thoroughly investigated reactions in this connection is the decomposition of nitrous oxide on platinum. The reaction is retarded by oxygen, but there is considerable disagreement about its action. Hinshelwood and Prichard[1] found that the rate was given by

$$-d/dt(N_2O) = K(N_2O)/(1+b(O_2)).$$

Their experiments were made with electrically heated filament catalysts at temperatures between 600° and 1200°C. They found that added oxygen had the same retarding effect as oxygen formed during the reaction. Schwab and Eberle[2] investigated the reaction in a similar way. They came to the conclusion, however, that added oxygen had no retarding effect on the reaction. Low pressure measurements have also been made by Cassel and Glückauf[3] and by van Praagh and Topley.[4]

[1] Hinshelwood and Prichard, J. Chem. Soc. **127**, 327 (1925).
[2] Schwab and Eberle, Zeits. f. physik. Chemie **B19**, 102 (1932).
[3] Cassel and Glückauf, Zeits. f. physik. Chemie **B9**, 427 (1930).
[4] van Praagh and Topley, Trans. Faraday Soc. **27**, 312 (1931).

In view of the above discrepancies it seemed worth while investigating the retarding effect of oxygen in a more thorough manner. Instead of filament catalysts we have used platinum sponge.

Experimental

Reaction velocities were followed in the usual way by observing the rate of pressure change in a system at constant volume. The reaction vessel was of fused silica and had a capacity of about 125 cc. The apparatus was similar to one which has been used in a number of previous investigations.[5] The required temperatures were obtained by means of an electric furnace, which could be maintained constant to within 0.5°C. Before each run the system was evacuated to about 10^{-4} mm by means of a mercury vapor pump.

The catalyst was platinum sponge prepared by the ignition of ammonium chloroplatinate. Approximately 5 grams of catalyst were used in each series of runs. Nitrous oxide was obtained in cylinders from the Ohio Chemical and Manufacturing Co. It was dried over phosphorus pentoxide. Oxygen was also obtained from cylinders and was dried in the same way. It contained 4.5 percent nitrogen.

Experimental Results

The temperature range used was from 450 to 570°C. Even at the highest of these temperatures the homogeneous reaction is far too slow to introduce any complication. Since the reaction has been shown to be homogeneous in quartz vessels, it follows that the vessel walls have no effect in this case.

[5] Steacie, Can. J. Research **6**, 265 (1932).

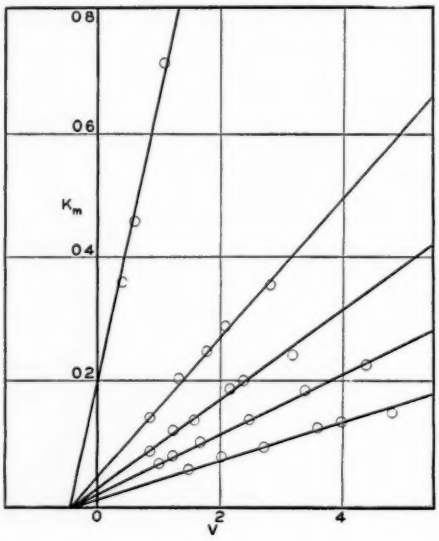

FIG. 1. $1/t \ln a/(a-x)$ *vs.* x/t.

I. The decomposition in the absence of added oxygen

The results obtained were in excellent agreement with the equation previously given by Hinshelwood and Prichard. This is shown by Fig. 1, in which $1/t \ln a/(a-x)$ is plotted against x/t. Good straight lines are obtained. The reaction is evidently retarded by the oxygen formed in the manner suggested by previous workers, in spite of the fact that previous investigations were made at high temperatures on filaments, while this work was done at comparatively low temperatures on spongy platinum.

The experimental results were quite definitely reproducible, there being no noticeable aging effects. It was also found that the vacuum treatment between runs was comparatively unimportant. Thus evacuating between runs to 1 or 2 mm pressure gave the same result as a prolonged evacuation to 10^{-4} mm. This is rather surprising in view of the fact that the reaction is retarded by the products. It was also found that it was almost immaterial whether the evacuation was carried out at the temperature of the experiments (say 532°C) or at 800°C.

A number of runs were made at various temperatures and with three different catalysts to determine the effect of the nitrous oxide concentration on the rate. The equation previously given was found to fit the results excellently for any individual run. The data are summarized in Table I.

TABLE I.

Temp. °C	Initial pressure, cm	T_{50} mins.	Temp. °C	Initial pressure, cm	T_{50}, mins.
		Catalyst No. 1.			
529.5	2.15	0.94	485.0	7.80	(38.9)
529.5	8.10	5.4	485.0	12.85	29.0
529.5	12.90	8.3	485.0	13.45	49.0
529.5	20.00	9.6	485.0	16.30	67.4
529.5	29.90	15.7	485.0	18.30	>75.0
485.0	4.15	17.5			
		Catalyst No. 2.			
532.5	5.35	1.8	532.5	15.45	4.0
532.5	5.50	1.9	532.5	19.15	4.1
532.5	6.30	2.1	491.0	10.00	24.2
532.5	11.25	2.5	491.0	11.10	24.4
532.5	12.20	3.5	491.0	30.40	>60.0
532.5	13.70	3.0	491.0	31.50	>60.0
532.5	15.00	5.5			
		Catalyst No. 3.			
570.0	5.50	0.85	570.0	19.40	2.0
570.0	6.20	1.6	570.0	20.85	2.7
570.0	6.80	1.1	570.0	24.00	2.4
570.0	7.15	1.2	570.0	29.35	3.1
570.0	11.15	1.9	570.0	36.00	3.5
570.0	11.40	1.6	570.0	40.00	4.0
570.0	11.60	1.5	570.0	48.40	5.5
570.0	14.45	1.7			

If we integrate the rate equation given previously, and solve for T_{50}, we obtain

$$T_{50} = 0.69/k + 0.19ba/k,$$

where a is the initial concentration of nitrous oxide. Hence, if the equation fits the data over the concentration range, we should obtain a straight line by plotting T_{50} against a, from the slope and intercept of which we can evaluate both b and k for any temperature or catalyst. Fig. 2 shows a typical T_{50} a plot. The values of K and b obtained from curves of this type are given in Table II.

TABLE II.

Catalyst No.	Temp. °C	K	b
1	529.5	0.460	1.125
1	485.0	0.099	0.912
2	532.5	0.812	0.812
2	491.0	0.066	0.800
3	570.0	1.38	0.635

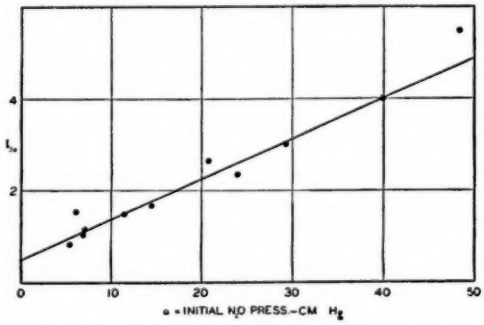

FIG. 2. Variation of T_{50} with initial pressure.

It may therefore be concluded that the rate of decomposition of nitrous oxide in the absence of added gases is satisfactorily given by

$$-(d/dt)(N_2O) = K(N_2O)/(1+b(O_2)).$$

II. The effect of added oxygen

(*a*). *Gases mixed prior to admission to the reaction vessel.* An investigation was made of the effect of added oxygen on the rate of reaction over a wide range of oxygen concentrations. There is found to be a definite diminution in rate in the presence of added oxygen. If the added oxygen has the same effect as the oxygen formed during the reaction, then the equation previously given should hold as before. If we let y be the concentration of added oxygen, and use the other symbols as before, we obtain

$$(1+by+ab)/t \ln a/(a-x) - bx/t = K.$$

Following Hinshelwood and Prichard's procedure and putting $1/t \ln a/(a-x) = K_m$, and $x/t = V$, we have

$$V = (a+y+1/b)K_m - K/b.$$

Hence V should be a linear function of K_m, the intercept being $-K/b$ as before. The slope, however, is now $(a+y+1/b)$ instead of $(a+1/b)$.

It follows that plotting K_m against V we should obtain straight lines as before. This is actually the case, as is shown by Fig. 3, curves 1 and 2. Curve 3 shows the same plot for a run with no added oxygen. All three curves are for runs with a constant initial pressure of nitrous oxide (6 cm). Hence the slopes should vary greatly in virtue of the y term. Actually the slopes are identical within the experimental error, as is also the case in some 30 similar runs. We must therefore conclude that $y=0$ or, in other words,

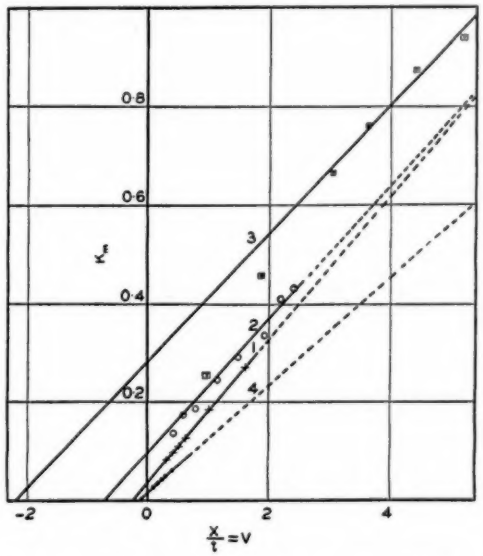

FIG. 3. $K_m - V$ curves: 1 and 2, oxygen mixed with nitrous oxide: 3, no added oxygen: 4, oxygen followed by nitrous oxide.

that the oxygen formed during the reaction exerts its customary effect without interference from the oxygen added. This is confirmed by the fact that the values of b obtained from the slopes of the lines in Fig. 3 are in excellent agreement with the value given in Table II for the same temperature and catalyst in the absence of added oxygen. We have therefore adopted this value of b for the calculation of K for these runs. The summarized data for runs of this kind are given in Table III.

The variation of T_{50} with added oxygen for a constant nitrous oxide pressure of 6 cm is shown by Fig. 4. It will be seen that T_{50} is proportional to the amount of oxygen added. It follows that added oxygen must exert an initial blocking effect on the surface which persists throughout, and is independent of the retarding effect of the oxygen formed during the reaction.

(*b*). *Oxygen admitted first.* The results described in this section were obtained by admitting oxygen to the reaction vessel, letting it stand for 5 minutes and then adding N_2O. (It was found that the time of standing in contact with oxygen had no effect within the limits 2 minutes to 12 hours.) The previous equation again fitted the results, the value of b being the same as that for runs in the absence of added oxygen. Hence any retarding effect due to the added oxygen is

TABLE III. *Oxygen-nitrous oxide mixtures. 570.0° C. Catalyst No. 3.*

P_{O_2} cm	T_{50} min.	K	P_{O_2} cm	T_{50} min.	K
Initial nitrous oxide pressure = 6 cm					
0.00	1.56	1.395	20.64	4.24	0.279
5.05	3.08	0.584	28.10	7.00	0.229
12.72	3.47	0.501	44.60	10.00	0.121
20.60	5.82	0.222			
Initial nitrous oxide pressure = 12 cm					
0.00	1.88	1.208	22.60	8.10	0.241
5.30	5.16	0.451	33.35	9.60	0.159
11.17	5.20	0.381	48.38	14.40	0.127
Initial nitrous oxide pressure = 18 cm					
0.00	2.87	1.194	27.88	8.04	0.216
9.30	4.55	0.552	39.25	10.58	0.171
17.05	5.44	0.375			

TABLE IV. *Oxygen followed by nitrous oxide. 570.0° C. Catalyst No. 3.*

P_{O_2} cm	T_{50} min.	K	P_{O_2} cm	T_{50} min.	K
Initial nitrous oxide pressure = 6 cm					
0.00	1.56	1.395	23.95	>60	0.056
11.85	4.51	0.302	49.05	>24 hrs.	0.015
18.30	23.8	0.089			
Initial nitrous oxide pressure = 12 cm					
0.00	1.88	1.208	36.05	20.0	0.121
12.10	6.00	0.235	48.45	>60	0.054
24.25	11.10	0.178			
Initial nitrous oxide pressure = 18 cm					
0.00	2.87	1.194	27.15	12.50	0.248
9.00	4.32	0.635	36.00	17.70	0.102
17.90	6.46	0.318	44.95	>60	0.076

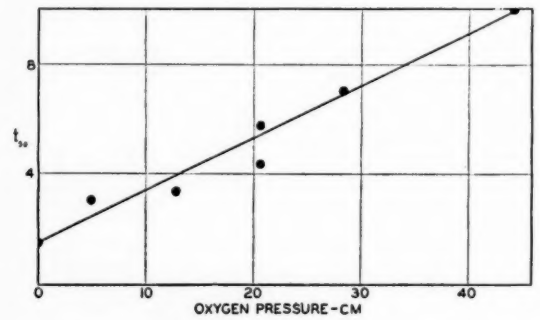

FIG. 4. Oxygen-nitrous oxide mixtures. Variation of T_{50} with added oxygen. $P_{N_2O} = 6$ cm.

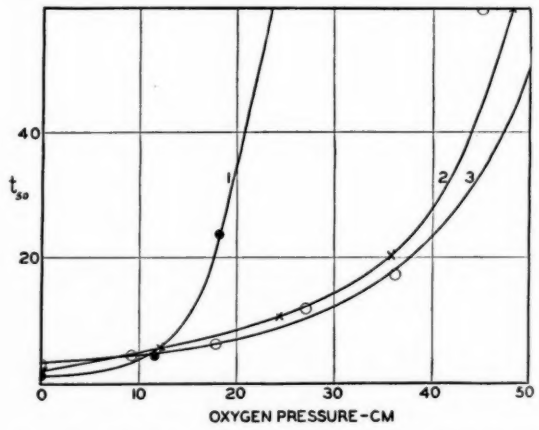

FIG. 5. Oxygen followed by nitrous oxide. Variation of T_{50} with oxygen concentration. 1, $P_{N_2O} = 6$ cm: 2, $P_{N_2O} = 12$ cm: 3, $P_{N_2O} = 18$ cm.

again entirely independent of the retarding effect of the oxygen formed during the reaction. The data are given in Table IV.

The variation of T_{50} with added oxygen for constant nitrous oxide pressures of 6, 12 and 18 cm is shown by Fig. 5. It will be seen that for oxygen pressures below 10 cm the order of admission of oxygen and nitrous oxide has little effect. At higher pressures, however, oxygen added first has a much more pronounced effect than oxygen added mixed with the reactant.

It is evident that the effect of oxygen is of three kinds, depending on whether it is formed in the reaction, mixed previously or added first. The effect of the three types of oxygen is illustrated by Fig. 6. The "addition" of oxygen formed in the reaction is accomplished by starting with a high pressure of nitrous oxide, letting it decompose until the partial pressure has fallen to 12 cm and calling this point zero time. In this way a certain amount of oxygen formed in the reaction is present at the start.

A number of experiments were carried out in which oxygen was left in contact with the catalyst for various lengths of time, pumped off partially or wholly, either quickly or slowly, and a new run made immediately. These showed conclusively that the adsorption and desorption of oxygen is complete within one or two minutes.

(*c*). *Diffusion.* A few experiments were performed in which oxygen was admitted to the catalyst first, followed by a mixture of oxygen and nitrous oxide. It was found that the reaction proceeded *faster* under these circumstances than would have been the case if the initial oxygen had been followed by the nitrous oxide alone. This immediately suggests that when oxygen is

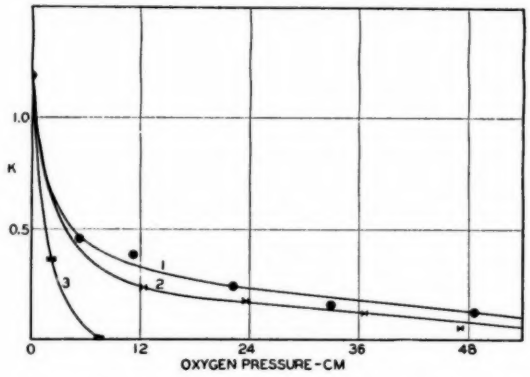

FIG. 6. Variation T_{50} with added oxygen. $P_{N_2O} = 12$ cm. 1, oxygen mixed with nitrous oxide: 2, oxygen followed by nitrous oxide: 3, oxygen formed in reaction.

admitted to the catalyst first its enhanced retarding effect is due to hindering the diffusion of the reactant into the pores of the catalyst. If more oxygen is added mixed with the nitrous oxide, a small additional retarding effect results, as has been shown in Table III. This effect, however, is more than offset by the compression of the gases into the pores of the catalyst, thus partially overcoming the slowing down of the reaction due to hindered diffusion. That this explanation is correct is proved by experiments with added nitrogen, the results of which are given in Table V.

The following conclusions may be drawn from Table V: (*a*). Mixing nitrogen with nitrous oxide in the absence of oxygen causes a very small retardation of the reaction. This may obviously be explained on the basis of hindered diffusion. (*b*). If nitrogen is admitted to the reaction vessel before nitrous oxide, the retarding effect due to hindered diffusion is considerably greater, as would be expected. The effect, however, is small compared to that of a similar amount of oxygen. (*c*). If oxygen is admitted first, followed by nitrogen mixed with nitrous oxide, there is an accelerating effect. This effect is greater than when the initial oxygen is followed by oxygen mixed with nitrous oxide. Hence oxygen under these circumstances has two effects, (i) acceleration due to aided diffusion, (ii) retardation due to an increase in the total oxygen concentration. The latter effect is absent with nitrogen, and hence the net acceleration is greater than with oxygen.

TABLE V. *The effect of nitrogen. 570.0°C. Catalyst No. 3. Initial nitrous oxide pressure = 6.00 cm.*

Nitrogen added first, cm	Oxygen added first, cm	Nitrogen added with N_2O, cm	K
			1.395
		20.00	1.240
39.85			0.508
	39.70		0.015
	39.90	5.65	0.079
	39.90	12.77	0.078
	39.90	15.02	0.087
16.95	22.90		0.025
27.60	12.35		0.035
34.05	5.95		0.069

DISCUSSION

The results of this investigation may be qualitatively explained as follows. In agreement with Schwab and Eberle it may be assumed that the oxygen formed in the reaction is adsorbed in the atomic condition and that the rate of desorption is comparatively slow (but not excessively slow, since the gas can be removed by evacuation in one or two minutes). Added oxygen may be assumed to be adsorbed as molecules. It is less effective than oxygen formed in the reaction either because it is only adsorbed to a comparatively small extent or because it can be displaced more easily by nitrous oxide. The form of the rate equation indicates fairly strong adsorption of oxygen but, as we have seen, this equation holds only for the oxygen formed in the reaction. We have therefore no definite indications as to the extent to which added oxygen is adsorbed.*

Added gases also retard the reaction by hindering the diffusion of the reactant to the catalyst. The order of admission of the gases is therefore of importance. If oxygen is admitted to the reaction vessel first it thus has a larger total retarding effect than when it is admitted mixed with nitrous oxide. Other effects due to hindered diffusion have already been discussed.

* We can obviously substitute 'activated' and 'van der Waals' adsorption for atomic and molecular adsorption without in any way affecting the argument. Since, however, the decomposition of the nitrous oxide molecule leads to the formation of atomic oxygen (the reaction being first order with respect to nitrous oxide), atomic adsorption seems to be the simpler and more plausible explanation.

The Solubility of Biphenyl in Non-Polar Solvents

J. C. Warner, R. C. Scheib and W. J. Svirbely, *Chemistry Laboratory, College of Engineering, Carnegie Institute of Technology*

(Received March 16, 1934)

The solubilities of biphenyl, between 30° and 60°, in benzene, carbon disulphide, carbon tetrachloride, heptane, dioxane and *p*-dichlorobenzene have been determined. The solubilities, in all cases, are lower than ideal. The freezing point-composition diagram for the system biphenyl-*p*-dichlorobenzene has been determined. These components yield a simple eutectic at 27.7° and at 42.5 mole percent biphenyl. Hildebrand's equation, based upon the simple Baud-Heitler equation for the heat of mixing, yields fairly satisfactory results for solutions of biphenyl in benzene, carbon disulphide, *p*-dichlorobenzene and dioxane. The results are not very satisfactory when the equation is applied to the solutions of biphenyl in carbon tetrachloride and heptane. Hildebrand's more recent equation, based upon the Menke probability function, yields fairly satisfactory results considering the nature of the assumptions made in its derivation. It is concluded that regular solution behavior should be expected only when the molecules of the constituents, in addition to being non-polar, possess spherical symmetry.

IN recent years, the properties of "regular solutions" have been the subject of a number of experimental and theoretical studies.[1] In regular solutions, due to the absence of special orientations of the molecules of the constituents with respect to each other, the partial molal entropies are assumed to be the same as in an ideal solution of the same composition. Since it has been postulated that orientation results through the operation of dipole and coulomb forces and not from shorter range forces of the van der Waal type, it has been assumed that solutions in which both constituents are non-polar should behave like regular solutions. In this investigation, we have determined the solubility of biphenyl in six non-polar solvents over a range of temperature and have examined our results to see what support they lend to current theories.

Materials and Purification

The chemicals used were all Eastman's "Best-Grade." The *n*-heptane and *p*-dichlorobenzene were used without further purification. Benzene (thiophene free) and carbon tetrachloride were dried over calcium chloride and redistilled. Only the middle fractions were used. Carbon disulphide was dried over calcium chloride and twice redistilled over mercury to remove sulphur. Dioxane was dehydrated by refluxing over metallic sodium and then fractionated over phosphorous pentoxide. Biphenyl, melting point 69.0°, was prepared by recrystallizing three times from alcohol, washing with ether and drying in an oven at 100°.

Experimental Method

Preparation of samples

All solubility measurements were made by a sealed tube method. Small pieces of Pyrex tubing (approximately seven-tenths cm in diameter and twelve cm long) were sealed at one end, cleaned, dried and weighed accurately. A small quantity of the solute, biphenyl, was admitted to the tube and by melting allowed to run to the bottom. All solute clinging to the sides of the tube was removed. The tube was then restricted, reweighed and the weight of the biphenyl determined. An appropriate quantity of the solvent was added and the closed end of the tube immersed in ice water to decrease the vapor pressure of the solvent. The tube was partially evacuated, sealed and reweighed to determine the weight of solvent introduced.

Procedure

Samples in the sealed tubes were completely liquified and then rapidly cooled to insure small, uniform crystals of biphenyl. The tubes were then fastened to stirring flippers immersed in a water bath. The flippers were so arranged that they moved through an angle of ninety degrees and vibrated at a rate of about one hundred and eighty per minute. The temperature of the bath was rapidly raised to within five degrees of the

[1] *a*. Hildebrand, J. Am. Chem. Soc. **51**, 66 (1929); *b*. Hildebrand and Carter, J. Am. Chem. Soc. **54**, 3592 (1932); *c*. Negishi, Donnally and Hildebrand, J. Am. Chem. Soc. **55**, 4793 (1933); *d*. Hildebrand, Phys. Rev. **34**, 984 (1929); *e*. Hildebrand and Wood, J. Chem. Phys. **1**, 817 (1933); *f*. Scatchard, Chem. Rev. **8**, 321 (1931).

actual solution temperature and the heating continued from this point at the rate of one-half degree per minute. The tube was shaken for about thirty seconds, stopped just long enough to examine for disappearance of solid and again set in motion. After determining approximately the temperature at which complete liquefaction occurred, the experiment was repeated, the temperature of the bath being raised at a rate of only one-tenth degree per minute. Four determinations, agreeing within 0.2° were made on each sample. The average of these four readings was taken as the actual solution temperature.

Temperatures were measured with 100° thermometers graduated in tenths suspended rigidly with the bulb not more than one centimeter from the path of one end of the sealed tube. All thermometers were compared with one of the same type which had been calibrated by the Bureau of Standards.

Experimental Results

The results of the measurements are summarized in Table I and represented graphically in Fig. 1 in comparison with the ideal solubility of biphenyl. Because of the rapid change in the slope of the curve with heptane as the solvent

Table I. *Solubility of biphenyl in non-polar solvents. Summary of calculations.*

Mole fract. sol'y of biphenyl	Temp. °C	"k"	$\bar{F}_2^r - \bar{F}_2^i$ cal.	$\bar{E}_2 - E_2^0$ cal.
	Solvent-Heptane			
0.972	68.1	1090	4	
.934	66.0	300	6	7
.892	64.0	235	13	
.857	62.5	220	21	
.836	61.6	212	26	43
.806	60.5	211	36	
.803*	59.5	151	26	
.726	57.5	200	68	
.665	55.3	192	99	
.475	49.1	186	235	478
.468	49.0	187	243	
.409	46.7	186	298	
.335	43.1	184	373	
.2735	39.9	188	456	942
.216	35.2	192	540	
.140	26.5	197	659	
	Solvent-Carbon tetrachloride			
0.939	66.0	140	2	
.906	64.3	140	6	7
.782	57.4	83	18	
.714	53.6	82	31	63
.534	41.3	57	57	
.518	40.0	56	59	170
.401	30.7	58	96	
.372	28.1	59	107	
	Solvent-Benzene			
0.713	52.3	40	15	
.677	49.4	25	17	55
.626*	45.5	18	17	
.605	44.3	27	19	
.585	43.1	29	24	87
.410	27.9	30	47	

Mole fract. sol'y of biphenyl	Temp. °C	"k"	$\bar{F}_2^r - \bar{F}_2^i$ cal.	$\bar{E}_2 - E_2^0$ cal.
	Solvent-Carbon disulphide			
0.810*	58.3	40	7	
.694	51.3	50	20	14
.674*	49.5	32	17	
.637*	47.6	46	28	
.595	44.1	35	26	23
.553	40.7	30	28	
.520	38.2	32	34	
.514	37.7	32	34	
.498	36.6	35	41	28
.404	28.4	38	62	
	Solvent-p-Dichlorobenzene			
0.923	65.0	66	2	
.859*	61.4	64	6	
.802	57.4	11	2	
.692*	49.8	6	3	
.575	41.2	11	10	
.496	34.1	9	11	
.425	27.7E	11	23	
	Solvent-Dioxane			
0.969	67.7	418	2	
.896*	63.4	50	3	
.796	57.7	58	11	
.752	55.0	52	15	
.725	53.1	41	14	
.638	47.3	32	23	
.535	39.3	31	32	
.457	32.4	29	39	
.398	26.4	28	47	
	Ideal Solubility			
1.0000	69.0			
.9266	65.0			
.8451	60.0			
.7679	55.0			
.6966	50.0			
.6317	45.0			
.5708	40.0			
.5149	35.0			
.4632	30.0			

* These solubilities seem least reliable inasmuch as they do not lie on the smooth solubility curves.

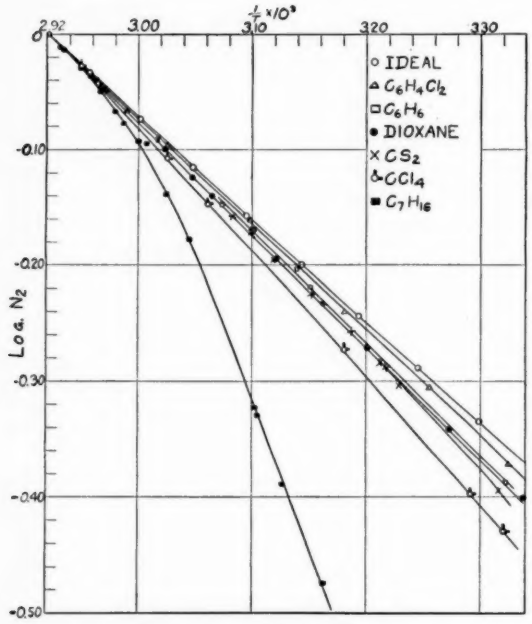

FIG. 1. Biphenyl-*p*-dichlorobenzene.

at about 58°, it was considered important to show that the solid phase separating out was the same over the complete temperature range. The solid phase must be either pure biphenyl or a solvate. That no solvate exists at room temperature and that pure biphenyl is the solid phase separating from all the saturated solutions was established by the fact that primary crystals obtained at room temperature melted sharply within 0.05° of the melting point of pure biphenyl. The ideal solubility, expressing the heat of fusion as a function of the temperature, is given by the equation:

$$\log N_2^i = -274/T + 4.38 \log T - 10.2996.$$

ΔH_f at the melting point is taken as 4235 cal. per mole. This is the mean of 4020 cal. per mole reported by Washburn and Read[2] and 4450 cal. per mole reported by Spaght, Thomas and Parks.[3] That the latter value is too high is indicated by the fact that it would require biphenyl to show negative deviations from Raoult's law in some non-polar solvents. C_p for solid biphenyl at the melting point equal to 54.82 cal. per mole was obtained from what appear to be very reliable data by the above authors.[3] These authors also give data from which we obtain 63.53 cal. per mole as the molal heat capacity of liquid biphenyl at the melting point. This value seems much more reliable than could be obtained from the previous discordant data.[4, 5]

The freezing point-composition data for the system biphenyl-*p*-dichlorobenzene are given in Table II and graphically represented in Fig. 2. According to the intersection of the liquidus curves, the eutectic composition is 42.5 mole percent biphenyl and the eutectic temperature is 27.7°. Assuming ideal solution behavior and constant heats of fusion, the calculated eutectic composition is 42.0 mole percent biphenyl and the eutectic temperature is 26.4°. For *p*-dichlorobenzene, we have taken $\Delta H_f = 4120$ cal. per mole.[6]

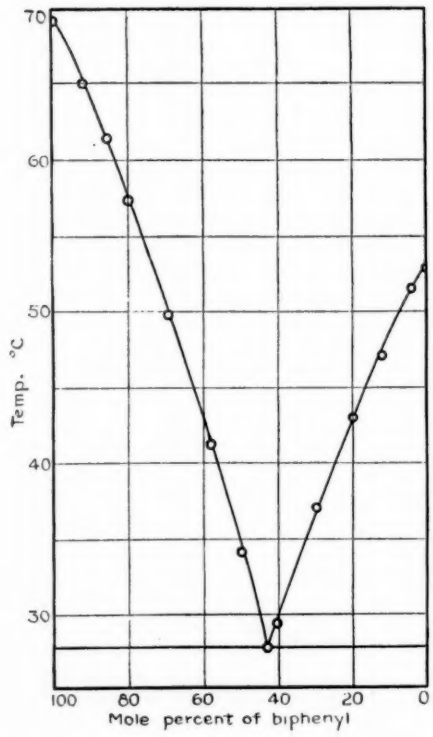

FIG. 2. Solubility of biphenyl in various solvents.

[2] Washburn and Read, Proc. Nat. Acad. Sci. **1**, 191 (1915).
[3] Spaght, Thomas and Parks, J. Phys. Chem. **36**, 882 (1932).
[4] Forrest, Brugmann and Cummings, J. Ind. Eng. Chem. **23**, 37 (1931).
[5] Newton, Kaura and DeVries, J. Ind. Eng. Chem. **23**, 35 (1931).
[6] Int. Crit. Tables **5**, p. 133.

TABLE II. *The binary system biphenyl-p-dichlorobenzene.*

Mole percent biphenyl	Initial cryst. temp. °C
100.0	69.0
92.3	65.0
85.9	61.4
80.2	57.4
69.2	49.8
57.5	41.2
49.6	34.1
42.5	27.7 E
40.2	29.3
29.1	37.0
20.0	42.8
18.55	43.4
11.85	47.1
3.8	51.5
0.0	52.9

DISCUSSION

In order to estimate the relative values of intermolecular forces between solute and solvent, certain physical constants such as heats of vaporization and molal volumes must be obtained at various definite temperatures for the constituents in the liquid phase. Since we are interested in the solubility of biphenyl below its melting point, it is necessary to use the values of ΔH_v and V_m for the supercooled liquid. The density[7] of liquid biphenyl is a linear function of the temperature from 70° to 130°. The heat of vaporization[8] of liquid biphenyl is also a linear function of the temperature from 69° to 105°. In each case, the curves were extrapolated to give densities and ΔH_v's of the supercooled liquid. Molal volumes of benzene, carbon tetrachloride, heptane and carbon disulphide were obtained from the densities reported in the I. C. T.[9] The heats of vaporization of benzene, carbon tetrachloride and heptane were calculated by use of the specific heat equations.[10] The heats of vaporization of carbon disulphide[11] were taken from the I. C. T. These constants are summarized in Table III.

In any saturated solution

$$\bar{F}_2^r - \bar{F}_2^i = RT \ln a_2/N_2 = RT \ln N_2^i/N_2. \quad (1)$$

$\bar{F}_2^r$ and $\bar{F}_2^i$ represent the partial molal free energies of solute in a regular and in an ideal solution. Since $\Delta F = \Delta H - T\Delta S$, one may say that for regular solutions

$$\bar{F}_2^r - \bar{F}_2^i = \bar{H}_2^r - H_2^0 = \bar{L}_2,$$

inasmuch as it is assumed that $\Delta S = 0$. Starting with the Baud-Heitler[12] equation for the heat of formation of a mole of solution

$$\bar{L}_2 N_2 + \bar{L}_1 N_1 = \Delta H = bN_1N_2, \quad (2)$$

Hildebrand[13a] obtained the equations $\bar{L}_1 = bN_2^2$, $\bar{L}_2 = bN_1^2$

$$\log N_2^i/N_2 = bN_1^2/2.303RT = KN_1^2/T. \quad (3)$$

His method cannot be justified on rigorous mathematical grounds but only because equations of the correct general form for regular solutions are obtained, namely, $L_1 \to 0$ as $N_2 \to 0$, $L_2 \to 0$ as $N_1 \to 0$ and $L_2 = L_1$ when $N_2 = N_1$. For regular solutions b, and hence k, is assumed to

TABLE III. *Physical constants of biphenyl and the non-polar solvents.*

Temp. °C	Molal vol. cc	Heat of vap. cal.
	Biphenyl	
25	149.4	18,870
35	150.6	18,310
45	151.8	17,730
55	153.0	17,160
65	154.3	16,570
	Benzene	
35	90.5	7,860
45	91.7	7,780
55	92.8	7,660
65	93.9	7,550
	Carbon disulphide	
35	61.2	6,520
45	61.9	6,410
55	62.8	6,310
65	63.6	6,200
	Carbon tetrachloride	
35	97.8	7,790
45	98.9	7,680
55	99.8	7,560
65	101.0	7,410
	Heptane	
35	148.2	8,547
45	149.8	8,400
55	151.3	8,260
65	152.6	8,110

[7] Private communication from Professor W. L. McCabe, University of Michigan.
[8] Bulletin, Swann Chemical Co., Birmingham, Ala.
[9] Int. Crit. Tables, **3**, pp. 28, 29.
[10] Int. Crit. Tables, **5**, pp. 115, 107, 81; Parks and Huffman, *Free Energies of Some Carbon Compounds*, pp. 68–93; Parks, Huffman and Thomas, J. Am. Chem. Soc. **52**, 1032 (1930).
[11] Int. Crit. Tables, **5**, p. 138.
[12] Baud, Bull. Soc. Chim. (4) **17**, 324 (1915); Heitler, Ann. d. Physik (4) **80**, 630 (1926).

be independent of composition and essentially independent of the temperature. Values of k calculated from our solubility data are listed in Table I. Reasonably constant values of k are obtained in all cases when the mole fractions of solute are less than 0.65. With higher mole fractions of biphenyl there is a drift toward increased values of k. This drift may not be very significant in the carbon disulphide, dioxane, *p*-dichlorobenzene and benzene solutions since the departure from Raoult's law is slight in each of these solvents. Furthermore, values of k are fairly sensitive to small errors in solubility when the mole fraction of solute is high. With carbon tetrachloride and especially with heptane as solvents the drift in k can hardly be attributed to experimental error. The drift is equally evident when k is calculated from the smoothed curves representing our solubility data (Fig. 1). We must conclude therefore, that Eq. (3) does not apply well to our data; particularily to the solutions of biphenyl in heptane and carbon tetrachloride.

That Eq. (3) should not apply to many solutions even when both constituents are non-polar is indicated by the fact that the Baud-Heitler equation, as shown by Coleman and Germann,[13] is not adequate for expressing the heat of mixing as a function of the composition. These investigators have developed the following empirical equation from an analysis of the dependence of ΔH on N.

$$\Delta H = N_1 N_2(\alpha + \beta e^{\gamma N_1}). \qquad (4)$$

α, β and γ are constants or functions of the temperature. This equation becomes identical with Eq. (3) when either β or γ is zero. However, an examination of the data compiled by Coleman and Germann shows that neither β nor γ is zero for a variety of solutions in which both components are non-polar and it seems likely that neither β nor γ would be zero in some of our solutions.

In a recent investigation, Hildebrand and Wood,[1e] by making use of the probability function of Menke[14] as a basis for a statistical treatment of intermolecular potentials in solution, has arrived at the equation

$$\overline{E}_2 - E_2^0 = \left[\frac{n_1 V_1}{n_1 V_1 + n_2 V_2}\right]^2 V_2 \left[\left(\frac{\Delta E_2}{V_2}\right)^{\frac{1}{2}} - \left(\frac{\Delta E_1}{V_1}\right)^{\frac{1}{2}}\right]^2. \qquad (5)$$

$\overline{E}_2$ represents the partial molal total energy and E_2^0 the molal total energy of the solute. The V's and ΔE's represent the molal volumes and the energies of vaporization. It is assumed that for regular solutions

$$\overline{E}_2 - E_2^0 = \overline{F}_2^r - \overline{F}_2^i = RT \ln N_2^i / N_2.$$

We possess sufficient data for the calculation of $\overline{E}_2 - E_2^0$ by Eq. (5) only for the solutions of biphenyl in carbon disulphide, carbon tetrachloride, benzene and heptane. For these four systems, $\overline{E}_2 - E_2^0$ is compared with $\overline{F}_2^r - \overline{F}_2^i$ in Table I. The agreement is as good as could reasonably be expected considering the nature of the assumptions made in the derivation of Eq. (5). The probability function is certainly not the same function of distance in all radial directions from the central molecule for non-spherical molecules. Moreover, the potential function must be dependent upon the shape of molecules and upon the presence or absence of polar bonds in the molecule even when the molecule as a whole possesses a zero moment. It seems likely that the conditions of Hildebrand's original definition of the regular solution can be met only when the molecules of the constituents, in addition to being non-polar, possess spherical symmetry.

[13] Coleman and Germann, J. Chem. Phys. **1**, 847 (1933).

[14] Menke, Phys. Zeits. **33**, 593 (1932).

Studies on Glass. XI. Some Thermodynamic Relations of Glassy and Alpha-Crystalline Glucose

GEORGE S. PARKS, LOILOR J. SNYDER AND FRANCIS R. CATTOIR, *Department of Chemistry, Stanford University, California*

(Received June 4, 1934)

Although the properties of a glass depend to some extent upon its thermal history, the view is expressed that fairly satisfactory thermodynamic data can be obtained for *well-annealed* glasses. In the present study the difference between the heat contents of glucose glass and α-crystals has been determined calorimetrically at 20°C and with the aid of this result the corresponding differences in entropy and free energy have also been computed. The value for this last quantity is $\Delta F^\circ_{293} = 1670$ cal. per mol. Solubility measurements have been made for glucose α-crystals and glass in methyl, ethyl and isopropyl alcohols at 20°. The free energy values thereby obtained for the conversion of α-crystals into glassy glucose are in good agreement with the preceding value derived from the thermal data.

THERE are three distinct forms, *viz.*, α-crystals, β-crystals and glass, in which pure *d*-glucose can exist in the neighborhood of room temperature. Of these, crystalline α-glucose has long been recognized as the most stable. As a partial, quantitative corroboration of this view Parks and Huffman,[1] employing the solubilities of the α- and β-crystalline forms in 80 percent alcohol, have recently calculated $\Delta F^\circ_{298} = 400$ cal. for the free energy change in the process

$$C_6H_{12}O_6\ (\alpha\text{-crystals}) \rightarrow C_6H_{12}O_6\ (\beta\text{-crystals}).$$

In the past, however, suitable thermodynamic data have not been available for a similar comparison between glucose in the α-crystalline form and the glassy form. The latter is readily produced by heating up the α-crystals through their melting point (146°C) and then undercooling the resultant liquid, which undergoes with falling temperatures an increase in viscosity to about $10^{13.5}$ poises at 25°C. Below this point the amorphous glucose becomes a hard, brittle glass and shows a marked falling off in both heat capacity and coefficient of thermal expansion.

The properties of such a glass depend to some extent upon its thermal history. This dependence is especially marked in the neighborhood of the transition region where the glass softens and changes into a very pasty liquid, as the previous studies by Thomas and Parks[2] and by Spaght and Parks[3] have shown. Hence it almost seems logical to consider that the thermodynamic properties of a glass system are a function of the three variables, temperature, pressure and *time*, instead of simply temperature and pressure as with a pure crystalline material. This is really equivalent to stating that a glass lacks a sharply specifiable energy content, so characteristic of a crystal or mobile liquid at a given temperature and pressure, and can possess any energy value within a certain range, depending upon its mode of formation and previous annealing. Accordingly, it can be argued that rigorous thermodynamic calculations involving a glass system are impossible.

In practice, however, the properties of a glass sample become fairly reproducible with *sufficient annealing* and those of different *well-annealed* samples of a given kind of glass agree reasonably well. In other words, with the lapse of sufficient time a definite condition of internal equilibrium is apparently approached and then this time factor becomes relatively unimportant in influencing further the energy content and other properties of a glass system. And, of course, the time actually required for sufficient annealing becomes progressively less as the temperatures involved approach those of the softening or transition region. Thus in the case of glucose glass the transition region centers around 25°C and glass samples at temperatures of 0° to 20° appear to be reasonably well annealed at the end of merely one or two days maintenance in the neighborhood of these temperatures. Under such conditions we

[1] Parks and Huffman, *The Free Energies of Some Organic Compounds*, p. 179, The Chemical Catalog Co., New York, 1932.

[2] Thomas and Parks, J. Phys. Chem. **35**, 2091 (1931); J. Am. Chem. Soc. **56**, 1423 (1934).

[3] Spaght and Parks, J. Phys. Chem. **38**, 103 (1934).

have been able to make satisfactory determinations of the heat content, entropy, free energy and even solubilities of glassy glucose. These results, expressed in relation to the corresponding values for the α-crystalline form, are given in the following sections of this paper.

Materials

The crystalline α-glucose employed in the present study was the C.P. material prepared by the Pfanstiehl Chemical Co. Its water content was guaranteed to be less than 0.10 percent. Polarimetric measurements, interpreted with the aid of the optical rotation values of Hudson and Yanovsky,[4] indicated that it perhaps contained a few percent of the β-form. Accordingly this material was further purified by the method of Hudson and Dale[5] to yield α-crystals for the solubility measurements. The glass samples were made from it in the manner described previously by Parks, Huffman and Cattoir.[6]

The Heat Content of Glucose Glass

The difference between the heat contents of glassy glucose and the crystalline α-form was evaluated by measurements of the heats of solution of these two forms in water under comparable conditions.

The calorimetric method employed was essentially that which had been previously used by Parks, Hablutzel and Webster[7] in their determination of the heat of solution of zinc oxide in hydrochloric acid. The calorimeter was a three-liter Dewar jar, equipped with a glass stirrer of the propeller type and a Beckmann thermometer, which had been calibrated by the United States Bureau of Standards. In the determinations 200 g samples of glucose, either glass or crystals, were dissolved in about 2500 cc of water to which a small amount of ammonia had been added to promote mutarotation and thus give the same end point in each solution. Whether this precaution was actually necessary is of course doubtful, since the work of Nelson and Beegle[8] indicates that the mutarotation of glucose in aqueous solution probably involves zero heat effect.

At 20°C three determinations of the heat of solution of the glass and six determinations for the α-crystals were made. The solution process for the glasses was exothermic, while that for the crystals was decidedly endothermic. In our calorimetric system the corresponding temperature changes were about +0.5° and −1.0°, respectively. The results are tabulated in Table I.

Table I. *Heat of solution of glucose samples at 20°C.*

ΔH_{293} for glass (cal./g)	ΔH_{293} for α-crystals (cal./g)	(cal./g)
6.85	−13.72	−13.88
6.79	−13.77	−13.52
7.01	−13.74	−13.72
Mean 6.88	Mean −13.73	

Our mean value for the heat of solution of the crystals is a little lower than the results (−13.96 cal./g and −13.85 cal./g) reported previously by Barry[9] and by Hendricks, Dorsey, LeRoy and Moseley.[10] However, these investigators dissolved α-glucose in water to yield much more dilute solutions than the approximately 0.44 molal involved in our present study.

From the mean results in Table I the difference between the heat contents of the glass and crystals is 20.61 (±0.15) cal./g at 20°C. This yields for the molal process

$$C_6H_{12}O_6\ (\alpha\text{-crystals}) \rightarrow C_6H_{12}O_6\ (\text{glass}); \quad \Delta H_{293} = 3712(\pm 25)\ \text{cal.} \quad (1)$$

Above 20°C the glass softens and in the neighborhood of 40° the product in this process becomes obviously a very viscous liquid. An examination of the available specific heat data for crystalline[11] and undercooled liquid[6] glucose indicates that the difference between the heat capacity of the undercooled liquid and the crystalline form is almost independent of the

[4] Hudson and Yanovsky, J. Am. Chem. Soc. **39**, 1035 (1917).

[5] Hudson and Dale, J. Am. Chem. Soc. **39**, 324 (1917).

[6] Parks, Huffman and Cattoir, J. Phys. Chem. **32**, 1366 (1928).

[7] Parks, Hablutzel and Webster, J. Am. Chem. Soc. **49**, 2792 (1927).

[8] Nelson and Beegle, J. Am. Chem. Soc. **41**, 574 (1919).

[9] Barry, J. Am. Chem. Soc. **42**, 1911 (1920).

[10] Hendricks, Dorsey, LeRoy and Moseley, J. Phys. Chem. **34**, 418 (1930).

[11] Simon, Ann. d. Physik **68**, 258 (1922).

temperature; and accordingly we shall now take the value $\Delta C_p = 33$ cal. per mol between 20° and 146° (the melting point of pure α-glucose crystals). Hence, by Kirchhoff's law, we can calculate for the conversion of a mol of α-crystals into liquid glucose at 146°C

$$\Delta H_{419} = 3712 + 33(146 - 20) = 7870(\pm 150) \text{ cal.} \quad (2)$$

This result for the heat of fusion of α-glucose crystals is in fairly good agreement with the experimental one recently obtained by Thomas and Parks[2] with their radiation calorimeter. Their value for a glucose sample, somewhat contaminated with decomposition products, was 41.7 cal. per gram at 141°, which corresponds to about 7675 cal. per mol at 146°C.

Entropy and Free Energy Differences Between Glass and Crystals

The entropy increase on fusion of the α-crystals at 146° follows directly from the data of Eq. (2):

$$\Delta S_{419} = 7870/419 = 18.78 \text{ E. U.} \quad (3)$$

The entropy change for the hypothetical conversion of a mol of the crystals into glucose glass at 20°C can be evaluated next with the aid of the ΔC_p value given in the previous section:

$$\Delta S_{293} = 18.78 - 33 \ln (419/293) = 6.98(\pm 0.25) \text{ E. U.} \quad (4)$$

By means of the fundamental thermodynamic equation, $\Delta F = \Delta H - T\Delta S$, and the data of Eqs. (1 and 4) we can then obtain the molal free energy change for the crystal-to-glass transformation at 20°C:

$$\Delta F^\circ_{293} = 1670(\pm 100) \text{ cal.} \quad (5)$$

Solubility Data

The free energy difference between the glass and crystals can also be evaluated from the relative solubilities of these two forms in various solvents. In the present study we have made such measurements in methyl alcohol, ethyl alcohol and isopropyl alcohol.

The experimental procedure was simple. Samples of finely ground glucose glass or purified α-crystals were placed in 125 cc Erlenmeyer flasks containing the alcohol solvent. These flasks were then vigorously agitated in a small thermostat at 20°. At suitable time intervals samples of the alcohol saturated with glucose were pipetted out through fine filter paper and weighed. The alcohol was then evaporated off and the residual glucose was also weighed. The solubilities were calculated as the weight of glucose per 1000 g of solvent. On the assumption that the chief impurity was water, the purity of the three solvents was estimated from density determinations to be: methyl alcohol, 99.5 percent; ethyl alcohol, 99.3 percent; and isopropyl alcohol, 99.2 percent. As we were primarily concerned with comparative solubilities, no effort was made to eliminate such small amounts of water in these solvents.

The determinations on the α-crystals offered no particular difficulty. With the ethyl and isopropyl alcohols saturation was completed in about five minutes. In the case of methyl alcohol, however, the solubility was much greater and about thirty minutes was required for saturation. During this time there was also considerable mutarotation of the dissolved α-glucose into β-glucose and a polarimetric analysis of the solution with the aid of the optical rotation data of Hudson and Yanovsky[4] indicated that over 30 percent was in the β-form. Thus the total dissolved glucose at the end of 45 minutes amounted to 20.2 g per 1000 g of methyl alcohol, of which only 12.5 g represented α-glucose. This production of dissolved β-glucose continued with further lapse of time so that at the expiration of several hours 20.7 g of glucose had dissolved, of which the α form represented only 58 percent or about 12.0 g.

The solubility determinations on the glass yielded somewhat less definite results. Agitation of the alcohol and glass mixtures for several hours was required to approach what appeared to be a saturation value and, since the solutions during this time were already supersaturated with respect to the α-crystalline form, glucose crystals were very prone to appear and interfere with the measurements. In the cases of the ethyl and isopropyl alcohols fairly consistent solubility values were obtained over a period of fifteen to twenty hours, although these data may be somewhat too low. In the case of methyl alcohol, however, a maximum value of 289 g of glucose glass per 1000 g of solvent was obtained at the end of about three hours. Profuse crystal formation

then prevented the extension of these measurements over longer periods of time and accordingly we are not inclined to place great reliance on this particular result.

The data derived from these measurements are summarized in Table II. Our mean solubility

TABLE II. *Solubility and related data for glucose glass and α-crystals at 20°C.*

Solvent	Glass solubility (in g/1000 g	Crystals solubility of solvent)	Solubility ratio	$\Delta F°_{293}$ (cal./mol)
Methyl alcohol	289	12.2	23.7	1810
Ethyl alcohol	32.0	1.55	20.6	1760
Isopropyl alcohol	10.1	0.62	16.3	1630

results are recorded in the second and third columns and the next column gives the ratio of the value for the glass to that for the α-crystals in each instance. On the assumption that these ratios for ethyl and isopropyl alcohols are also the ratios of the corresponding activities we have calculated the free energy changes for the conversion of glucose α-crystals into glass by the formula

$$\Delta F° = RT \ln a_{\text{glass}}/a_{\text{crystals}}. \qquad (6)$$

In the case of the methyl alcohol solutions, the solubilities being much greater, the calculation was made by using the ratio of the mol fractions of glucose ($N_{\text{glass}}/N_{\text{crystals}} = 22.4$) in the saturated solutions instead of the weight solubilities. These molal $\Delta F°$ values are tabulated in the last column. They are in good agreement with the corresponding value derived in Eq. (5) from the thermal data.

This agreement would seem to indicate the essential correctness of our solubility values. There is, however, one objection which can be adduced toward these calculations as we have made them; i.e., we have not allowed for mutarotation in considering the glucose glass solubilities. Moreover, some measurements, recently carried out by Mr. Charles Jacobs (of this laboratory) on the optical rotation of glucose glasses, indicate that our glasses, as made up, contain both α- and β-glucose in roughly equal proportions and consequently the alcohol solutions directly obtained by dissolving the glasses would represent an approximately similar division between these two forms. Hence, if we aim to compare simply the amounts of α-glucose dissolved from both the glasses and the crystals, our ratios in the fourth column of Table II should be approximately halved. This means that the tabulated values of $\Delta F°_{293}$ should be reduced by an amount equal to $RT \ln 2$, or about 400 cal., if we wish to deal with the free energy change for the process of converting one mol of α-glucose crystals into this glass containing roughly equal amounts of the α- and β-forms. On the other hand, if we wish to consider the process of converting the α-crystals into an idealized glass containing only α-glucose molecules, the $\Delta F°_{293}$ quantities given in Table II need not be altered, as doubling the activity of the α-form in the glass would produce a corresponding effect on the activity of this form in the alcohol solution.

CONCLUSION

In our judgment, the results obtained in this study justify the view that fairly satisfactory thermodynamic data can be obtained for *well-annealed* glasses, especially at temperatures close to the softening region. The free energy values hereby derived show clearly that annealed glucose glass possesses a thermodynamic potential which is only slightly higher than that of glucose in either the α- or β-crystalline forms.

Deviations from Ohm's Law in Weak Electrolytes

LARS ONSAGER,* *Sterling Chemistry Laboratory, Yale University*

(Received May 29, 1934)

The effect of an external electric field on the electrolytic dissociation is computed kinetically from the equations for Brownian motion in the combined Coulomb and external fields. The result is an increase of the dissociation constant, by the factor $K(X)/K(0)=F(b)=1+b+(1/3)b^2+\cdots$, where the parameter b is proportional to the absolute value of the field intensity, and inversely proportional to the dielectric constant. In water at 25°, $F(b)=F(1)=2.395$ for a field of 723 kilovolt/cm, while in benzene, the same increase of the dissociation constant is obtained for a field of only 21 kilovolt/cm. The theory is quantitatively confirmed by the deviations from Ohm's law which have been observed for solutions of weak electrolytics in water and in benzene. For solutions of salts in acetone, and for solid electrolytes such as glass, mica, celluloid, etc., the observed increments of conductance are smaller than those expected from the theory, but still of the predicted type and order of magnitude. The kinetic constants of dissociation and recombination can be computed separately on the assumption that the recombination proceeds as rapidly as the mutual approach of two ions due to the Coulomb attraction. The derivation is equivalent to that of Langevin, and leads to the same result. In the Langevin case, the coefficient of recombination is independent of the field; that of dissociation is increased by the factor $F(b)$. Slower reactions may occur when a (chemical) rearrangement of the ion pairs is involved. In the most general case, it is necessary to consider the successive reversible reactions *ions*$\rightleftarrows$*pairs*$\rightleftarrows$*molecules*, where the former takes place with the Langevin velocity; only the reaction rate *pairs*$\rightarrow$*ions* depends on the field. On the basis of this picture, the saturation phenomena observed in dielectrics are discussed in relation to the field effect.

INTRODUCTION

IN recent years, it has been definitely established that the conductance of electrolytes increases with the intensity of the field, so that Ohm's law has only a limited range of validity.[1]

For the case of strong electrolytes, this effect has been successfully interpreted as a destruction of the "ionic atmosphere." The initial effect is proportional to the square of the field intensity, and for very strong fields the equivalent conductance approaches a limiting value, which is not greater than the limiting equivalent conductance for small concentrations. Weak electrolytes, on the other hand, show much enhanced deviations from Ohm's law; the conductance increases linearly over a considerable range of the field intensity, and the limit of the increase, if any, corresponds to complete dissociation of the total amount of electrolyte present.[2]

It has been considered an open question whether the prevailing theory for the electrostatic interaction of the ions could account for this increased dissociation of weak electrolytes, and several explanations have been offered. Without entering into the possible merits and defects of these various approaches to the problem, I shall present a result which has been computed on the basis of the interionic attraction theory, and discuss its significance. The agreement with the available measurements of conductance in strong fields may be considered satisfactory. In addition, the theory allows some predictions concerning the rates of dissociation and recombination of the ions, and the considerations involved by this question are extended with equal ease to the case of high field intensities.

The computed relative increase of the dissociation constant is given by the formula

$$K(X)/K(0)=J_1(4(-\beta q)^{\frac{1}{2}})/2(-\beta q)^{\frac{1}{2}}$$
$$=1+2\beta q+\frac{(4\beta q)^2}{2!3!}+\frac{(4\beta q)^3}{3!4!}+\cdots, \quad (1)$$

where

$$q=-e_1e_2/2DkT>0;$$
$$2\beta=|X(e_1\omega_1-e_2\omega_2)|/kT(\omega_1+\omega_2). \quad (2)$$

Here, e_1 and e_2 denote the charges of the ions, X the intensity of the field (in electrostatic units), D the dielectric constant of the solution, k Boltzmann's constant, $kT\omega_i$ the coefficients of diffusion, and $e_i\omega_i$ the velocities of electrolytic migration in a field of one e.s.u.=300 volt/cm. The most remarkable feature of (1) is the proportionality with the absolute value of the field. This paradoxical *linear law* is borne out by the

* Research Fellow in Yale University.

[1] M. Wien, Phys. Zeits. **29**, 751 (1928).

[2] M. Wien, Phys. Zeits. **32**, 545 (1931).

experiments for all but the lowest field intensities, where deviations occur due to an effect that has been neglected in the derivation of (1). A complete theory would eliminate the discontinuity which (the differential quotient of) the function (1) possesses for $X=0$, in a manner dependent on the concentration; the result (1) of the approximate theory is *independent of the concentration.*

Kinetic Theory of the Dissociation Equilibrium

The formula (1) is derived from a detailed study of the mutual approach and parting of pairs of ions; we shall assume that these events are governed by the laws of Brownian motion. It will be necessary to make a somewhat arbitrary distinction between "free" and "bound" ions (i.e., in molecules); we may adopt Bjerrum's[3] convention, that a pair of ions at a distance $r<q$ are considered as "bound" to each other. Our considerations will apply primarily to cases where the concentration of "free" ions is sufficiently small, so that the Debye-Hückel "radius" $1/\kappa$ of the ionic atmosphere is much greater than the "effective range" q of the ions; i.e.,

$$\kappa q = -\kappa e_1 e_2/2DkT \ll 1, \tag{3}$$

with Bjerrum's convention

$$\kappa^2 = 4\pi(n_1 e_1^2 + n_2 e_2^2)/DkT, \tag{4}$$

where n_1 and n_2 denote the concentrations of "free" ions. The effects of interionic forces in *strong electrolytes* are of the order κq; the condition (3) implies that these effects are small. In *weak electrolytes*, the electrostatic (and other) forces may still cause considerable "association" of ions into "bound" pairs, even when κq is small. As pointed out by Bjerrum, this process is practically governed by the mass-action law, no matter what are the forces that keep the pairs together. Here we are interested in the modification of the mass-action equilibrium by an external electric field.

Let us first examine briefly the structure of the ionic atmosphere in a case of the type (3). When no external field is present (equilibrium), the density of ions of the species i in the neighborhood of ions of the species j is given by the formula

$$n_{ji}(r) = n_i \exp(-w_{ji}(r)/kT), \tag{5}$$

where $w_{ji}(r)$ is the potential of the average force between two ions i and j, with the understanding that both ions should be "free" or (for $r<q$) bound to each other. According to Bjerrum,

$$w_{ji}(r) = \frac{e_j e_i}{D}\frac{\exp(\kappa q - \kappa r)}{(1+\kappa q)r} \quad \text{for } r>q, \tag{6}$$

and

$$w_{ji}(r) = e_j e_i/Dr \quad \text{for} \quad r<q, \tag{7}$$

approximately. In Bjerrum's theory, (7) contains a correction of the order $\kappa q kT$, which may be neglected under the assumption (3). The total concentration of "bound" pairs equals

$$\nu_{ji} = \nu_{ij} = n_j \int_a^q n_{ji}(r) 4\pi r^2 dr, \tag{8}$$

where a denotes the "diameter" (the least distance of approach) of the ions i, j. It is important that in the case of typical weak electrolytes, and quite generally in solvents of *low dielectric constant*, the main contribution to (8) arises from distances r that are but slightly greater than a. The upper limit of the integral in (8) is fixed by an arbitrary convention due to Bjerrum, but if the limit q were replaced by $q/2$ or by $2q$, the difference would be negligible for our purposes, as for his.

We take the opportunity to point out one peculiar characteristic of the Eqs. (6) and (7). The factor $\exp(-\kappa r)$ in (6) is due to the gradual screening off of the electric field of an ion by the surrounding space charge; without this factor, Eq. (5) would lead to an infinite total space charge. Nevertheless, under the assumption (3) it is possible to neglect the factor $\exp(-\kappa r)$ up to some distance $r'>q$; in fact, this distance may be chosen so as to fulfill the condition

$$q \ll r' \ll 1/\kappa, \tag{9a}$$

and we may extend (7) up to the distance r':

$$w_{ji}(r) = e_j e_i/Dr \quad \text{for} \quad r<r', \tag{9b}$$

without appreciable error. This method of approximation is very well adapted to the purpose in hand; because the phenomenon of incomplete

[3] N. Bjerrum, Kgl. Danske Vid. Selskab, Math. -fys. medd. **7**, 9 (1926).

dissociation depends mainly on the innermost part (7) of the field of an ion, while the region beyond the limit given by (9) is of no importance whatever.

The customary procedure in the theory of *strong* electrolytes is to replace formula (5) by the abbreviated Taylor series

$$n_{ji}(r)\sim n_i(1-w_{ji}(r)/kT). \tag{10}$$

This approximation is good where $w/kT\ll 1$, that is for large distances r; for small distances it is poor and leads to absurd consequences (n_{ji} negative for $w>kT$). The approximation expressed by (8) and (9) has the opposite characteristics: It is good for small distances, in fact wherever w/kT is appreciable, but it would lead to absurd results if extended to all distances ($r'=\infty$). For the purpose of convenient computation, we shall nevertheless remove the outer boundary r' in (9) to infinity, and it will turn out that we still obtain intelligible results for the significant region of small distances r; only the disastrous effects due to the infinite total charge in the distant part of the "ionic atmosphere" must be disregarded.

In the presence of an external electric field $\mathbf{X}$ the Boltzmann Eq. (5) is no longer applicable, because we are not dealing with a true equilibrium. We must now develop a kinetic theory for the electrolytic dissociation and the recombination of the ions; we shall base this theory on the laws of Brownian motion. The general procedure in applying the equations of Brownian motion to the problem of two particles is well known.[4]

We now consider a distribution-function

$$f_{ji}(\mathbf{r})=f_{ij}(-\mathbf{r})=n_jn_{ji}(\mathbf{r})=n_in_{ij}(-\mathbf{r}), \tag{11}$$

where the distance $\mathbf{r}$ must be regarded as a vector, because now the direction is important. The mean relative velocity of two ions j and i at a distance $\mathbf{r}=\mathbf{r}_2-\mathbf{r}_1$ from the former to the latter is

$$\begin{aligned}\mathbf{v}_{ji}(\mathbf{r})-\mathbf{v}_{ij}(-\mathbf{r})&=\omega_i(e_i\mathbf{X}+\mathbf{k}_{ji}(\mathbf{r})\\&\quad-kT\,\mathrm{grad}_2\log f_{ji}(\mathbf{r}))-\omega_j(e_j\mathbf{X}+\mathbf{k}_{ij}(-\mathbf{r})\\&\quad-kT\,\mathrm{grad}_1\log f_{ij}(-\mathbf{r})),\end{aligned} \tag{12}$$

where $\mathbf{k}_{ji}(\mathbf{r})$ and $\mathbf{k}_{ij}(-\mathbf{r})$ denote the average of the ionic forces on the ions in this position, and the stationary condition is

$$\begin{aligned}\partial f/\partial t&=-\mathrm{div}_2\,(f_{ji}(\mathbf{r}_2-\mathbf{r}_1)\mathbf{v}_{ji}(\mathbf{r}_2-\mathbf{r}_1))\\&\quad-\mathrm{div}_1\,(f_{ij}(\mathbf{r}_1-\mathbf{r}_2)\mathbf{v}_{ij}(\mathbf{r}_1-\mathbf{r}_2))\\&=\mathrm{div}_2\,(f_{ji}(\mathbf{r})\{\mathbf{v}_{ij}(-\mathbf{r})-\mathbf{v}_{ji}(\mathbf{r})\})=0.\end{aligned} \tag{13}$$

On account of the difference between the ionic atmospheres of the ions j and i, there is, in general, no simple relation between $\mathbf{k}_{ji}(\mathbf{r})$ and $\mathbf{k}_{ij}(-\mathbf{r})$. However, if we assume (3), then the screening effect of the atmosphere is negligible in the region of interest, as shown above for the equilibrium case; with a strong field $\mathbf{X}$ the approximation is even better, because the field tends to sweep the atmosphere away from the ion. For simplicity, we put $r'=\infty$ in (9); then $\mathbf{k}_{ji}$ and $\mathbf{k}_{ij}$ possess everywhere the same potential $w_{ji}(r)$:

$$\begin{aligned}\mathbf{k}_{ji}(\mathbf{r}_2-\mathbf{r}_1)&=\mathbf{k}_{ji}(\mathbf{r})=-\mathrm{grad}_2\,w_{ji}(r),\\\mathbf{k}_{ij}(\mathbf{r}_1-\mathbf{r}_2)&=\mathbf{k}_{ij}(-\mathbf{r})=-\mathrm{grad}_1\,w_{ji}(r),\end{aligned} \tag{14}$$

where w is simply the Coulomb potential (9), and (12) becomes

$$\begin{aligned}f_{ji}(\mathbf{r})(\mathbf{v}_{ji}(\mathbf{r})-\mathbf{v}_{ij}(-\mathbf{r}))&=(e_i\omega_i-e_j\omega_j)\mathbf{X}f_{ji}(\mathbf{r})\\&\quad-(\omega_j+\omega_i)\{f_{ji}(\mathbf{r})\,\mathrm{grad}\,(e_je_i/Dr)\\&\quad+kT\,\mathrm{grad}\,f_{ji}(\mathbf{r})\}.\end{aligned} \tag{15}$$

We now choose a frame of reference such that the x axis is parallel to the external field $\mathbf{X}$, with the potential $-Xx$, and assume

$$Xe_j>0;\qquad Xe_i<0.$$

Then with the notation (2), and dropping the indices for f, the mean relative velocity $\mathbf{v}$ of the two ions in a given configuration is given by

$$\begin{aligned}f(\mathbf{r})\mathbf{v}(\mathbf{r})&=f(\mathbf{r})(\mathbf{v}_{ji}(\mathbf{r})-\mathbf{v}_{ij}(-\mathbf{r}))\\&=kT(\omega_j+\omega_i)(-\mathrm{grad}\,f\\&\quad+f\,\mathrm{grad}\,((2q/r)+2\beta x)).\end{aligned} \tag{16}$$

The stationary condition (13) takes the form

$$\mathrm{div}\,(f\,\mathrm{grad}\,(2\beta x+(2q/r)))-\mathrm{div}\,\mathrm{grad}\,f=0, \tag{17}$$

which, since the field of the potential $(2q/r)+2\beta x$ is divergence-free, may be written

$$\mathrm{div}\,\mathrm{grad}\,f=(\mathrm{grad}\,f\cdot\mathrm{grad}\,((2q/r)+2\beta x)). \tag{18}$$

In accordance with (16), the net rate of entry of (pairs of) ions into the interior of any closed surface S in the $\mathbf{r}=\mathbf{r}_2-\mathbf{r}_1$ space equals

[4] M. v. Smoluchowski, Phys. Zeits. **15**, 593 (1916); Onsager, Phys. Zeits. **28**, 277 (1928); Onsager and Fuoss, J. Phys. Chem. **36**, 2689 (1932), Section 2.

$$\int(\partial f/\partial t)dv=(\omega_j+\omega_i)kT\int(\mathrm{grad}_n f - f\,\mathrm{grad}_n((2q/r)+2\beta x))dS, \quad (19)$$

where grad_n denotes the normal component of the gradient at the surface S.

Now if the phenomenon of incomplete dissociation can be dealt with entirely by Bjerrum's picture, our task is to solve the partial differential Eq. (18)[5] with the boundary conditions:

$$f=n_j n_i \quad \text{for} \quad r=\infty, \quad (20)$$

and $fv_r=0$, (radial component of the flow); that is according to (16):

$$\mathrm{grad}_r f=f\,\mathrm{grad}_r((2q/r)+2\beta x) = f(2\beta\cos\Theta-2qr^{-2}) \quad \text{for} \quad r=a. \quad (21)$$

For the purpose of computation, the boundary condition (21) is unduly complicated, but the limit of a solution fulfilling (21) for $a=0$ is relatively simple. We shall actually apply a boundary condition for $r=0$ which will lead directly to this limiting solution.

If the formation of undissociated molecules involves special configurations and possibly the passage of a potential barrier, then the boundary condition (21) for small distances must be modified accordingly. The result (1) for the dissociation constant will not be materially affected by this complication, but the time required to establish equilibrium may be increased, because the passage of a potential barrier may be the slowest step involved in the process.

Rather than to search directly for a solution of (18) fulfilling both the boundary conditions (20) and (21), we shall compute separately the parts of f that correspond to the two processes of dissociation and recombination, so as to obtain the rate constants KA and A in the chemical kinetic equation

$$dv_{ji}/dt=-dn_j/dt=-dn_i/dt = An_jn_i-KAv_{ji}. \quad (22)$$

The state of complete dissociation we shall represent by the random distribution, which conforms to (18). Thus

$$f(\mathbf{r})=n_j n_i=\text{const.}, \quad (23)$$

whence, by (19), the rate of recombination becomes

$$An_jn_i=kT(\omega_j+\omega_i)\int n_jn_i((2q/r^2) - 2\beta\cos\Theta)r^2\sin\Theta d\Theta d\varphi = 8\pi qkT(\omega_j+\omega_i)n_jn_i. \quad (24)$$

Here, (r, Θ, φ) denote polar coordinates. For a binary electrolyte, $e_1=-e_2=e$, we obtain simply

$$A=4\pi\Lambda/D=4\pi(e_1^2\omega_1+e_2^2\omega_2)/D, \quad (25)$$

where Λ denotes the conductance per molecule in e.s.u.

When the field X (and hence β) vanishes, the undissociated molecules are according to (5), (9) and (23) represented by the part

$$f(r)=(v_{ji}/K(0))(e^{2q/r}-1)=n_jn_i(e^{2q/r}-1), \quad (26)$$

of the distribution-function, which by itself satisfies (18). This distribution corresponds to a stationary flow from a source at the origin, of the magnitude (24) but in the outward direction. It is possible to show that (26) is the only solution of (18) that satisfies the following set of boundary conditions: that $f=0$ for $r=\infty$, that there is a source of the given yield at the origin, and that the *flow from the origin through any space angle is finite.*

For $X\neq 0$, the solution of (18) under these same boundary conditions involves elaborate analysis. However, the unique result can be expressed by a definite integral in terms of known functions, as follows

$$f(r,\Theta)=gr^{-1}e^{-\beta r+\beta r\cos\Theta+(2q/r)} \times\int_{s=0}^{s=2q}J_0((-8\beta s)^{\frac{1}{2}}\cos\tfrac{1}{2}\Theta)e^{-s/r}ds, \quad (27)$$

where $J_0(z)=\sum(-)^n(z^{2n}/2^{2n}n!n!)$ denotes the ordinary Bessel function of order zero. For small values of r, the upper limit of the integral in (27) may be replaced with very good approxi-

[5] The general solution of this equation has the form:

$$f=r^{-\frac{1}{2}}e^{(q/r)+\beta x}\Sigma_n T_n(\cos\Theta)F_n(\tfrac{1}{2}i\log(\beta r^2/q)).$$

Here, T_n denotes the nth wave function of a dumb-bell dipole rotator in an electric field, and F_n a linear combination of the corresponding Mathieu functions of indices $\pm\frac{1}{2}$; $r^{-\frac{1}{2}}F_n$ is a single-valued transcendental function of r. The functions F_n and T_n are related by a Laplace transformation. The general properties of these functions will be the subject of a separate treatise.

mation by ∞, which yields

$$f(r, \Theta) \sim g e^{2q/r} e^{2\beta r \cos\Theta}, \tag{28}$$

whereby the error is of the order

$$g(\beta q)^{-\frac{1}{4}} \exp\,(4(\beta q)^{\frac{1}{2}}) \tag{29}$$

when βq is large, otherwise of the order g, and may be neglected whenever

$$\exp\,((2q/r) - 4(\beta q)^{\frac{1}{2}}) \gg 1. \tag{30}$$

By means of (28), we can easily establish the relation between the undetermined factor g and the total number of "undissociated" ion pairs. As before in discussing (8), we disregard the region $r > q$. For the region of small r, which contains practically all the "bound" pairs, we admit the approximation (28) and go one step further in that we replace the factor $\exp\,(2\beta r \cos\Theta)$ by unity.[6] We then have practically the same distribution as in the equilibrium case (26), where $1 \ll \exp\,(2q/r)$, and by comparison,

$$\nu_{ji} = gK(0). \tag{31}$$

It remains to evaluate the rate of dissociation that corresponds to the distribution (27). For this purpose, the complete function (27) must be substituted in (19); if the integral in (27) be written

$$\int_0^{2q} = \int_0^{\infty} - \int_{2q}^{\infty},$$

it turns out that only the second term on the right contributes to the flow (19). Most easily by specialization to small r, one obtains

$$-K(X)A\nu_{ji} = \int (\partial f/\partial t)dv$$
$$= -8\pi q k T(\omega_j + \omega_i) g J_1(4(-\beta q)^{\frac{1}{2}})/2(-\beta q)^{\frac{1}{2}}.$$

By comparison with (24) and (31), we see that the rate constant for the dissociation is increased by the factor

$$AK(X)/AK(0) = K(X)/K(0)$$
$$= J_1(4(-\beta q)^{\frac{1}{2}})/2(-\beta q)^{\frac{1}{2}}, \tag{32}$$

verifying (1), while the rate constant A for the recombination (cf. (24)) is not affected by the field.

[6] The corresponding error in $K(X)/K(0)$ is measured approximately by the factor $2\beta a/\sinh\,(2\beta a)$; an error of the same order has probably been made already by neglecting the hydrodynamic interaction of the ions.

Critique of Approximations

Our principal result, given by Eq. (32), may be considered a consequence of the boundary condition (21) for the limiting case $a = 0$. In this case, too, the condition (30) for allowing the approximation (28) is ideally fulfilled. In order to estimate the effect of changing the boundary condition for small r, e.g., by another choice of a in (21), we observe that the approximate distribution (28) corresponds to a *local Maxwell-Boltzmann equilibrium* for small r, in the combined Coulomb and external field.[7] Hence the distribution (28) fulfills not only the boundary condition (21) for every value of a, but (at least for binary electrolytes[7]) any possible alternative condition as well. Since it is only the difference (29) between the distribution (27) and the equilibrium distribution (28) that must be modified in order to fit a particular boundary condition for small r, we may expect that the error of (28) will not be of much greater order of magnitude than (29). Indeed, if the differential Eq. (18) is assumed valid for all distances $r = a$, with arbitrary boundary conditions for $r < a$, and provided that the Coulomb field at contact is stronger than the external field, i.e.,

$$1 - a(\beta/q)^{\frac{1}{2}} = h > 0, \tag{33}$$

then it can be shown that the relative error of (28) for $r = a$ is at most of the order

$$(q^2/a^2 h) \exp\,(-2h^2 q/a). \tag{34}$$

Therefore, as long as (34) is small, the boundary condition for small r is immaterial and our idealization of the interior region contributes but a small error to the result (32). In (34), a is of molecular dimensions and does not vary greatly from one case to another.

The variation of β is limited by the available intensities of electric fields, which do not exceed 500 kv/cm, to the range $0 < \beta < 10^7$ cm^{-1}. The most important quantity that enters into (34) is the length q, which depends on the valence type of the electrolyte and on the dielectric constant of the solvent. For uni-univalent elec-

[7] When the charges of the ions are unequal, i.e., $e_1 + e_2 \neq 0$, a true equilibrium in the external field is impossible on account of the resultant net force $(e_1 + e_2)X$ on the ion pair. Nevertheless, the ambiguity due to this force is only of the same order of magnitude as the correction discussed in footnote 6, and therefore of slight importance.

trolytes in water at ordinary temperatures, with $D=80$, we find $q=3.5\times10^{-8}$ cm, while for similar electrolytes in acetone, $q=14\times10^{-8}$ cm, and in benzene, $q=125\times10^{-8}$ cm.

From this analysis, we must be prepared to find considerable deviations from (32) in solvents of high dielectric constant like water and, to a lesser extent, acetone. Still, we know that in such solvents, the only *weak electrolytes* are those for which a very close approach of the ions can occur and if a is computed from the dissociation constant according to Bjerrum's theory,[3] then for any weak electrolyte in any solvent

$$\exp(2q/a)\gg1.$$

The weight that can be given to this reassuring consideration depends on the actual laws of motion for small distances between the ions. Rather than to utilize unlimited opportunities for interesting conjecture, it seems proper to wait until adequate experimental material can guide the theory, if one should be required.

For distances r that are substantially greater than molecular and ionic dimensions, the laws of motion are known with practical certainty; but the exact equations which result lead to excessive mathematical difficulties. Our fundamental equation (18), which we were able to solve, represents several simplifications of the physical picture. We shall discuss the nature of these approximations, and estimate their effects.

First of all, we must admit that in formulating the equations for ionic motion, the hydrodynamic interaction was neglected. Except for structure-dependent terms of the order $1/r^3$, this interaction decreases the mutual mobility of the ions,

$$\omega_1+\omega_2,$$

by the amount

$$1/2\pi\eta r, \qquad (\eta=\text{viscosity}),$$

in the direction connecting the two ions, and by half this amount in any perpendicular direction. It is very difficult to estimate how much this effect will modify the distribution (27) and the result (32) for the dissociation constant. So much seems certain, that the correction will be inversely proportional to $\omega\eta$, that is proportional to the Stokes "radius,"

$$\rho=1/6\pi\eta\omega.$$

Moreover, in case $q=0$ (one ion neutral), the hydrodynamic interaction does not disturb the uniform distribution which results from (23) alone, while (27) vanishes. Therefore, the hydrodynamic correction is probably proportional to some power of q. Every power of ρ or q must be multiplied by β to make the result dimensionless, so that we obtain the following estimate for the order of the hydrodynamic correction:

$$K(X)/K(0)=F(2\beta q)+O(\beta^{n+1}\rho q^n)$$
$$=1+2\beta q+\cdots+O(\beta^{n+1}\rho q^n).$$

This correction increases with the intensity of the field. For high field intensities it may become important in any solvent, but even so, it ought not to change the order of magnitude of the principal effect.

Finally, we have to discuss the shielding of the Coulomb forces due to the Debye-Hückel "ionic atmosphere," which has been neglected so far. When no external field is present, this shielding decreases the work required to separate a pair of ions by the amount

$$-kT\log\Pi(\gamma)=2\kappa qkT,$$

where κ is the mean inverse distance of the shielding charge. The factor $\Pi(\gamma)$ is called the activity coefficient product, and is usually written

$$\gamma_1\gamma_2/\gamma_{12}=\Pi(\gamma).$$

It enters as a correction to the mass-action law when the concentration of free ions becomes appreciable, in the form

$$c_1c_2/c_{12}=K_c=K_0/\Pi(\gamma),$$

where K_c is called the "stoichiometric" or apparent dissociation constant for the concentration in question, and K_0 the "true" dissociation constant.

We shall show next that for high field intensities, that is when

$$\beta\gg\kappa,$$

the value of $K(0)$ to be employed in (32) is the true dissociation constant K_0, and not K_c. The reason is that, as seen from (27), the modification of the distribution due to the external field proceeds by peeling off the excess density of ions from the outside inwards to a distance of the order $1/\beta$ in all directions except $\Theta=0$. The only effect of the ionic atmosphere is to

reduce the concentration gradients for distances of the order $1/\kappa$. Now if the external field is strong enough to break down the concentration gradients for all distances $r>1/\beta$, where $1/\beta \ll 1/\kappa$, then the shielding charge in the ionic atmosphere can have no further effect.

Conversely, the field requires a leverage of the length $1/\beta$ to modify the distribution; because over a path of this length, the work of the field is comparable to kT. When $\kappa \gg \beta$, then the atmospheric shielding levels the concentrations for all distances r that afford sufficient leverage for the field. In this case, it is the effect of the field that becomes very small.

The conclusions from these considerations can be summarized as follows:

$$\begin{aligned} K(X)&=K_0F(2\beta q)+O(\kappa^2 q/\beta)=K_0(1+2\beta q+\cdots)\\ &\quad +O(\kappa^2 q/\beta), \quad \text{when} \quad \beta\gg\kappa;\\ K(X)&=K_c+O(\beta^2 q/\kappa)=K_0(1+2\kappa q+\cdots)\\ &\quad +O(\beta^2 q/\kappa), \quad \text{when} \quad \beta\ll\kappa. \end{aligned} \tag{35}$$

The estimated orders of the corrections are probable conjectures.

When κq and $\kappa\rho$ are appreciable, it is also necessary to allow for the effect of the "atmosphere" on the migration of the free ions, and for the modification of this action by the field, that is the "ordinary" Wien effect as observed for strong electrolytes. This correction does not affect the dissociation equilibrium itself, but only the relation between the free ion concentration and the conductance of the solution.

A computation of these effects for small β has been given by Joos and Blumentritt.[8] A computation of all terms of the orders q and ρ = Stokes radius, homogeneous of the first order in κ and β, is in progress.[9] The results for very strong fields are simple: the asymmetry of the ionic atmosphere becomes negligible, but a part of the "electrophoresis" remains. For binary electrolytes, the conductances in weak and in strong fields are

$$\begin{aligned} &\Lambda=\Lambda_0-(A\Lambda_0+B)(c)^{\frac{1}{2}}, \quad \beta=0;\\ &\Lambda=\Lambda_0-(B/2^{\frac{1}{2}})(c)^{\frac{1}{2}}, \quad \beta\gg\kappa. \end{aligned} \tag{35a}$$

The constants A and B are the same for all binary electrolytes of the same valence.

Discussion of Theoretical Results

The increase of the dissociation constant due to the field is measured by the parameter

$$\begin{aligned} b=2\beta q&=\frac{z_1\omega_1+z_2\omega_2}{\omega_1+\omega_2}z_1z_2\frac{|X|\epsilon^3}{2Dk^2T^2}\\ &=\frac{z_1^2z_2^2(\Lambda_1+\Lambda_2)}{z_2\Lambda_1+z_1\Lambda_2}\cdot 9.636\frac{V}{DT^2}, \end{aligned} \tag{36}$$

where z_1 and z_2 are the valences of the ions, Λ_1 and Λ_2 the equivalent conductances, ϵ the electronic charge, X the field in e.s.u., and V the field measured in volt/cm. For uni-univalent electrolytes, (36) reduces to the simple result,

$$b=9.636V/DT^2. \tag{37}$$

The function (1) can be computed from the power series

$$K(X)/K(0)=F(b)=1+b+\frac{b^2}{3}+\frac{b^3}{18}+\frac{b^4}{180}+\frac{b^5}{2700}+\frac{b^6}{56700}+\cdots \tag{38}$$

or, for large values of b, from the asymptotic expansion

$$F(b)\sim(2/\pi)^{\frac{1}{2}}(8b)^{-3/4}e^{(8b)^{\frac{1}{2}}}\times\left\{1-\frac{3}{8(8b)^{\frac{1}{2}}}-\frac{15}{128.8b}-\frac{105}{1024((8b)^{\frac{1}{2}})^3}-\cdots\right\}, \tag{39}$$

where, for $b\geqq 3$, the remainder of the series is less than $1/130b^2<10^{-3}$.

The increase of the concentration c_i of free ions due to the altered dissociation constant is given by the mass-action law. For binary electrolytes this law takes the form

$$c\alpha^2/(1-\alpha)=K=K_0F(b), \tag{40}$$

where c denotes the total concentration of electrolyte, and $\alpha=c_i/c$ the degree of dissociation. The increase of the conductance λ is proportional to the displacement of the dissociation equilibrium:

$$\lambda/\lambda_0=c_i/c_{i0}=\alpha/\alpha_0.$$

[8] M. Blumentritt, Ann. d. Physik [5] **1**, 195 (1929).

[9] For an approximate treatment of this problem see H. Falkenhagen, Phys. Zeits. **32**, 353 (1931).

It is seen from (40) that the displacement due to a given change of K depends on the initial degree of dissociation, α_0.

The change of K with the field for binary electrolytes depends only on one individual characteristic, the valence (cf. Eq. (36)). We shall see that the uniformity, thus predicted by the theory, is indeed borne out by experience. In spite of its simplicity, this law has remained undiscovered because previous workers have only paid attention to the variation of λ with the field, and have failed to properly allow for the effect of α.[10]

In discussing the influence of α, we shall limit ourselves to binary electrolytes. Further complications are to be expected in mixed electrolytes and in cases of step-wise dissociation, but the binary case is the most important, and will suffice for illustration.

In general, α/α_0 decreases with increasing α_0. It is instructive to specialize (40) for small values of b. If we neglect all terms of the order b^2 and higher in (38) and in (40), we get

$$\frac{\Delta\lambda}{\lambda}=\frac{\Delta\alpha}{\alpha}=\frac{(1-\alpha)}{(2-\alpha)}\frac{\Delta K}{K}=\frac{(1-\alpha)}{(2-\alpha)}b. \qquad (41)$$

When the dissociation is nearly complete, the change due to the field is proportional to the remaining fraction, $1-\alpha$, of undissociated electrolyte. In the other extreme, $\alpha\ll 1$, the effect approaches a maximum which is given for all values of b by the simple formula,

$$\lambda/\lambda_0=\alpha/\alpha_0=(K/K_0)^{\frac{1}{2}}=(F(b))^{\frac{1}{2}}$$
$$=1+\frac{1}{2}b+\frac{1}{24}b^2+\cdots. \qquad (42)$$

The function $(F(b))^{\frac{1}{2}}$ is represented graphically in Fig. 1.

Formula (42) applies whether the molecules and the ions are simple or complex, as long as all kinds of ions have the same charge (± 1 or ± 2, etc.), and the total number of ions is small compared to the number of molecules. This is important for the application to solvents of low dielectric constant, where complexity is the rule, but the ionized fraction of the solute is always small.[11]

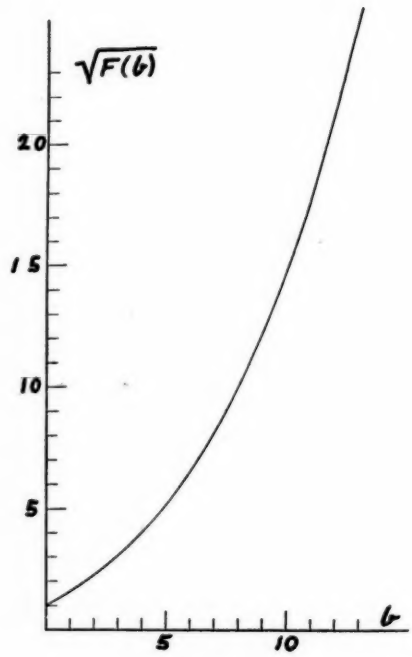

FIG. 1.

The characteristic parameter b is proportional to the cube of the valence, and inversely proportional to the dielectric constant of the solvent. It is illuminating to compare extremes among solvents. For uni-univalent electrolytes in water at 25°C, with $D=78.57$, we get

$$b=1.384\times 10^{-6}V, \qquad (43)$$

but in benzene, with $D=2.280$, at the same temperature,

$$b=47.5\times 10^{-6}V. \qquad (44)$$

Since in either medium, the strongest practically obtainable fields are about the same, of the order 5×10^5 volts/cm, the greatest effect that can be obtained in water is approximately

$$\lambda(X)/\lambda(0)=c_i(X)/c_i(0)$$
$$=(F(b))^{\frac{1}{2}}=(F(0.7))^{\frac{1}{2}}=1.37,$$

while in benzene, for $X=5\times 10^5$ volts/cm,

[10] It is but fair to point out that in many cases, reliable determinations of α are lacking. The qualitative effect of α has been recognized by Schiele, Ann. d. Physik [5] **13**, 811 (1932).

[11] Kraus and Fuoss, J. Am. Chem. Soc. **55**, 21 (1933); Fuoss and Kraus, ibid. **55**, 2387 (1933).

$$\lambda(X)/\lambda(0) = c_i(X)/c_i(0) = (F(b))^{\frac{1}{3}} = (F(23.7))^{\frac{1}{3}} = 121.$$

Even in water, however, very large effects could be expected if it were possible to dissolve a weak electrolyte of high valence type.

When an electric field is applied suddenly to a solution, some time will pass before the new dissociation equilibrium becomes established. The approach to equilibrium is described by the mass-action law (22). The recombination constant A, which determines the reaction velocity, is equal to our theoretical value (24) whenever the mutual approach of the ions is the slowest step in the reaction; otherwise it is smaller. For a binary electrolyte, the solution of (22) can be written in the form,

$$(\alpha-\alpha_0)/(\alpha+\alpha_0/(1-\alpha_0)) = Ce^{-t/\tau}, \qquad (45)$$

where α denotes the degree of dissociation at the time t, α_0 the steady value of α, C is an integration constant, and the time-lag equals

$$\tau = (1-\alpha_0)/(2-\alpha_0)n\alpha_0 A.$$

For binary electrolytes, our computed maximum A takes the very simple form (25), and if we may adopt this value, we get the interesting result

$$\tau = \frac{1-\alpha_0}{(2-\alpha_0)n\alpha_0 A} = \frac{(1-\alpha_0)}{(2-\alpha_0)}\frac{D}{4\pi\lambda}, \qquad (46)$$

where $1/\lambda$ denotes the specific resistance of the solution, measured in electrostatic units, i.e., seconds (1 sec. $= 9\times10^{11}$ ohm cm). When $\alpha_0 \ll 1$, the time-lag is simply

$$\tau = D/8\pi\lambda. \qquad (46a)$$

This is substantially the same as the time needed for any readjustment of charges in an electrolytic conductor. For example, suppose that a pair of charges $\pm e$ be introduced on a pair of ideal electrodes, so arranged that practically all the force lines run between the electrodes. Without any further restrictions, the time needed for neutralization or shielding of the charges will be:

$$\text{capacity} \times \text{resistance} = D/4\pi\lambda,$$

i.e., twice that given by formula (46a). The relaxation of the Debye-Hückel "ionic atmosphere" is a similar process, and the time involved is of the same order of magnitude.

In formulas (45), (46) and (46a), α_0 and λ refer to the steady state in a field of intensity X, and both α_0 and λ increase with X. Hence *the time-lag decreases with increasing field intensity.* This consequence of the theory is important for the application to saturation in strong fields. The saturation current may increase more rapidly with the field intensity than the conductance.

Experimental Verification

The increased conductances due to strong electric fields have been measured for a number of substances, in several solvents. The following have been selected as a fair sample: Acetic and chloroacetic acids in aqueous solution,[16] cobalt chloride in acetone,[19] and picric acid in benzene containing some alcohol.[21]

Acetic and chloroacetic acids are among those electrolytes whose dissociation constants in aqueous solution have been determined with great precision. We shall base our computations on the conductance data of MacInnes and Shedlovsky,[12] who give $K = 1.753\times10^{-5}$ for acetic acid at 25°, and those of Saxton and Langer,[13] who give $K = 1.396\times10^{-3}$ for chloroacetic acid at the same temperature. The values found by electromotive force measurements at 25° are $K = 1.754\times10^{-5}$ for acetic acid[14] and $K = 1.378\times10^{-3}$ for chloroacetic acid.[15] Incidentally, the latter sources[14, 15] give data over ranges of temperature from 0° to 60° and from 0° to 40°, respectively.

Unfortunately, Schiele does not specify the concentrations of acids used in his experiments, nor the temperatures, but only the conductances of his solutions. Probably, the temperatures were not far from 25°, perhaps 5 or 10 degrees lower. In the absence of better directions, the added labor involved by computation for some temperature different from 25°, even if slightly more plausible, was not considered worth while.

---

[12] MacInnes and Shedlovsky, J. Am. Chem. Soc. **54**, 1429 (1932).

[13] Saxton and Langer, J. Am. Chem. Soc. **55**, 3638 (1933).

[14] Harned and Ehlers, J. Am. Chem. Soc. **55**, 652 (1933).

[15] Donald D. Wright, J. Am. Chem. Soc. **56**, 314 (1934).

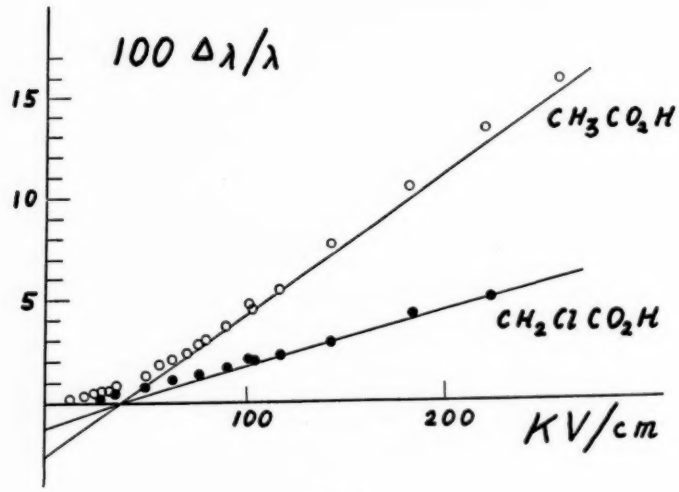

FIG. 2.

The overall error that arises from our overestimate of the temperature is probably of the order 0.3%. Since the sensitivity in Schiele's measurements was of the order 0.03%, a later revision of our calculations to the correct temperatures may be justified. It must be borne in mind, however, that in the experiments where Schiele found a reasonably large effect, the field intensities could not be determined with an accuracy comparable to the sensitivity for small differences of resistance.

Schiele did not measure directly the entire increase of the conductance due to the field, but instead, the difference between the conductances of weak electrolytes and a strong acid, HCl, as a function of the field intensity. This procedure practically eliminates the error due to heating and in addition, the "general" Wien effect of the free ions. In the cases which we have selected, two electrolytes of the same valence type and nearly equal conductances were compared. In consequence, the compensation of the general Wien effect was particularly good, within 0.03% as estimated from formula (35a). This means that we make no appreciable error when we attribute the differential effects measured by Schiele for monobasic acids entirely to the increased ionization of the weak acids.

In Fig. 2, Schiele's[16] measurements for acetic acid and for chloroacetic acid are compared with the computed concentrations of free ions. The calculation is based on a *stoichiometric* dissociation constant $K(X)=K_0F(b)$. For $X=0$, this computed dissociation constant is in error by the factor[3]

$$\gamma^2=\exp\,(-2\kappa q/(1+\kappa q))$$

due to the weakening of the interionic attraction by the "atmosphere." With increasing field intensity, the effect of the atmosphere is eliminated. The agreement between theory and experiment is most striking, all the more when one considers that the computation of the theoretical curves involves no adjustable constants.

The discrepancies between theory and experiment in Fig. 2 are within the limits of uncertainty of this comparison, and perhaps of the measurements. The difference between the two acids depends entirely on the degree of dissociation. Other acids investigated by Schiele fit equally well into the picture. Propionic acid behaves almost exactly like acetic, as it should. Phosphoric acid, conductance 2×10^{-4}, shows a small effect, 1.8 percent at 260 kv/cm, which agrees quantitatively with Nims' result,[17] $K=8\times10^{-3}$ at 20°, for the first dissociation constant; the second dissociation is negligible.

For weak bases, Schiele[18] found somewhat smaller effects than expected from the theory. On the other hand, the effect found for NaOH

[16] J. Schiele, Ann. d. Physik [5] **13**, 811 (1932).

[17] Nims, J. Am. Chem. Soc. **56**, 1110 (1934).

[18] Schiele, Phys. Zeits. **34**, 60 (1933).

was surprisingly high, in fact, equal to that of $Ba(OH)_2$. This strange coincident could perhaps be explained by the absorption of CO_2 from the air; it would not be safe to draw conclusions until this question has been settled.

In view of the approximations which we have discussed before, we must be prepared to find appreciable deviations from our theoretical formula for the highest field intensities. It is a bit surprising that the acids in water agree as well as they do. This may be due to the small Stokes' radius, in which case the slower ions of the bases might lead to greater deviations. However, it would be easier and even more interesting to investigate a weak salt, so as to get a still greater hydrodynamic effect. A possible suggestion is mercuric chloride, which dissociates according to the scheme

$$HgCl_2 \rightleftarrows HgCl^+ + Cl^-.$$

A strong salt, for example NaCl, could be used for comparison. Since weak salts may be liable to greater time-lags than acids, the effect of time should be investigated.

Some di- and tribasic acids, among them sulfuric, tartaric and ferricyanic acids, also were investigated by Schiele. In these cases, the differential effects against HCl is partly due to the general Wien effect, and partly to the increased dissociation. For this reason, and in view of the inaccurate data on the dissociation of the acids in question, it is not practicable at present to use these cases for a test of the theory. The general trend of the results seems to be in accord with the theory.

In applying the data of F. Bauer[19] for the Wien effect in acetone we meet with similar difficulties. Bauer was more interested in the general Wien effect of free ions, than in the increased dissociation of weak electrolytes. In the cases where he extended his experiments to the highest field intensities that he could get, his main purpose was to determine the upper limit of the general Wien effect. For weak electrolytes he then found very large effects, which gave little indication, if any, of approaching a limit. As outstanding examples he mentions, in the order of increasing effects, LiBr, $CoCl_2$ and $Co(NO_3)_2$. The results for the last named substance are not given in his article, except by a qualitative description. The next best case from our point of view is $CoCl_2$. Adequate data for the dissociation of this salt are not available. Bauer describes measurements but fails to publish the complete results. In Fig. 3, the solid curves and the points represent Bauer's data for the Wien effect of $CoCl_2$ in acetone, while the theoretical curve (dashes) has been computed on the assumptions $\alpha \ll 1$; $\gamma^2 = 1$, which necessarily lead to an overestimate of the effect. The predicted effect is evidently large enough to account for Bauer's results. In fact, a prediction based on reasonable estimates of α and γ still leads to values which are somewhat greater than those observed by Bauer. The discrepancy might arise from errors in our estimates of α and γ, or else from the time-lag of the dissociation equilibrium, which would then have to be considerably *greater than our theoretical minimum* (46a). The latter explanation finds support in Bauer's remarks about the time-effect, and with the data given in his Fig. 4. Unfortunately, the interpretation of these data remains ambiguous, for Bauer failed to specify the conductances of the solutions in connection with the time-lag.

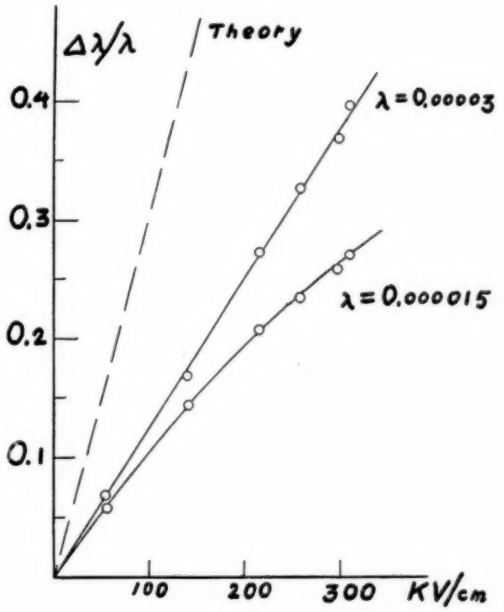

FIG. 3.

[19] F. Bauer, Ann. d. Physik [5] **6**, 253 (1930).

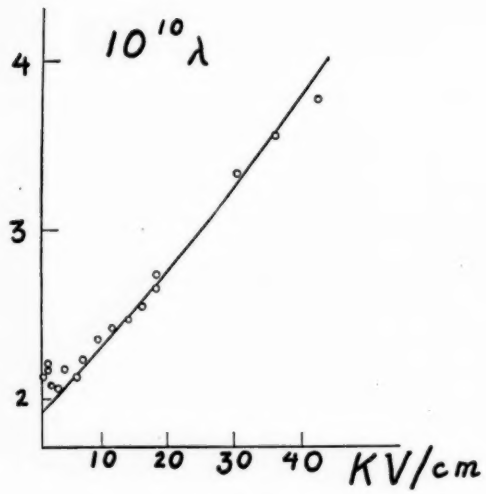

FIG. 4.

In solvents of very low dielectric constant, such as benzene, the application of the theory is no longer complicated by the variation of the degree of dissociation α, which is always very small. Moreover, in most cases the activity coefficients will be practically equal to unity; in benzene, only a few very good electrolytes provide exceptions.[11, 20] We therefore expect the great majority of conducting solutions in solvents of low dielectric constant to exhibit the simple variation of conductance with the field intensity, which is described by our formula (42). When the dielectric constant is as low as that of benzene, a field of less than 40 kv/cm will suffice to double the conductance.

This class of conductors includes the liquid insulators used in electrotechnics. It is common knowledge that the conductance of a transformer oil increases with the field intensity. However, most investigators have failed to separate the opposing effect of saturation, so that their results are by no means direct measurements of the conductance. Only A. Gemant[21] made successful efforts to find "semiconducting" solutions that would lend themselves more readily to a quantitative study of the field effect. In order to obtain reproducible results, he replaced the transformer oil by a mixture of benzene and ethyl alcohol for solvent, with picric acid as electrolyte. By the addition of phenol or mineral oil in moderate amounts, the temperature coefficients of the conductances could be adjusted to zero. Thanks to the higher conductance of his solutions as compared to transformer oil, the saturation of the current was negligible in his experiments, at least if the time-lags for his electrolytes are of the order given by our minimum estimate (46). Gemant used a steady direct current, and derived the resistances of his solutions from measurements of voltage and current.

The dielectric constants of Gemant's solutions have not been measured, but they can be estimated with reasonable certainty from available data on solutions of ethyl alcohol in benzene.[22] For a solution containing 1 percent picric acid, 5 percent ethyl alcohol and 1 percent mineral oil, of conductance $\lambda=2\times10^{-10}$, the estimated dielectric constant is $D=2.71$ at 20°. For another solution, which contained 1 percent picric acid, 8 percent ethyl alcohol and 3 percent mineral oil, of conductance $\lambda=4\times10^{-9}$, our estimate is $D=3.03$ at 20°. Both estimates involve extrapolation of Stranathan's data,[23] which only cover concentrations of ethyl alcohol up to 4.3 percent.

In Figs. 4 and 5, Gemant's data for the two solutions referred to are compared with the theoretical formula (42). Both the magnitude and the general type of the effect conform approximately to the theory. The agreement in Fig. 4 is almost as good as for Schiele's data in aqueous solutions, Fig. 2. However, both figures 4 and 5 indicate a flattening out of the experimental curves for low field intensity, which cannot be explained by the present theory. While some flattening of the curves due to the effect of the atmospheres should indeed be expected, the observed effects seem much too large. The concentrations of free ions can be estimated from the conductances, if reasonable assumptions about the equivalent conductances Λ are allowed. For the case represented in Fig. 5, $\Lambda=40$ is hardly an overestimate. On this basis,

[20] Kraus and Vingee, J. Am. Chem. Soc. **56**, 511 (1934).

[21] A. Gemant, *Elektrophysik der Isolierstoffe*, p. 78, Springer, Berlin, 1930.

[22] J. Stranathan, Phys. Rev. **31**, 653–71 (1928).

[23] A. Gemant, *Elektrophysik der Isolierstoffe*, p. 80, Springer, Berlin; Phys. Zeits. **29**, 289 (1928).

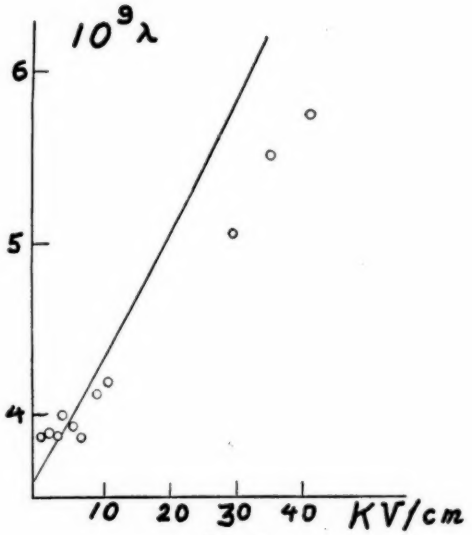

FIG. 5.

the concentrations of free ions would be 10^{-7}, and the activity coefficient would be $\gamma=0.95$. The value of λ for $X=0$, computed by the theory from the three highest points, is 3.17×10^{-9}; the given activity coefficient would raise this value to 3.34×10^{-9}, but by no means up in the neighborhood of 4×10^{-9}, as indicated by the data.

In one other respect, the present theory fails to agree with Gemant's results. Since the theory predicts an increase of electrolytic dissociation, the resultant increase of the conductance should be independent of the direction. Gemant[23] made special arrangements to measure the conductance perpendicularly to a strong field, and found that the transverse conductance increased much less with the field intensity than the longitudinal, if at all.

On the whole, the verification of the theory is satisfactory. In some instances, the numerical agreement is excellent, and with one exception, an effect of the predicted order of magnitude has been observed. The only qualitative discrepancy is Gemant's failure to find a substantial transverse effect.[23] The discrepancies cannot be interpreted without further experimental evidence.

APPLICATIONS TO SOLID ELECTROLYTES

Most ionic solids possess an intrinsic conductance, which is ordinarily electrolytic. In addition, a photoconductance induced by sunlight or by natural γ-radiation may be present. The intrinsic conductance is characterized by its regular variation with the temperature. Its electrolytic mechanism can often be established by the verification of Faraday's law for suitable temperatures, or by the evidence of polarization. For part of the time at least, the mobile ions must occupy abnormal positions in the structure of the solid. If a process of exchange takes place regularly between the mobile and the normal ions, perhaps something like the process,

$$2H_2O \rightleftarrows H_3O^+ + {}^-OH,$$

which takes place in pure water, then the solid will behave like a weak electrolyte. If the mobile ions should arise from permanent faults in the lattice, then the solid electrolyte would be weak or strong, according to the frequency of recombination of the ions. There is no conclusive evidence that strong solid electrolytes exist.

There is no reason why the present theory for the dissociation of weak electrolytes in strong fields could not be applied to solids, except that for highly anisotropic crystals, the quantitative relation between conductance and field intensity might be different.

It was first shown by H. H. Poole[24] that solid dielectrics exhibit deviations from Ohm's law. Poole demonstrated this effect in fields of the order 10^6 volt/cm for glass, mica, shellac and celluloid (Kodak film). He could describe his results fairly well by the formula,

$$\log_{10}\lambda = A - B|X|.$$

His values of B range from 1.2×10^{-6} for mica to 3.80×10^{-6} for celluloid. In the case of glass, but not in the case of mica, the constant B was found to decrease with increasing temperature.

H. Schiller and N. Albrecht[25] found similar results for glass, mica and gypsum. In their experiments with glass, considerable polarization was evident. For mica, which will stand up in very strong fields if thin enough, Poole's formula was found valid only for a limited range of field intensities. In the range $10^6<X<3\times10^6$ volt/cm, log λ increases less rapidly with the field than for $X<10^6$ volt/cm. A field of the in-

[24] H. H. Poole, Phil. Mag. **32**, 112 (1916); ibid. **34**, 204 (1917); ibid. **42**, 488 (1921).

[25] H. Schiller, Ann. d. Physik [4] **81**, 32 (1926).

tensity 3×10^6 volt/cm increases the conductance of mica by a factor of more than a thousand.

The effects found by these investigators were not quite as large as those predicted by the present theory, but of the expected order of magnitude. The agreement is comparatively good for very high field intensities, which tend to suppress polarization and time-lags. The deviations from Poole's formula observed by Schiller are in the direction expected by the theory, cf. our asymptotic formula (39).

Finally, it may be pointed out that Poole's values for his characteristic parameter B were about inversely proportional to the dielectric constant of the materials, which may be taken as a crude verification of our theoretical prediction $b\sim1/D$ (formula (37)).

As yet, the deviations from Ohm's law in solids have not been explored to any great extent. It would be advantageous to eliminate the complicating effect of polarization. This could probably be achieved by appropriate choice of electrodes, such as silver electrodes for the investigation of silver halides, or *alkali metal electrodes* for glasses and other alkali silicates.

Time-Lags and Polarization

In many cases it is important to know not only the dissociation constant as a function of the field intensity, but the actual reaction velocities of electrolytic dissociation and recombination as well.

We have shown that the time required for the mutual approach and departure of the ions determines a certain maximum value (Eqs. (24) and (25)) for the kinetic coefficient constant of recombination. For binary electrolytes, the corresponding minimum time-lag for adjustment of the dissociation equilibrium is given by Eq. (46),

$$\tau=\tau_L=\frac{(1-\alpha_0)}{(2-\alpha_0)}\frac{D}{4\pi\lambda}.$$

This minimum time of adjustment we shall call the Langevin time-lag, because the underlying theory of ionic recombination was first derived by Langevin.[26] When the steady degree of dissociation α_0 is very small, the Langevin time-lag equals half the Maxwell time-lag, $\tau_M=D/4\pi\lambda$, for the readjustment of charges in a conductor.

The mutual approach of two ions will not in all cases complete the recombination, which may involve a molecular rearrangement of the pair. If the time needed for this rearrangement is smaller than the Langevin time-lag, then it is of no importance. Otherwise, we have to consider two reversible reactions with different time-lags:

$$\begin{aligned}&\text{cation}+\text{anion}\rightleftarrows\text{pair};\quad(\tau=\tau_L);\\&\text{pair}\rightleftarrows\text{molecule};\quad(\tau=\tau_c>\tau_L).\end{aligned}\tag{47}$$

When $\tau_c<\tau_L$, all the molecules may be counted as ion pairs. The Langevin time-lag τ_L depends on the degree of dissociation α_0 of the ion pairs, and on the conductance λ in the steady state. Both of these depend on the intensity of the electric field (although, when $\alpha_0\ll1$, only the change of λ matters). As a result, the Langevin time-lag decreases with increasing field; when $\alpha_0\ll1$, the relation between the two is

$$\tau_L=D/8\pi\lambda(X)=D/8\pi\lambda(0)(F(b))^{\frac{1}{2}}.\tag{48}$$

The chemical time-lags, τ_c, will not be affected by the field. *Only one of the four reactions represented in the scheme* (47) *is affected by the field, namely the dissociation:*

$$\text{pair}\rightarrow\text{cation}+\text{anion};$$

the kinetic constant of this reaction is increased by the factor $F(b)$.

It is reasonable that cases of the type (47) should exist, and some experimental indications have been found, although there is no certain evidence of chemical time-lags from measurements of conductance in strong fields. Two conditions must be satisfied in order that the chemical time-lag can be measured. First, the concentration of molecules must obviously be at least comparable to the concentration of free ions. Secondly, *the concentration of free ions must be at least comparable to the concentration of ion pairs*. Otherwise, even a large displacement of the equilibrium between ions and pairs will not

[26] Langevin, Ann. chim. phys. **28**, 433 (1903), applied his theory to ionized gases. See Herzfeld, Phys. Rev. **34**, 791 (1929); ibid. **37**, 287 (1931), for applications to dielectrics.

materially disturb the equilibrium ratio between pairs and molecules, and the subsequent adjustment of the latter will involve changes too slight to be detected. The condition for detecting chemical time-lags by saturation currents is somewhat milder: The rate of removal of free ions must be comparable to the rate of conversion of molecules into pairs.

In Schiele's measurements (Fig. 2), the electric fields were applied for time intervals of the order 10^{-6} sec., about the shortest admissible in view of the Langevin time-lag for acetic acid of conductance $\lambda = 2 \times 10^{-4}$. We calculate

$$\tau_L = 1.7 \times 10^{-8} \text{ sec.}$$

Since Schiele's conductances agree with the theoretical steady values, any chemical time-lag involved in the dissociation of acetic, chloroacetic and phosphoric acids in water must likewise be of the order a few times 10^{-8} sec. or less. The slightly lower field effects found by Schiele for bases might be due to greater time-lags (between 10^{-6} and 10^{-7} sec.); but as we have pointed out, it does not appear certain that sufficient precautions were taken to exclude carbon dioxide in his experiments with bases.

It would be worth while to investigate by this method the possible time-lags in the dissociation of other electrolytes as well. The dissociation of weak salts ought to be slower, in general, than the proton exchange involved in the dissociation of acids and bases.

For solutions in acetone, F. Bauer[19] made some interesting observations of time-lags. He worked with conductances in the range

$$0.000015 < \lambda < 0.0004;$$

the corresponding Langevin time-lags for sparingly dissociated electrolytes lie in the range

$$2 \times 10^{-9} < \tau_L < 4 \times 10^{-8} \text{ sec.}$$

The data represented in Bauer's Fig. 4 indicate time-lags of the order 10^{-7} sec. for cobalt chloride, and two or three times greater for mercuric chloride.

In liquid and solid electrolytic semiconductors, the Langevin time-lag can range from fractions of a second to the order of an hour. However, as I have pointed out in discussing the conductance of such substances, in most experiments the field effect and the polarization have not been separated. It will therefore be necessary to discuss the interaction of the two effects.

The observed polarizations are of the order of kilovolts, and are probably analogous to the saturation phenomena in gases. When the electrodes furnish no ions, which is frequently the case, the total current cannot exceed the rate of production of ions by dissociation of molecules (ion pairs) in the interior of the dielectric. For a given rate of dissociation, the saturation current is evidently proportional to the volume.

The removal of ions starts at the electrodes: The region near the cathode becomes depleted of anions, and *vice versa*. As long as the current remains considerably below that necessary for complete saturation, the concentrations of both ions midway between the electrodes will be maintained by the normal kinetic equilibrium of dissociation and recombination. Near the electrodes, the dissociation must exceed the recombination by an amount that equals the rate of removal of ions. Therefore, the thickness of each electrode layer will be proportional to the intensity of the field, unless the field itself affects the rate at which the dissociation takes place. The electrode layers contain space charges, which intensify the fields near the electrodes. The resultant excess potential drop appears as a "polarization." For transformer oils, the excess fields near the electrodes have been demonstrated by Whitehead and Marvin,[27] and the space charges by A. Gemant.[28]

There also is evidence of genuine polarization from some of the experiments performed by Whitehead and Marvin, in which a considerable increase of the conductance was observed after reversal of the current. The quick appearance of the carriers would seem to exclude the possibility that they were formed after the current was reversed. Hence, the only reasonable explanation for the increased conductivity is the accumulation of undischarged ions in the immediate vicinity of the electrodes. Since the layer involved ought to be very thin in the case of strong fields, the polarization is not likely to become greater than a few volts. However, the local

[27] Whitehead and Marvin, A. I. E. E. Trans. **48**, 299 (1929), ibid. **49**, 647 (1930). See also Herzfeld.[26]

[28] A. Gemant, Elektrotech. Zeits. **54**, 468 (1933).

field in the polarization layer might become quite considerable, and could possibly play a part in the breakdown of dielectrics.

For the interpretation of certain experiments on the initial conductance of dielectrics, it might be worth while to consider the adsorption of ions by the electrodes due to the electrostatic image force. This effect would tend to increase the equilibrium concentration of ions, and to accelerate the separation of ion pairs in a layer of the thickness $q \sim 10^{-6}$ cm near the electrodes. The effect would be greater, the smaller the distance of closest approach between the ions and the metal. In order to interpret any part of the charging current curves found by Whitehead and Marvin as due to adsorption, it is necessary to assume a least distance of approach smaller than 3×10^{-8} cm. The current of adsorbed ions ought to exhibit a Schottky effect, which might account for the observed increase of the initial conductance with field intensity.

The experiments of Whitehead and Marvin are outstanding in the detailed study of individual factors, such as time-lags, and in the consistent limitation to relatively weak fields. Thanks to the latter precaution, the increase of the dissociation constant due to the field in their experiments could not have exceeded fifty percent (for 10^4 volt/cm), except in the cases where the fields were locally enhanced by space charges. Therefore, their investigation represents a rather clear-cut study of the saturation phenomena, without serious complications due to the field effect.

In most other investigations recorded in the literature, the experimenters sought one of the effects, and apparently measured a combination of both. The task of separating the factors that enter into the results then becomes rather hopeless. Hence, it seems proper to discuss only the most pertinent simple deductions that can be made from the present theory, and to draw tentative general conclusions from the available mass of data.

In applying the scheme (47) to liquids of dielectric constant less than 3, we must bear in mind that at equilibrium, even when the concentration of free ions is as low as 10^{-10} mol/l, the concentration of ion pairs will almost certainly be large in comparison. This conservative inference from the data of Kraus and Fuoss[11] is another example of the valuable general information that can be gained by studying solutions of known electrolytes in well purified solvents.

We now recognize that when a considerable chemical time-lag exists, the saturation phenomena will develop through two essentially different stages.

At first, the ions removed by electrolysis will be replaced by dissociation of ion pairs at the Langevin rate. The modifications of the field by space charges will be moderate (a factor of the order 2), as long as the concentration of ion pairs is nowhere greatly reduced. However, after the electrode regions have been depleted of ion pairs, the subsequent production of ions in these regions will be determined by the slower transformation of molecules, and the electrode layers will expand accordingly. The conditions in this second stage permit the development of much greater fields, so that even the concentration of cations near the cathode and that of anions near the anode will be greatly lowered due to their high velocities.

With this general picture in mind, certain predictions can be made regarding the magnitude of the saturation current. First, if there is a chemical time-lag $\tau_c > \tau_L$, and the saturation current is measured after the ion pairs have been removed by electrolysis, then the current will be found independent of the field intensity. On the other hand, if there is no appreciable chemical time-lag, or if the saturation current is measured before any great fraction of the ion pairs have been electrolyzed, then we shall expect the saturation current to increase with field intensity X, in the ratio

$$i_{\text{sat}}(X)/i_{\text{sat}}(0) = K(X)/K(0) = F(b). \quad (49)$$

For comparison, the conduction current in the case of no saturation increases with the field intensity as

$$i = X\lambda(X) = X\lambda(0)(F(b))^{\frac{1}{2}} \sim b(F(b))^{\frac{1}{2}}.$$

It is seen from Fig. 1, that for $b > 4$, the ratio $(F(b))^{\frac{1}{2}}/b$ increases with the field intensity. Accordingly, for a field intensity that corresponds to a value of b somewhat less than 4, *the thickness of the space charge layer will reach a*

maximum. The field in question should be of the order 70 kv/cm for transformer oil, and 200 kv/cm for glass.

The data given by Toriyama[29] for the conductance of transformer oil indicate that the saturation current may indeed increase very rapidly with the field intensity. The effects found by Toriyama were somewhat larger than could be accounted for by the theory (assuming univalent ions); the cause of the discrepancy would have to be determined before definite conclusions could be drawn.

Where the saturation current is found to increase with the field intensity, it should be possible to find evidence of the Langevin time-lags. Where the saturation current is independent of the field intensity, the distribution of space charges ought to correspond to a greater, chemical time-lag.

In a given experiment, some electrolytes may show a Langevin time-lag, others a chemical time-lag. Whether a given electrolyte will show one or the other, will depend on two properties that cannot in general be predicted, namely, the ratio τ_c/τ_L and the reserve concentration of ion pairs. Incidentally, the pair concentration and τ_L will depend on the concentration of ions, the latter inversely as the conductance. The chemical time-lag ought not to depend on the concentration unless the electrolyte is polymerized, or cluster ions are formed. It must be pointed out, however, that cluster ions may form at surprisingly low concentrations.[11]

As yet, time-lags or saturation currents have not been measured for electrolytes of known constitution in solvents of low dielectric constants. By such methods, it should be possible to determine the mobilities of suitable free ions in benzene and similar solvents, where there is no hope that we should ever be able to extrapolate conductance curves. Moreover, the investigation of these phenomena in known electrolytes would greatly aid their application to the study of semiconductors of unknown constitution.

[29] Y. Toriyama, Archiv f. Electrotech. **19**, 31 (1927).

Caesium Nitrate and the Perovskite Structure

LOUIS WALDBAUER AND D. C. MCCANN, *Division of Analytical Chemistry, State University of Iowa*

(Received June 15, 1934)

1. The crystal structure of dysanalyte has been verified. 2. The crystal structure of $CsNO_3$ has been determined. 3. The so-called perovskite structure as a type of cubic symmetry is based on a mineral which is very probably not cubic but is orthorhombic. 4. The term "perovskite structure" should be discontinued.

THE authors' interest was first directed to the perovskite structure when a powder diffraction pattern of $CsNO_3$ was found to suggest cubic symmetry (Fig. 1) while the weak birefringence, as shown by the polarizing microscope, indicated some other symmetry.

Wyckoff[1] discussed the assignment of crystals, giving a pattern of this kind, to the so-called perovskite structure and expressed his doubt that these crystals were really isometric. Barth[2] made the first structure determination of perovskite and reported the mineral to be orthorhombic, $a:b:c=0.9881:1:1.4078$, and the space group to be V_h^{19}. Barth[2] also determined the structure of dysanalyte to be cubic with $a_0=3.826$. The authors of this paper were able to check Barth's work on dysanalyte, using a sample from Magnet Cave, Arkansas (see Table I).

The authors were unable to obtain a sample of perovskite but, in view of Table I, saw no reason to doubt Barth's work. It therefore seemed worthwhile to make a complete structure analysis of $CsNO_3$, since the "perovskite structure" was in question and the structure of $CsNO_3$ had never been determined.

[1] R. W. G. Wyckoff, *Structure of Crystals*, Chemical Catalogue Company, New York, 1931.
[2] T. Barth, Norsk. Geology Tidsskr. **8**, 201 (1925).

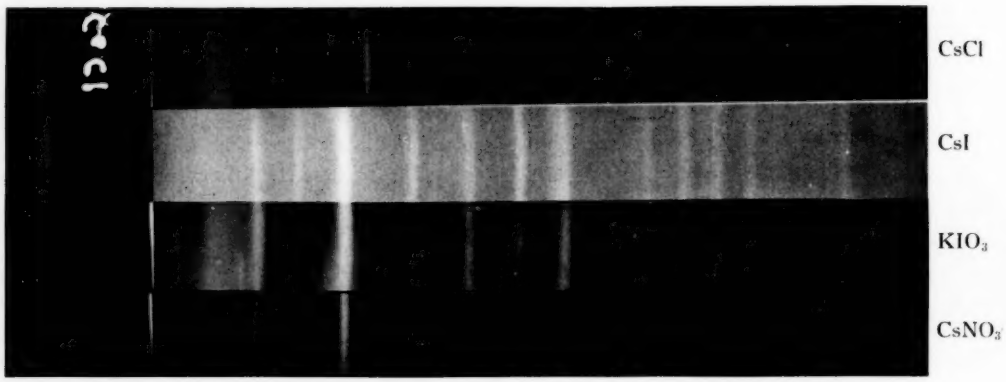

FIG. 1.

TABLE I. *Dysanalyte.*

	Barth	Waldbauer and McCann
Symmetry	cubic	cubic
Space group	O_h^1, O^1 or T_d^1	O_h^1, O or T_d^1
a_0	3.826	3.80

The usual methods of crystal analysis were used. Several Laue photographs were obtained, all of which indicated hexagonal symmetry. Oscillation photographs were used for measurement of spacings along the axes. A gnomonic projection (Fig. 2) of a Laue photograph of $CsNO_3$, with the x-ray parallel to the C axis, was made and indexed. From the indexed projection and the spacing measurements, values of $n\lambda$ were calculated and compared with the minimum possible wave-length. Wyckoff's statistical method and tables[3] were used to determine the space group. The results are given in Table II.

TABLE II. *Symmetry data on $CsNO_3$.*

a_0	10.74A
c_0	7.68A
mols per unit cell	9
Space lattice	Γh
Space groups (possible)	D_{3h}^1, D_{3h}^3, D_{3h}^4

The problem of the supposed inversion of $CsNO_3$ at 161°[4] was attacked by means of a heated camera built by the authors (Fig. 3). Powder diffraction photographs were obtained at temperatures of 165° and 200°. These showed a pattern exactly comparable to those at room temperature except for a very slight shift due to expansion. The inference was, therefore, that no structure change took place. In view of the determination of $RbNO_3$[5] a question arose, however. Rubidium nitrate was discussed both for the hexagonal and the orthorhombic symmetry, the conclusion being that it was very nearly hexagonal but actually orthorhombic. The decision seemed to be based on a biaxial interference figure. Caesium nitrate could be assigned to the orthorhombic axes with $a : b : c = 18.60 : 10.74 : 7.68$, a unit cell containing 18 mols. However, since $CsNO_3$ shows no biaxial interference figure and since the hexagonal cell is smaller, the orthorhombic assignment is not justified by any known data. The fact remains that $CsNO_3$ may be, through deviations within experimental error, orthorhombic at room temperature or above 161°.

A further discussion of Fig. 1 may be made. Caesium chloride and CsI are known to be cubic. Caesium nitrate has been shown to be hexagonal. Potassium iodate, which has been assigned to the perovskite structure, is highly birefringent and therefore not cubic. Several attempts were made to grow crystals of KIO_3 suitable for analysis but none were obtained which were useful, even with the microscope. The most striking point of Fig. 1 is the almost exact coincidence of the lines of CsI, KIO_3 and $CsNO_3$, both in number and position, and to

[3] Wyckoff, R. W. G., Zeits. f. Krist. **63**, 507 (1926).
[4] A. N. Winchell, *Microscopic Characters of Artificial Minerals*, p. 208, John Wiley and Sons, New York, 1931.
[5] Pauling and Sherman, Zeits. f. Krist. **84**, 213 (1933).

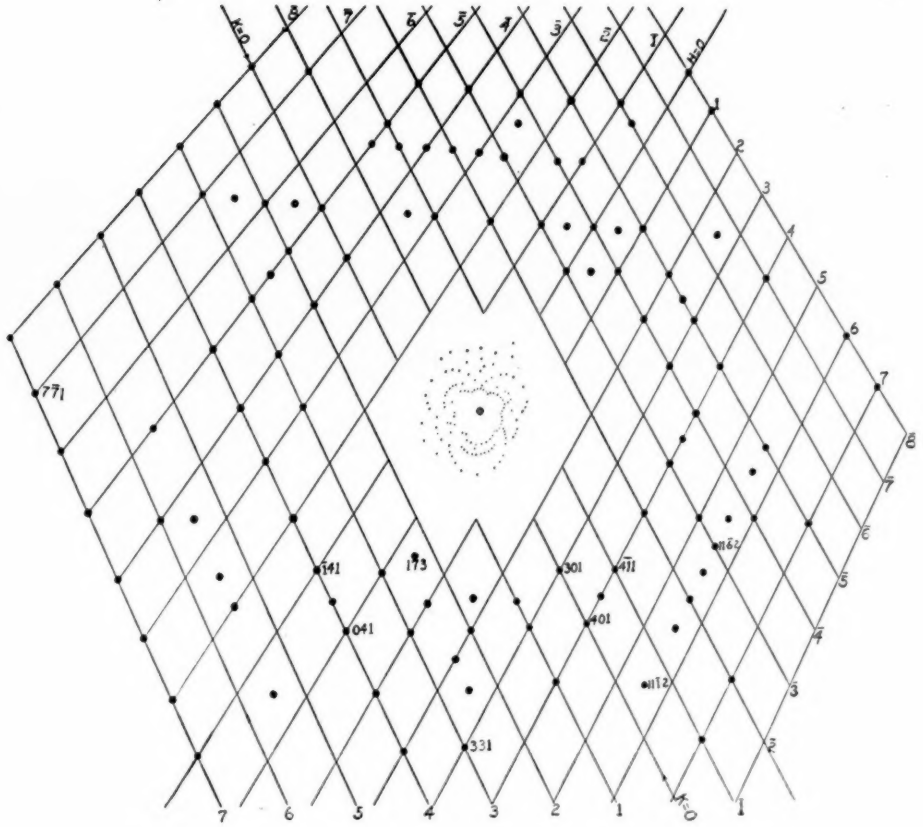

FIG. 2. Gnomic projection of $CsNO_3$. X-rays nearly parallel to c axis.

some extent in intensity. Very careful measurements showed a slight difference in position.

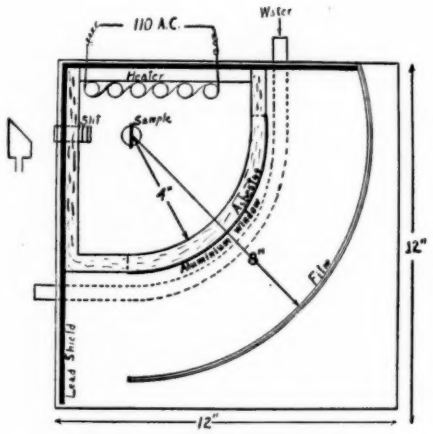

FIG. 3. Heated powder diffraction camera.

The authors therefore state that crystals giving an apparently cubic powder diffraction pattern are not necessarily cubic, as has been recognized for $LiCl.H_2O$ [6] and that practical identity of spacings of lines on the pattern are not proof of identity unless the intensity is taken into account.

The "perovskite structure" can be applied only to perovskite which is most probably orthorhombic but has been used as a type of cubic symmetry. The use of the term in this manner has apparently been based only on similarity of powder patterns. Obviously the term should be discontinued or the term "perovskite pattern" applied to pseudo-cubic powder diffraction patterns.

---

[6] S. B. Hendricks, Zeits. f. Krist. **66**, 131 (1927).

LETTERS TO THE EDITOR

This section will accept reports of new work, provided these are terse and contain few figures, and especially few halftone cuts. The Editorial Board will not hold itself responsible for opinions expressed by the correspondents. Contributions to this section must reach the office of the Managing Editor not later than the 15th of the month preceding that of the issue in which the letter is to appear. No proof will be sent to the authors. The usual publication charge ($3.00 per page) will not be made and no reprints will be furnished free.

The Raman Spectra of Some Isomeric Octanes

The Raman spectra of 3,4-dimethylhexane and 2,5-dimethylhexane have been examined using the technique described by Murray and Andrews.[1] The samples studied were synthesized in this laboratory for experiments on motor fuels by C.W.A. workers in an investigation of carbon monoxide elimination. They are believed to be of satisfactory purity having boiling ranges not greater than 0.2°. Spectra were excited by the violet and blue lines of the mercury arc separately, using appropriate filters. The following lines were observed.

3,4-dimethylhexane: 338(5*b*), 436(5), 462(1), 489(0), 558(1), 583(0), 733(5), 754(5), 801(3*b*), 840(4), 897(5), 955(4), 984(5), 1034(5), 1054(4), 1123(1), 1163(4), 1182(2), 1286(4*b*), 1355(2*b*), 1455(20*b*), 1658(1), 2732(2*br*), 2860(10), 2875(20), 2907(8), 2934(10), 2967(20).

2,5-dimethylhexane: 265(3), 313(2), 444(4*b*), 553(0) 778(2), 839(6), 962(3*br*), 1048(1), 1150(3), 1176(4), 1233(1/2), 1302(2*b*), 1338(4), 1453(10*b*), 2650(0), 2720(2), 2763(1), 2871(10), 2921(3), 2962(10). Estimated relative intensities are given in parentheses following the displacements of the Raman lines together with symbols to indicate the character of the lines; *b* meaning broad, and *r* shaded toward the red.

Whereas the molecules in question are too complex to permit detailed assignments of frequencies to types of motion, a few features of these spectra appear worthy of comment. It is to be expected that 2,5-dimethylhexane should have lower frequencies than the 3,4- isomer as the methyl groups are situated nearer the ends of the vibrating hydrocarbon chain. This is in accordance with the observed spectra. The 3,4-dimethylhexane has two asymmetric carbon atoms and hence should occur in three stereoisomeric forms. The synthesized product should be a mixture of all three and hence the spectrum should consist of two superimposed spectra as the *d* and *l* forms should have identical spectra. The fact that several more lines are found for this compound than for the 2,5- isomer is in accord with this expectation although the greater symmetry of the latter compound would also tend to produce this effect.

JOHN W. MURRAY

Johns Hopkins University,
July 17, 1934.

[1] J. W. Murray, and D. H. Andrews, J. Chem. Phys. **1**, 406 (1933).

The Thermodynamic Functions of a Diatomic Gas Whose Molecules Have a Multiplet Normal Electronic State Belonging to Hund's Case (a)

In Hund's case (a), which occurs only when $\Lambda \neq 0$, the energy levels of the multiplet are given in cm^{-1} by the formula

$$F_s(v,J) = B_s(v)[(J+\tfrac{1}{2})^2 - \Omega_s^2] + (s-1)D + E_s(v). \quad (1)$$

Here s numbers the components of the multiplet from 1 to m, m being the multiplicity; D is the separation between the successive components of the multiplet. In any given component of the multiplet J takes on the values Ω_s, Ω_s+1, etc. $E_s(v)$ is the vibrational energy in terms of the new quantum theory.

The partition sum is then

$$P_1 = \sum_{s,v,J} 2(2J+1)e^{-\sigma_s(v,J)+\sigma_0}, \quad (2)$$

where

$$\sigma_s(v,J) = hcF_s(v,J)/kT, \qquad \sigma_0 = \sigma_1(0,\Omega_1)$$

and $2(2J+1)$ is the statistical weight of the state $F_s(v,J)$, the factor 2 coming from Λ-type doubling.

Inserting the expression (1) in (2) and making the usual approximations,[1] it can be shown that the partition sum splits into a product of four factors, one due to rotation, one to vibration, one due to the multiplicity, and the factor e^{σ_0}. Designating by a subscript M the factor due to the multiplicity,

$$P_{1M} = (1-e^{-m\rho})/(1-e^{-\rho}), \quad (3)$$

where

$$\rho = hcD/kT. \quad (3a)$$

As a consequence the specific heat, entropy and free energy will each have an extra additive term due to the multiplicity. These terms are, respectively,

$$\frac{C_M}{R} = \frac{\rho^2 e^{-\rho}}{(1-e^{-\rho})^2} - \frac{m^2\rho^2 e^{-m\rho}}{(1-e^{-m\rho})^2}, \quad (4)$$

$$\frac{S_M}{R} = \frac{\rho e^{-\rho}}{1-e^{-\rho}} - \log(1-e^{-\rho}) - \left[\frac{m\rho e^{-m\rho}}{1-e^{-m\rho}} - \log(1-e^{-m\rho})\right], \quad (5)$$

$$\left(-\frac{F-E_0^0}{RT}\right)_M = \log(1-e^{-m\rho}) - \log(1-e^{-\rho}). \quad (6)$$

In each case the contribution due to the multiplicity is of the form

$$F\left(\frac{1}{\rho}\right) - F\left(\frac{1}{m\rho}\right) = F\left(\frac{kT}{hcD}\right) - F\left(\frac{kT}{mhcD}\right). \quad (7)$$

This means that if we plot the multiplet contributions to the thermodynamic functions against temperature, curves with the same m but different values of D will differ only in their scale along the temperature axis.

It is interesting to note that in the case of the specific heat, F is the Einstein function or the specific heat of a single vibration (cf. Einstein's theory of the specific heat of solids). It is easy to show that the curve for C_M has a maximum. The height of this maximum is determined entirely by the multiplicity m, and in no case can the height exceed the gas constant R. For a given m, the location of this maximum is determined entirely by the value of D.

ENOS E. WITMER

Randal Morgan Laboratory of Physics,
University of Pennsylvania,
Philadelphia, Pennsylvania,
July 24, 1934.

[1] E. Schrödinger, Handbuch der Physik, Bd. X, p. 275.

Raman Effect of Molecule Type XY_6

Yost, Steffens and Gross[1] have given three new valuable examples of the Raman effect of the type XY_6, first examined experimentally and theoretically by us;[2] they think, however, our theoretical treatment to be "oversimplified" and think it "necessary to treat the problem more thoroughly."

We have adopted the central force system exactly according to the form suggested by Bjerrum.[3] We were, of course, well aware of the fact, that several authors[4] have introduced the hypothesis, that apart from Bjerrum's forces there are other ones, acting in the equilibrium positions of the atoms; this hypothesis is a reasonable development of Bjerrum's assumption, the latter being a first approximation. We do not know, why Yost, Steffens and Gross take Bjerrum's original system as impossible; probably they assume that the forces present in equilibrium positions have an influence about as great as Bjerrum's forces. But as those forces can be substituted by forces perpendicular to the line connecting the two respective atoms,[5] it can be assumed, that they are really considerably smaller than Bjerrum's forces.[6]

In our case we think it perfectly adequate to dispense with those smaller forces; first, because their introduction involves the introduction of additional constants, which cannot be determined by the Raman frequencies; second, because our treatment of the problem gives a perfectly satisfactory interpretation of the experimental results.

In fact, the interpretation of the Raman frequencies given by Yost, Steffens and Gross is essentially identical with ours. That can be said not only of the vibration scheme, but also of the coordination of frequencies and vibrations; especially the relation between the three Raman frequencies given by Yost, Steffens and Gross was used already by us for coordination.

There is no material influence of the different theoretical treatment except in the calculations, leading to the numerical values of Table II, given by Yost, Steffens and Gross In performing these calculations, however, these authors are forced to introduce not only the new theory of Badger, but also a rather uncertain additional assumption regarding their constant j; moreover, this assumption seems to be incompatible with their putting the constant k_{24} of the analogous force of Bjerrum equal to zero.

Still, we think our theoretical treatment an adequate interpretation of our experimental results; on the other hand, we regard the calculations performed by Yost, Steffens and Gross, inasmuch as they go further than ours, as a trial of interpretation, very interesting, but necessarily rather uncertain.

O. REDLICH
T. KURZ
P. ROSENFELD

Technische Hochschule,
Institut für physikalische Chemie,
Wien,
July 25, 1934.

[1] D. M. Yost, C. C. Steffens and S. T. Gross, J. Chem. Phys. **2**, 311 (1934).
[2] O. Redlich, T. Kurz and P. Rosenfeld, Zeits. f. physik. Chemie **B19**, 231 (1934).
[3] N. Bjerrum, Verhandl. d. physik. Ges. **16**, 737 (1914).
[4] Cf. D. M. Dennison, Astrophys. J. **62**, 84 (1925).
[5] We do not know, whether this substitution has already been made heretofore.
[6] Cf. an analogous assumption made by R. Mecke, Zeits. f. physik. Chemie **B16**, 409 (1932).